NATIONAL CENTER FOR EARTHQUAKE
ENGINEERING RESEARCH
State University of New York at Buffalo

Experimental Performance and Analytical Study of a Non-Ductile Reinforced Concrete Frame Structure Retrofitted with Elastomeric Spring Dampers

by

G. Pekcan, J.B. Mander and S.S. Chen

State University of New York at Buffalo
Department of Civil Engineering
Buffalo, New York 14260

Technical Report NCEER-95-0010

July 14, 1995

This research was conducted at the State University of New York at Buffalo and was partially supported by the National Science Foundation under Grant No. BCS 90-25010 and the New York State Science and Technology Foundation under Grant No. NEC-91029.

NOTICE

PB96-137161

Experimental Performance and Analytical Study of a Non-Ductile Reinforced Concrete Frame Structure Retrofitted with Elastomeric Spring Dampers

by

G. Pekcan[1], J.B. Mander[2] and S.S. Chen[2]

July 14, 1995

Technical Report NCEER-95-0010

NCEER Task Number 94-3101

Jarret, Inc. Contract Number UBF-9103-339925

NSF Master Contract Number BCS 90-25010
and
NYSSTF Grant Number NEC-91029

1 Research Assistant, Department of Civil Engineering, State University of New York at Buffalo
2 Associate Professor, Department of Civil Engineering, State University of New York at Buffalo

NATIONAL CENTER FOR EARTHQUAKE ENGINEERING RESEARCH
State University of New York at Buffalo
Red Jacket Quadrangle, Buffalo, NY 14261

PREFACE

The National Center for Earthquake Engineering Research (NCEER) was established to expand and disseminate knowledge about earthquakes, improve earthquake-resistant design, and implement seismic hazard mitigation procedures to minimize loss of lives and property. The emphasis is on structures in the eastern and central United States and lifelines throughout the country that are found in zones of low, moderate, and high seismicity.

NCEER's research and implementation plan in years six through ten (1991-1996) comprises four interlocked elements, as shown in the figure below. Element I, Basic Research, is carried out to support projects in the Applied Research area. Element II, Applied Research, is the major focus of work for years six through ten. Element III, Demonstration Projects, have been planned to support Applied Research projects, and will be either case studies or regional studies. Element IV, Implementation, will result from activity in the four Applied Research projects, and from Demonstration Projects.

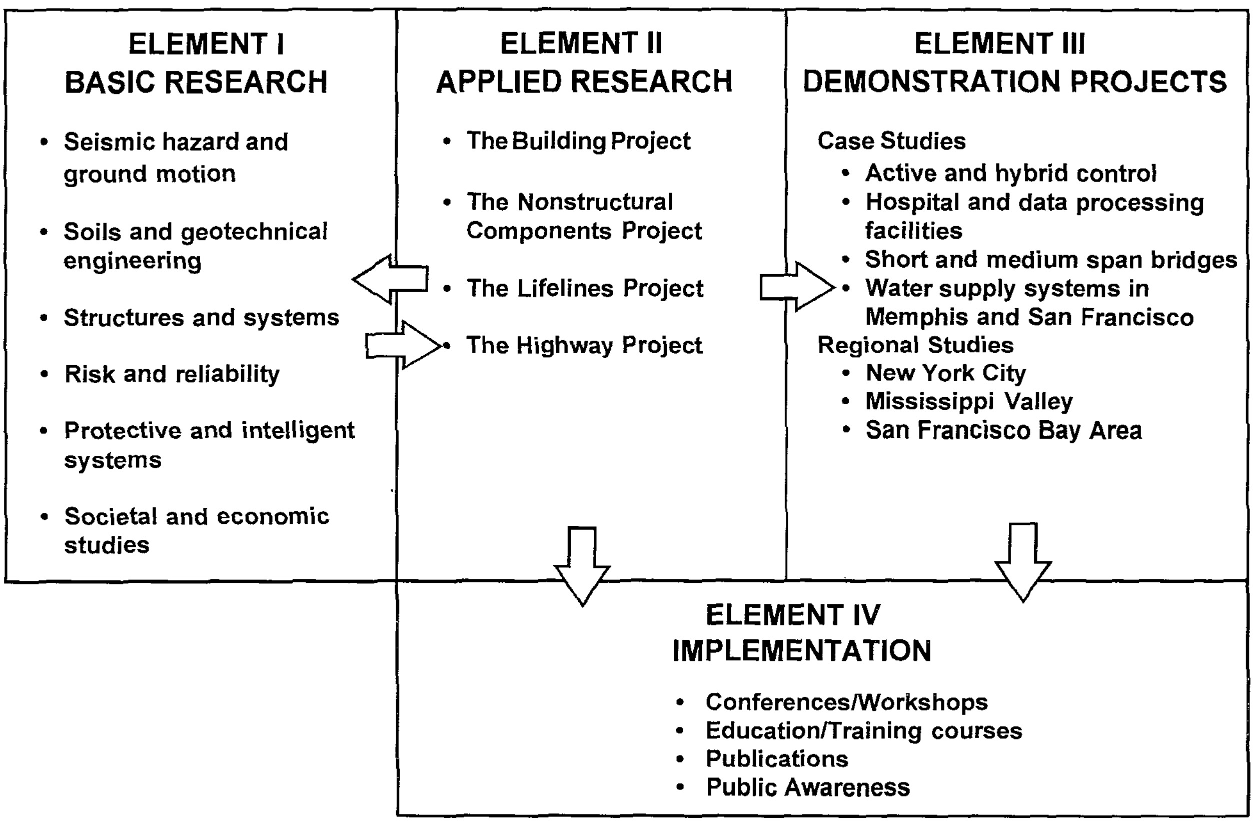

Research in the **Building Project** focuses on the evaluation and retrofit of buildings in regions of moderate seismicity. Emphasis is on lightly reinforced concrete buildings, steel semi-rigid frames, and masonry walls or infills. The research involves small- and medium-scale shake table tests and full-scale component tests at several institutions. In a parallel effort, analytical models and computer programs are being developed to aid in the prediction of the response of these buildings to various types of ground motion.

Two of the short-term products of the **Building Project** will be a monograph on the evaluation of lightly reinforced concrete buildings and a state-of-the-art report on unreinforced masonry.

The **protective and intelligent systems program** constitutes one of the important areas of research in the **Building Project**. Current tasks include the following:

1. Evaluate the performance of full-scale active bracing and active mass dampers already in place in terms of performance, power requirements, maintenance, reliability and cost.
2. Compare passive and active control strategies in terms of structural type, degree of effectiveness, cost and long-term reliability.
3. Perform fundamental studies of hybrid control.
4. Develop and test hybrid control systems.

As stated above, one of NCEER's current tasks in the protective systems area is to perform comparative studies of their capabilities and limitations. While a large variety of these systems exist and have found applications, there is a lack of common basis on which the performances of these systems can be evaluated and compared to arrive at a recommendation under certain specified conditions such as control objectives, structural type, loading conditions, and system configuration. This report documents one part of NCEER's efforts in this direction involving performance evaluation of several passive energy dissipation devices. It presents the evaluation of elastomeric dampers used as additional braces in reinforced concrete frame structures based on analysis and shaking table experiments performed on a 1:3 scale reinforced concrete frame. The elastomeric spring damper is a special type of fluid damper that possesses recentering characteristics.

ABSTRACT

This experimental study describes the use of elastomeric spring dampers, which have a distinct re-centering capability. The dampers were used to retrofit a non-ductile, previously damaged 1/3 scale model reinforced concrete building frame. The structure was then subjected to a variety of ground motions in shaking table tests. A velocity dependent analytical model is developed and verified for the elastomeric spring dampers. This model is implemented in the widely available non-linear dynamic time history analysis computer program DRAIN-2DX to produce response predictions which are in good agreement with experimental observations. The elastomeric spring damper devices significantly attenuate the seismic response of the structure and provide a considerable amount of energy dissipation while the main non-ductile reinforced concrete structural load carrying elements remain elastic. The effect of varying the damper configuration on the structural response was also investigated.

ACKNOWLEDGEMENTS

The damper specimens (modified BC1C devices) and partial funding for this study were provided by Jarret, Inc. The scale model building was constructed and initially tested under the direction of Prof. A.M. Reinhorn in conjuction with the second author and under financial support of the National Center for Earthquake Engineering Research (NCEER). NCEER technician, Mark Pitman, assisted with conducting the shaking table tests. After removal of the dampers, final testing of the bare frame under 0.3 g El Centro earthquake was undertaken by graduate student Mr. Chen Li. All are gratefully acknowledged.

TABLE OF CONTENTS

TABLE OF CONTENTS - CONT'D

TITLE **PAGE**

LIST OF ILLUSTRATIONS

LIST OF ILLUSTRATIONS - CONT'D

LIST OF TABLES

SECTION 1

INTRODUCTION

As modern structures become taller, more slender and lighter with the invention of new structural materials and the enhancement of design and construction techniques, control of effects of seismic excitation and/or wind on structures has become an important goal of researchers. Many design and analysis methods for structures subjected to seismic excitations have been proposed following analytical and experimental studies.

Conventional ductile design requires that structures passively resist earthquakes through a combination of strength, deformability and energy dissipation. Sufficient stiffness must also be provided to avoid excessive relative floor displacements (interstory drifts) which cause non-structural damage. Lateral strength to the structure must then be provided to resist seismic loads in the form of moment resisting frames, shear walls, concentric or eccentric braces or a combination of these. To prevent collapse during severe earthquake excitation and to achieve an economical design for frame structures, shear walls are permitted to crack and yield, concentric braces are permitted to buckle, and eccentric brace shear links are designed to yield so as to reduce the inertia forces during earthquake shaking. Thus, during strong ground motions, due to lack of lateral strength, structures invariably deform beyond their elastic limit.

Inelastic deformation takes the form of localized and/or spread plasticity in hinges which result in increased flexibility and energy dissipation. This inelastic action results in damage to the structural members, which is generally intended to occur in specially detailed critical regions of lateral force resisting systems, e.g., in the beams near the beam-column joints. Following a strong earthquake, damage to these plastic hinge regions is to be expected, but without structural collapse, to ensure the preservation of life-safety. To some designers, particularly designers of essential or critical structures, this ductile philosophy is untenable. This has led many researchers to investigate alternate forms of energy dissipation within the structures to minimize permanent damage through yielding of members.

There are indeed a number of situations where ductile structural behavior may be either unattainable, or desirable. Consider first many older structures especially those located in the eastern and central United States that were designed only for gravity loads (1.4D+1.7L) per non-seismic detailing provisions of the codes. During a moderate earthquake the non-seismic ductile detailing of the structural elements may lead to excessive interstory drifts resulting in distress of nonstructural elements. During strong shaking, an undesirable soft-story failure mechanism may form and subsequent collapse. Secondly, well designed and detailed reinforced concrete frame structures may be quite flexible, and under earthquake excitations the interstory drifts may be excessive leading to the distress of nonstructural elements; the result is often undesirable damage and permanent deformations. Secondly, important structures such as hospitals, schools and fire departments may be required to be serviceable after an earthquake; the ductile design philosophy with the associated permanent deformations in such cases is inappropriate. Thus, if seismic energy dissipation can be achieved by means of separate non-load-bearing supplementary damping devices which also provide a re-centering capability, the load-bearing structure can remain largely elastic with continuing serviceability.

A number of investigations have shown that a significant amount of seismic energy can be dissipated by specially designed non-structural damping elements, allowing the primary structural elements to remain within the elastic limits after a major seismic event. These elements can be categorized in three main groups: Friction Devices, Metallic Yielding Devices, Viscous (fluid) Devices and Viscoelastic Devices. A brief discussion of these groups of devices is given in what follows:

1.1 Friction Devices

Pall (1987, 1991) proposed a type of friction device which was located at the intersection of a cross-bracing as shown in Figure 1.1. This device has been used in three buildings in Canada. Seismic loading induces cycles of tension-compression forces in the braces such that the tension brace causes slippage at the friction joint, therefore forcing the compression brace to slip as well. A number of experimental studies (Filiatrault 1987, Aiken 1988) were performed using these devices after which design methodologies were developed

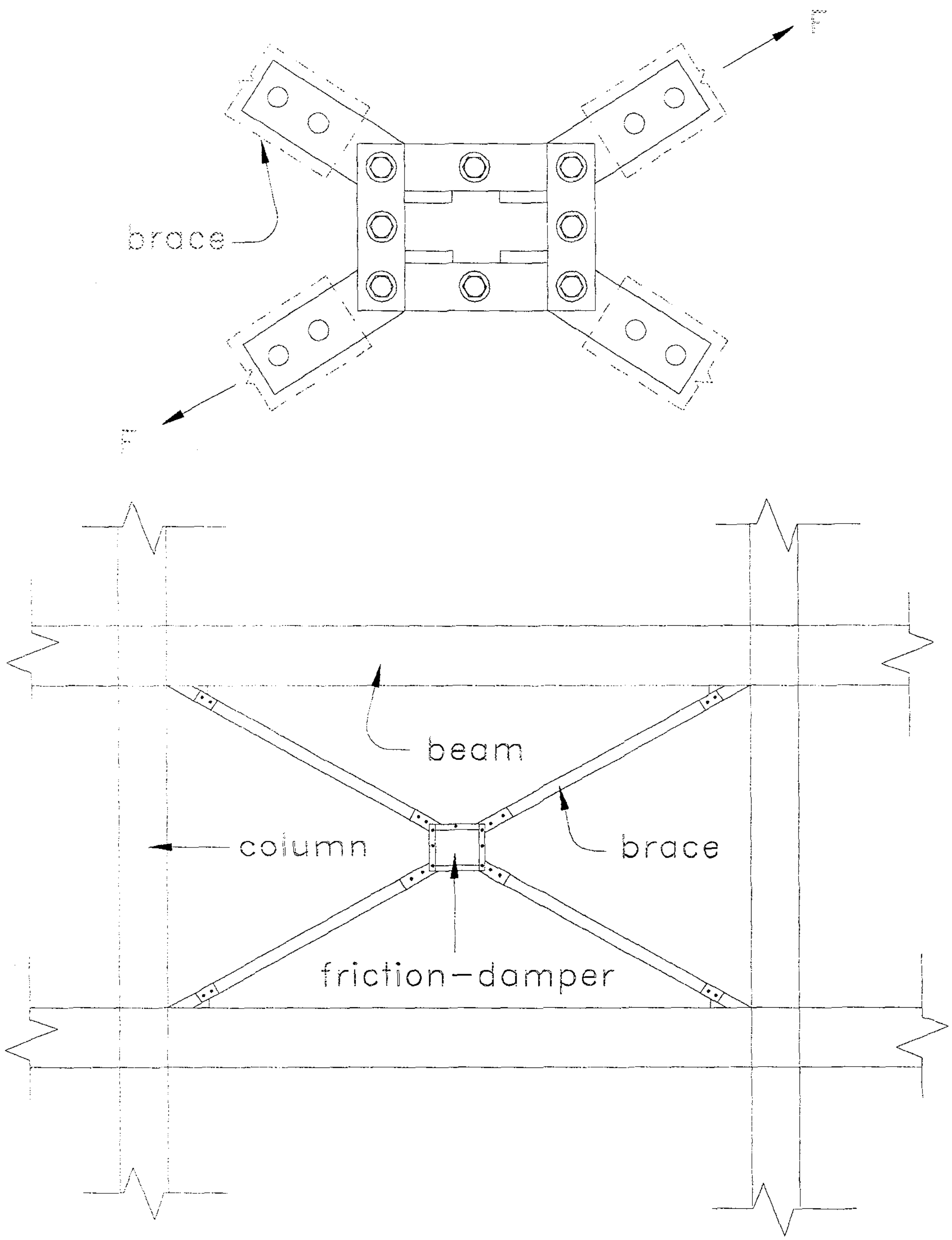

Figure 1.1 Friction Device (Pall 1987)

for friction-damped structures (Filiatrault 1990).

Sumitomo friction dampers (Figure 1.2) which were developed for railway applications, consist of copper alloy pads which generate friction due to contact with the inner surface of the steel casing. Aiken (1990) conducted shaking table tests of a 9-story model structure with Sumitomo dampers.

All of these friction dampers have Coulomb friction characteristics as they generate rectangular hysteresis loops. Fluor Daniel Inc., however, has developed a friction device called the Energy Dissipating Restraint (EDR) which has a double-flagged hysteresis loop. Richter et al. (1990) and later Nims et al. (1993) and Aiken et al (1993) investigated the self centering capabilities of EDRs.

Fitzgerald et al. (1989) used slotted bolted connections in the braces allowing slip and energy dissipation at the connection. Further investigation of this type of friction connections was done by Grigorian and Popov. (1992, 1994).

These studies have shown that friction devices could be utilized in building structures so as to enhance their seismic performance. In general, story drifts were reduced when compared to moment resisting frames, increasing the energy dissipation capacity. Story shears were also reduced moderately and transferred to braces which in turn allowed lower design forces for primary structural elements.

1.2 Metallic Damping Devices

In this group of damping devices, *yielding steel systems* are the most extensively investigated types of dampers. The most common characteristic of these devices is that they deform into the plastic range utilizing flexural, shear, or extensional deformation modes. The fact that the mild steel can go through a considerable number of stable inelastic cycles has led to the development of this class of device. After Kelly et al. (1972) and Skinner et al. (1980) have developed these dampers, Tyler (1978) and Stiemer et al. (1981) used mild steel plates with triangular or hourglass shapes so that the yielding would spread almost uniformly throughout the material. Tyler (1985) also developed an energy dissipating system which used mild steel round bars in cross-bracing as the energy absorbing elements.

Inspired by the X-shaped damping supports for piping systems (Stiemer et al. 1981), Whittaker et al. (1991) studied the Bechtel Added Damping and Stiffness (ADAS) devices. As shown in Figure 1.3, the ADAS device consists of multiple X-steel plates supported by rigid plates such that the X-plates deform in double curvature. ADAS elements have been experimentally tested by Bergman and Goel (1987) and Whittaker et al. (1991). It has been shown that these elements can increase the stiffness and strength of the structure while reducing the energy dissipation demand on the structural elements.

Lead Extrusion Devices (LED) and Shape Memory Alloys (SMA) are the other two types of metallic damping devices. LED (Skinner et al. 1993) has essentially the same rectangular hysteresis behavior as friction devices, and the effect of number of loading cycles is minimal. However, LED is rate-dependent and temperature dependence is observed as well either due to ambient changes or to the absorption of energy during an earthquake. These devices have been used mostly in New Zealand: in three bridges and to provide damping for a ten-story building supported by flexible piles. It has also been installed in the walls to improve the seismic performance of two buildings in Japan.

SMA can yield repeatedly without any permanent deformation. These devices are also shown to be effective in reducing the seismic response of structures (Aiken et al. 1992, Witting and Cozzarelli 1992).

1.3 Viscoelastic Devices

Mahmoodi (1969) first described the characteristics of a double-layer, constraint layer, viscoelastic (VE) shear damper. In his first attempt to model the VE damper, Mahmoodi used linear viscoelastic theory and did not consider frequency and temperature effects. Since then, studies have focused on the investigation of various parameters affecting the behavior of this class of dampers. It was found that the stiffness and damping properties of VE dampers are controlled by the temperature, the frequency of the loading and the level of induced shear deformation in the material.

Viscoelastic materials consist of polymers or glassy substances. They dissipate energy in the form of heat when subjected to deformations. A typical VE damper which is subjected

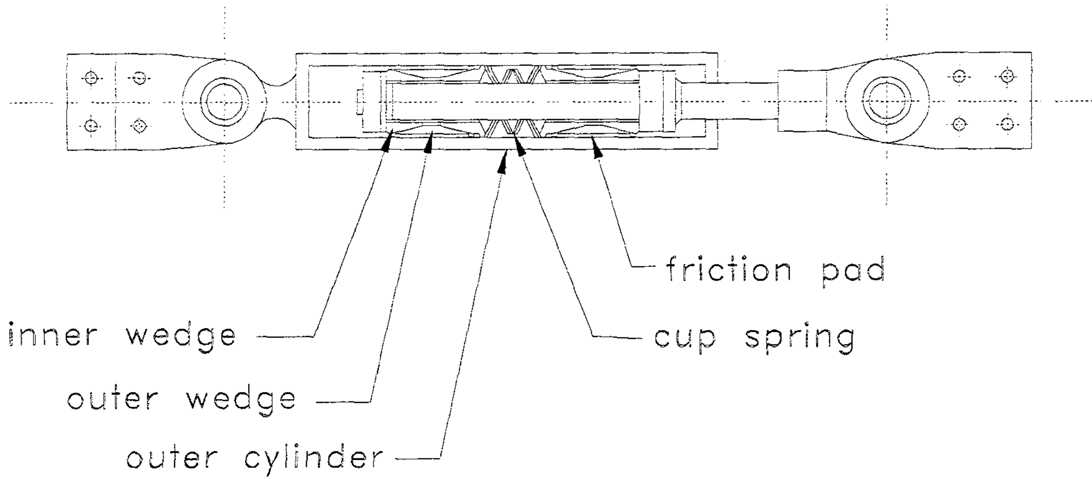

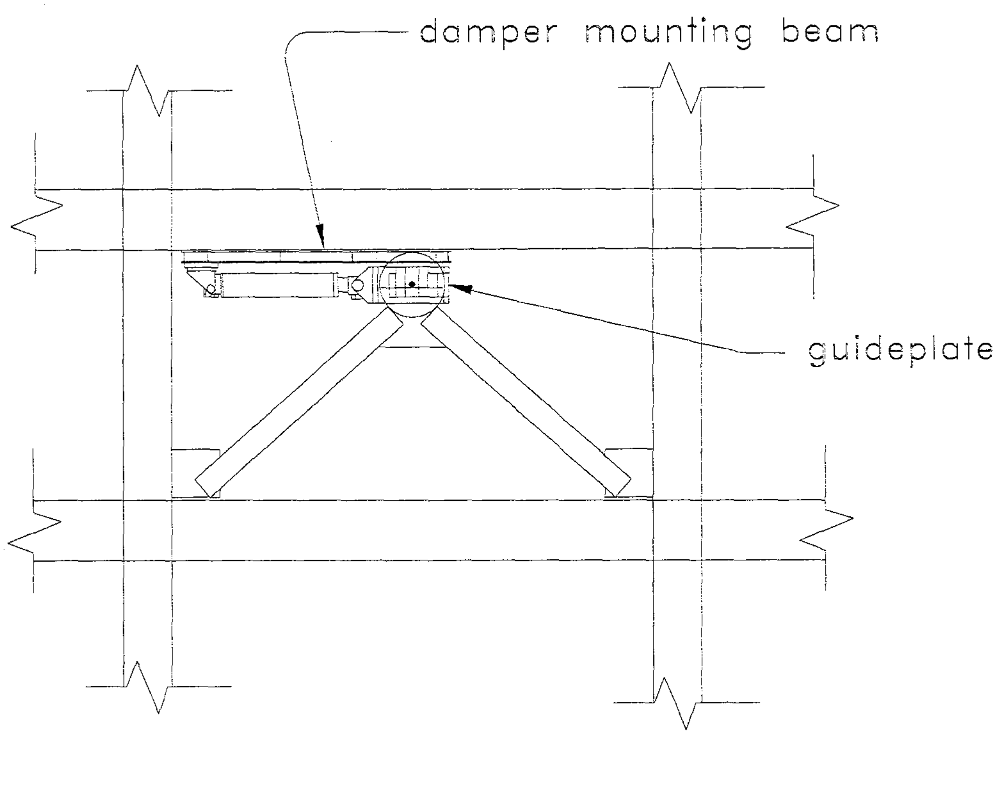

Figure 1.2 Sumitomo Friction Device (Aiken 1990)

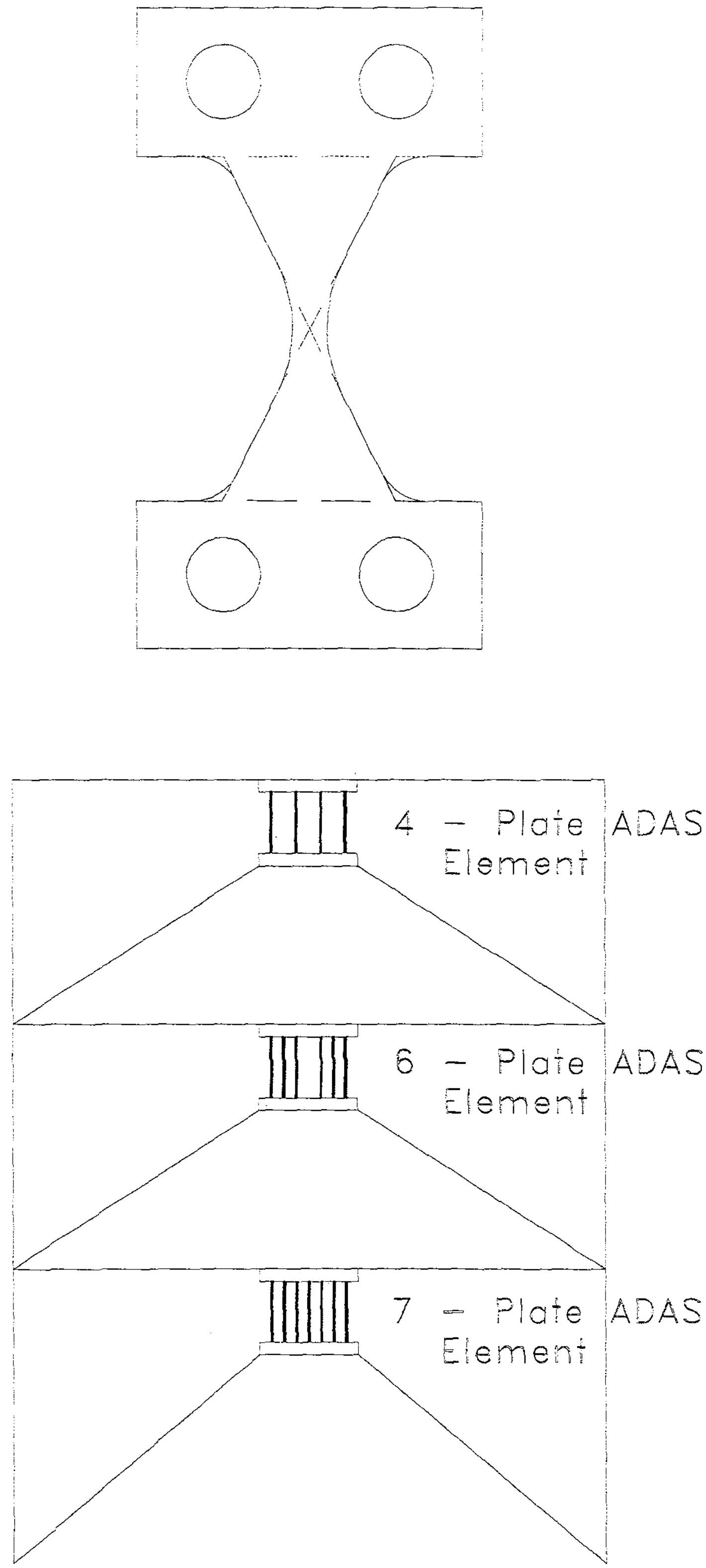

Figure 1.3 Added Damping and Stiffness Device (ADAS) (Whittaker et al, 1991)

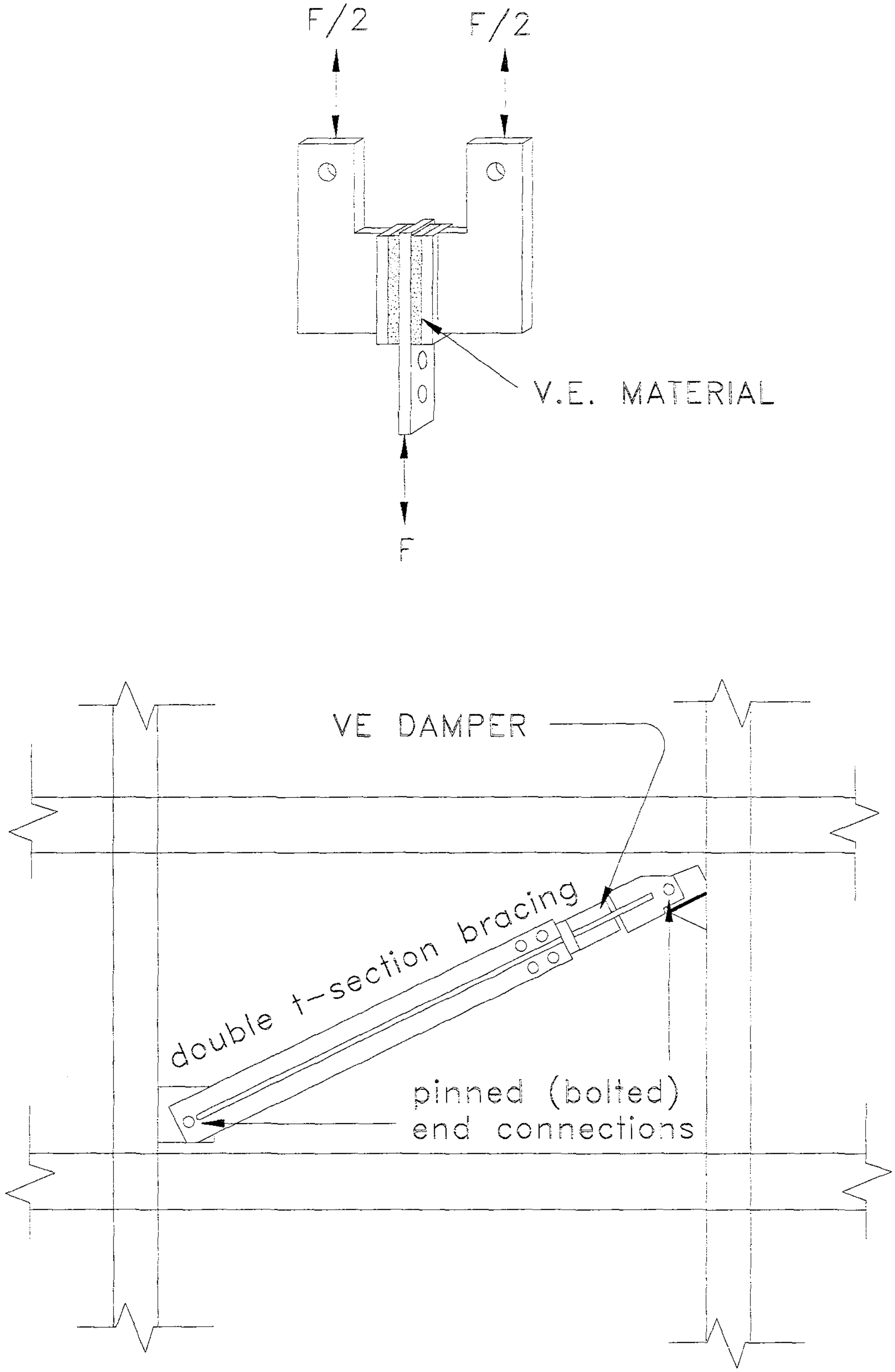

Figure 1.4 Viscoelastic Device (VE)

to longitudinal force is shown in Figure 1.4. VE dampers have been effectively used as energy dissipators in reducing the structural response due to dynamic loadings such as wind (Keel 1986, Mahmoodi et al. 1987), earthquake (Lin et al. 1988, Aiken and Kelly 1990). A number of earthquake simulator tests have been conducted on large-scale steel frames with VE dampers. Various desing methodoligies were suggested by Abbas and Kelly (1993) and Zhang and Soong (1992).

Recently Lobo et al. (1993) performed shaking table tests on a 1/3 scale, non-ductile reinforced concrete model structure which is also the model used in this study. Investigation of the influence of viscoelastic dampers on the inelastic response of reinforced concrete structures was carried out performing a series of simulated ground motion tests. Test results have shown that story drifts and story shears can be reduced significantly and the damping ratio can be increased up to 20 percent of critical. Hysteretic energy dissipation is transferred from the load bearing elements to non-load bearing elements, i.e., viscoelastic braces.

A viscous-damping wall system was developed by Oiles and Sumitomo Construction has been found to provide 10 to 30 percent damping with about 50 to 60 percent reduction in the maximum response in general.

1.4 Viscous (Fluid) Devices

There are no known applications of fluid viscous devices within the framework of a building structure for seismic protection. However, there have been a number of applications for the seismic protection of bridges. These devices maintain linear viscous behavior and very little temperature dependence is observed.

Experimental and analytical studies of a typical fluid viscous device on both building and bridge structures were performed by Constantinou et al. (1993). Very large response reductions were observed with the incorporation of fluid viscous dampers in structures. One of the major advantages of viscous dampers (compared to viscoelastic dampers) is that it appears to be more robust and is not temperature sensitive. A second advantage is that a pure viscous damper does not add any stiffness to the structure; therefore member forces are not increased in columns which may be seismically vulnerable. The most appealing characteristic of the pure viscous damper is that the damping is out-of-phase with the maximum forces (and the maximum displacement) in the structural elements.

1.5 Force-Deformation and Energy Absorption Characteristics of Various Dampers

Force-deformation relationships of some of the dampers discussed which are investigated both experimentally and analytically are shown on Figure 1.5. Sumitomo friction devices (Figure 1.5a) and LED devices (Figure 1.5b) essentially have "Coulomb damper" characteristics which consist of rectangular hysteresis loops. Energy absorbed is a maximum for a particular force and stroke. Experimental studies have shown that ADAS devices have stable hysteretic performance (Figure 1.5c). Design of EDR devices is similar to that of Sumitomo friction devices. Various forms of force-deformation relationships can be obtained by changing the preload and initial gaps in the damper. Analytical force-deformation relationship for an EDR with non-zero preload but no initial gap is shown in Figure 1.5d.

VE dampers have two components in their force-deformation behavior (Figure 1.5d): a viscous (energy absorbing) part andan elastic (energy restoring) part. Experimental studies have shown that VE devices have a significant temperature dependency due to which energy absorption capacity decreases. Finally, viscous (liquid) devices have linear viscous behavior characteristics and generally capability to operate over a temperature range of -40 °C to 70 °C.

Elastomeric spring dampers combine the shear and compressibility characteristics of silicone compounds which are stable over a wide range of temperature of -60 °C to 200 °C. Details of the behavior of elastomeric spring dampers are given in Section 2.

1.6 Present Study - Objectives and Scope

In the present study a type of single-acting damper device previously employed in the railroad and steel industries is used. These stock off-the-shelf devices, called *elastomeric spring dampers,* exhibit a distinct re-centering characteristic and were modified to operate in a double-acting fashion and used to retrofit a lightly reinforced, previously damaged 1/3 scale

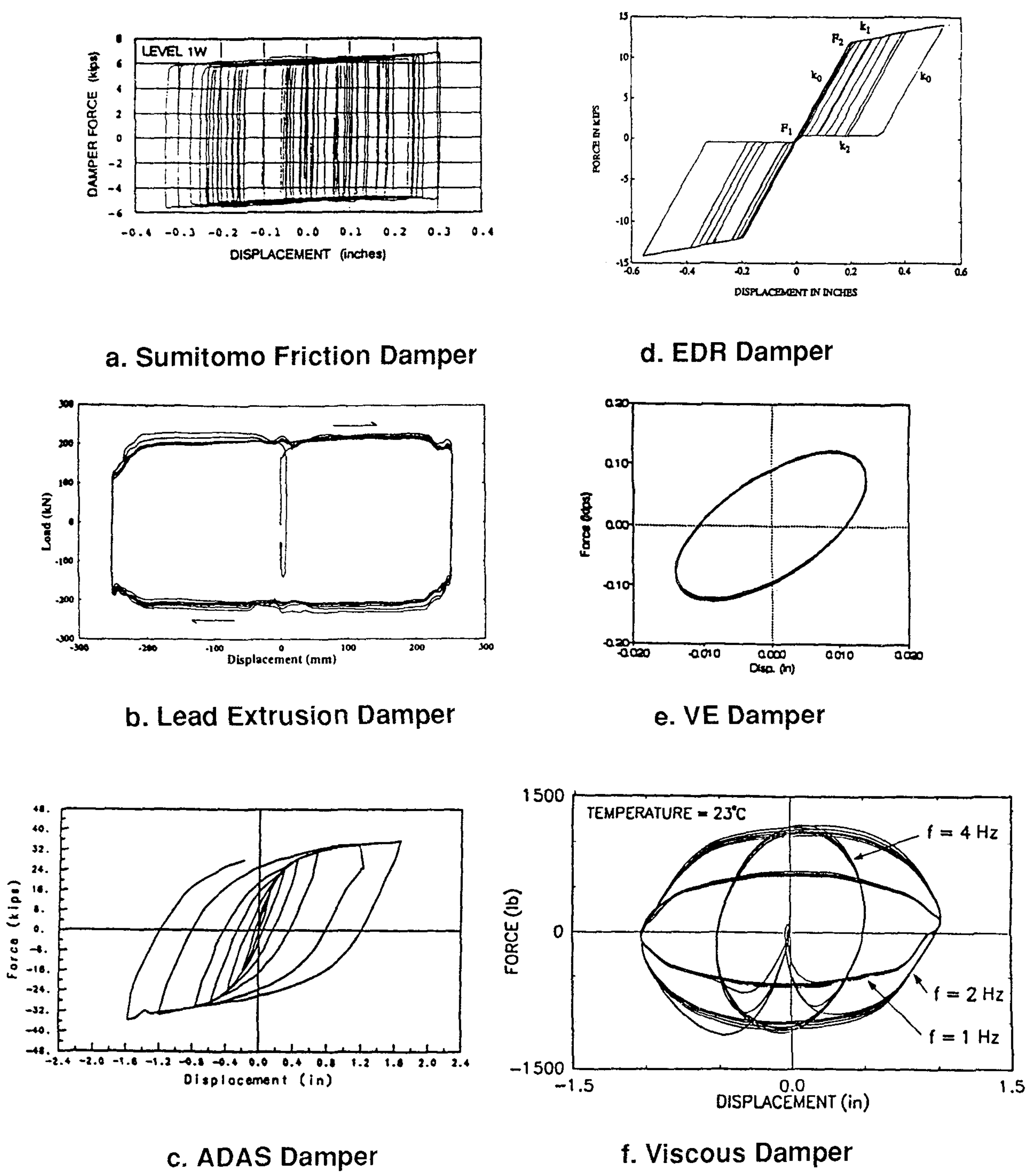

Figure 1.5 Force-Deformation Relationships of Various Dampers
(a. Aiken et al., 1990, b, c., Skinner et al., 1993,
d. Nims et al., 1993, e. Lobo et al., 1993,
f. Constantinou et al., 1993)

model of an office building. The model reinforced concrete structure was tested under simulated earthquake loading on the shaking table at the State University of New York at Buffalo. The structure was previously designed and tested by Bracci et al. (1992a). The model structure has already been retrofitted with various supplemental damping devices such as viscoelastic dampers (Lobo et al., 1993), as well as friction dampers, viscous dampers (Reinhorn et al, 1995) and tested under various earthquake ground motions.

The principal objectives of investigating the performance of the present supplemental elastomeric spring damper system are:

(1) to determine the mechanical properties of elastomeric spring dampers and analytically model their behavior,

(2) to investigate the experimentally-observed and analytically-predicted response characteristics of the building structure with such dampers,

(3) to investigate the alternate configurations for employing the elastomeric spring dampers in the tested building structure.

To achieve these objectives, the following tasks were undertaken:

(1) Perform preliminary tests of elastomeric spring dampers supplied by Jarret Inc. prior to shaking table tests,

(2) Develop a model to simulate the hysteretic behavior of the dampers,

(3) Incorporate the damper model into the DRAIN-2DX (Prakash et al. 1992) time-history dynamic analysis computer program, and predict structural responses prior to shaking table tests,

(4) Establish the instrumentation of the dampers and the three-story model structure to be tested on the shaking table,

(5) Perform shaking table tests of the structure with dampers, on each story, on the first and second stories, on the first story only, and without dampers,

(6) Set up an analysis procedure for determining the structural response of the structure from the experimental results.

SECTION 2

PROPERTIES OF ELASTOMERIC SPRING DAMPERS

2.1 Introduction

The dampers used in this study contain a silicone-based elastomer that has the appearance of silly-putty. The consistency of this material gives both compressibility and viscous attributes. Thus dampers can be designed to give both spring and hysteretic behavior. The performance of the elastomeric spring dampers results from the interaction of the following parameters; (1) the precharge pressure of the elastomer, (2) the compressibility characteristic of the elastomer, (3) the viscosity and shear characteristics of the elastomer, (4) the design of the piston head, (5) the size and the shape of the plunger, (6) the piston rod/plunger cavity volume relationship, and (7) seal friction. These parameters can be modified to produce a wide variety of required damper performance characteristics and energy absorption capability.

Over the last three decades the type of elastomeric spring damper investigated in the present study has enjoyed much use in a wide range of industrial, defense and civilian applications. Railway engineering applications in various parts of the U.S. and Europe for this class of shock absorbing device include end-of-track buffers and part of the car-to-car coupling systems on rapid transit trains. The dampers are used in many industrial applications including steel mills, manufacturing and process treatment industries, as well as heavy duty material handling systems such as cranes. Military applications include shock absorption devices on missile and torpedo launching systems, gun recoil systems, and suspension systems for tanks. This class of shock absorber has also been applied to a wide range of civil engineering systems including the seismic protection of highway and railroad bridge systems, swing and lift bridges, sliding roof and lock gate protection systems, and offshore drilling platforms. It is thus evident that this type of damper has historically exhibited good reliability and longevity in a variety of chemically and thermally hostile environments. It is therefore

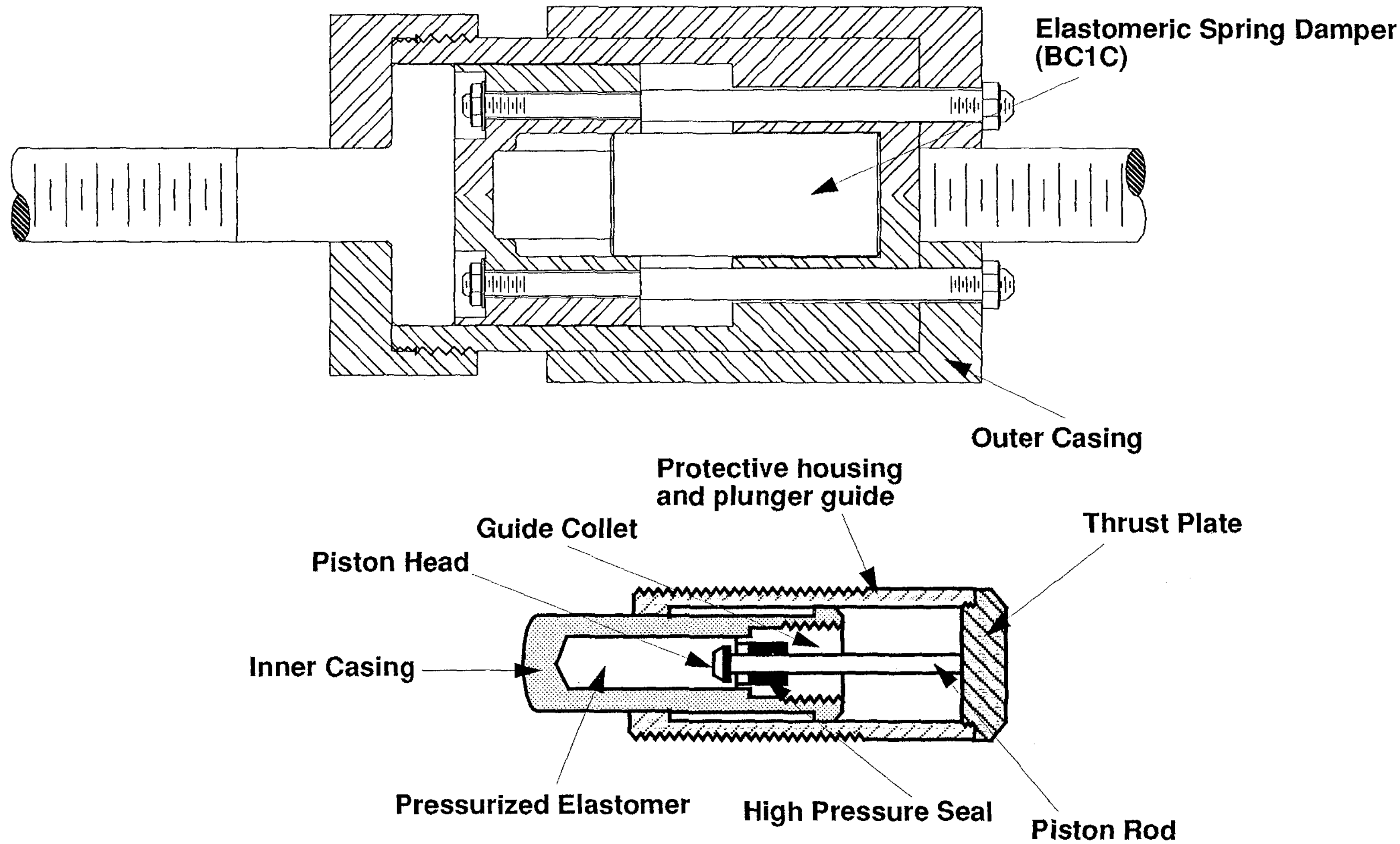

Figure 2.1 Elastomeric Spring Damper

considered, that based on this previous track record, that this class of shock absorber which utilizes the unique compressibility characteristics of silicon elastomer, is a viable candidate for the seismic protection of buildings.

Single-acting (compression only) dampers were modified to enable the application for seismic protection of building structures, by building a housing around the damper to give similar tension and compression attributes. Figure 2.1 shows the physical arrangement of the double-acting damper. The steel damper's inner cylindrical casing shown in Figure 2.1 is filled with the elastomer and pressurized to a predetermined level. When loaded, the piston head is driven into the cylinder, further compressing the elastomer. The damper thus acts as a soft spring. While the piston is being forced into the casing, some of the elastomer is free to flow around the annular space at the position head. This orificing effect provides velocity dependent resistance as well as hysteretic damping. When the piston velocity reduces to zero, the flow of the elastomer around the piston head ceases, thus allowing the pressure of elastomer to equalize on both sides of the piston. The internal spring force tends to push the piston out to its initial position. Figure 2.1 also shows a section of an outer casing which is used to convert an ordinary off-the-shelf, single-acting damper into a double-acting damper which was used in the present experimental studies.

2.2 Damper Testing

2.2.1 Model Damper - BC1C

Each damper was tested in order to investigate their force-deformation relationships prior to shaking table tests. Specimen tests consisted of applying 3-5 cycles of displacement-controlled sinusoidal motions at specific frequencies ($0.5 - 2\ Hz$) and amplitudes ($6.5 - 24\ mm$). Built-in load cells were designed and installed on the exposed rod protruding from the dampers. These were needed to accurately record the damper force history during the shaking table tests. Hence, initial specimen tests were also conducted for purposes of calibrating the load cells.

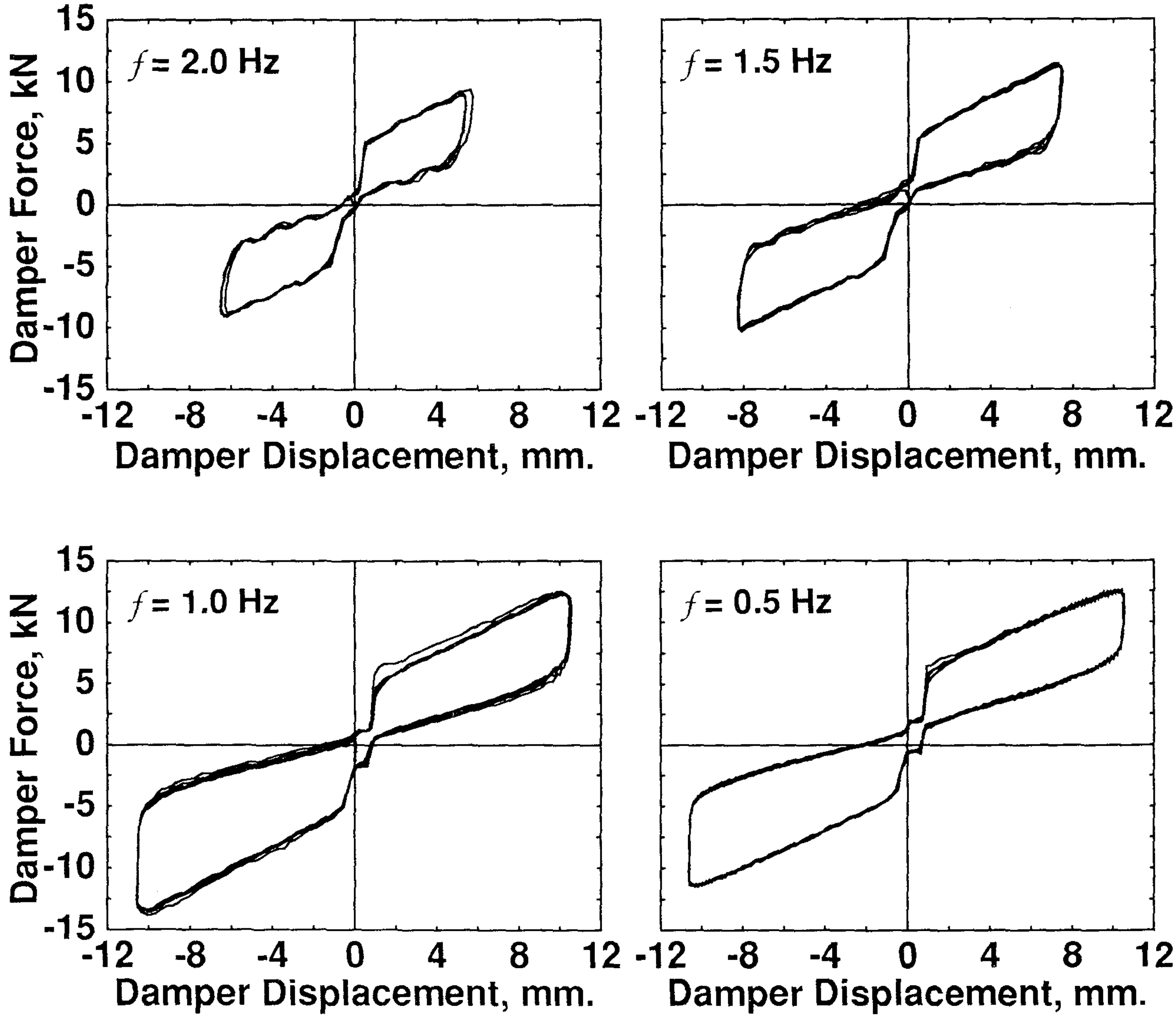

Figure 2.2 Effect of Test Frequency on the Force-Displacement Behavior of a Model BC1C Damper

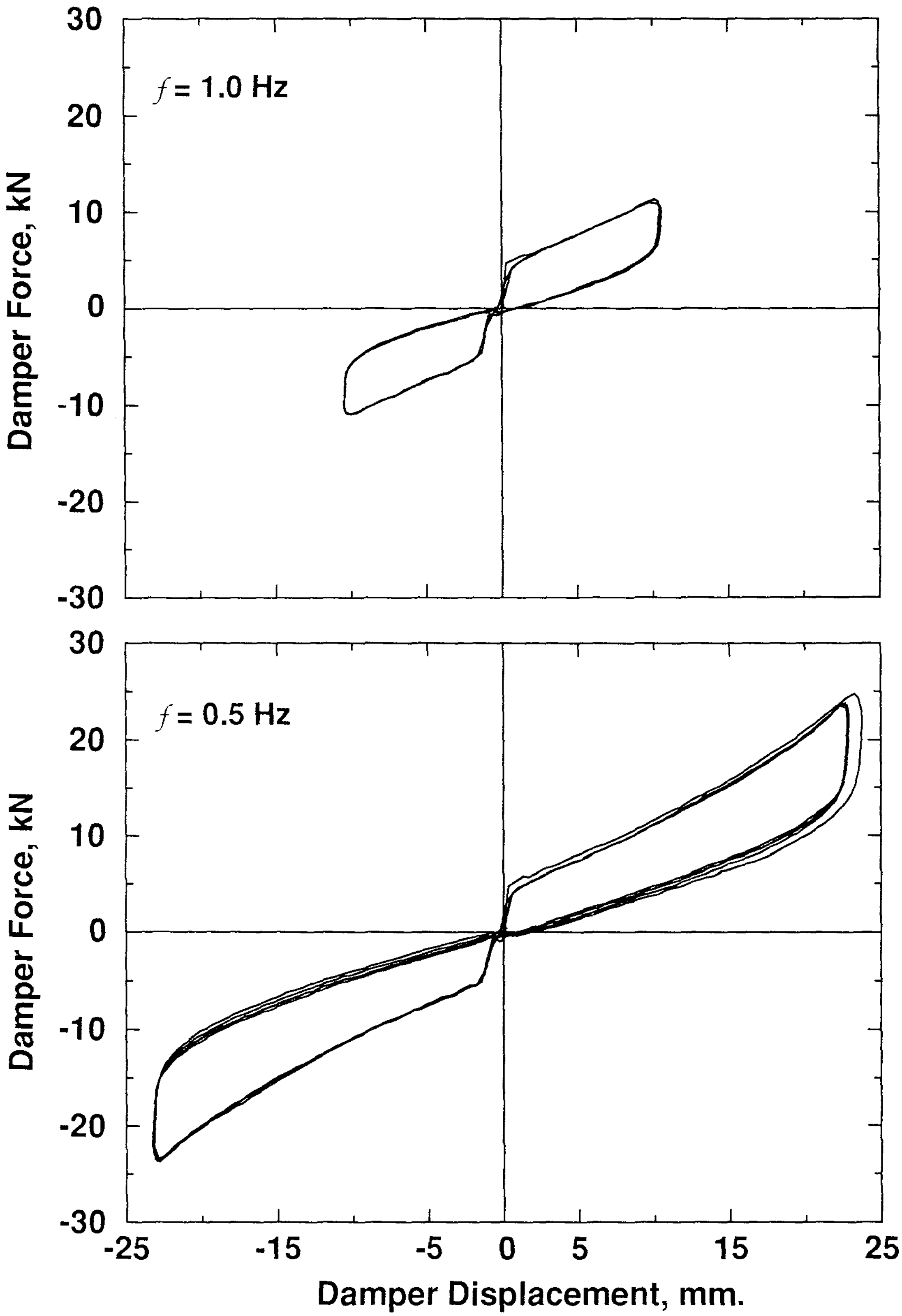

Figure 2.3 Effect of Amplitude on Response - BC1C

A total of 20 tests were performed on six damper specimens. Selected specimen test results for various amplitudes and test frequencies are plotted in Figure 2.2 and test results are summarized in Table 2.1. The table includes the maximum tension and compression side damper displacements as well as corresponding damper forces. Dissipated energy was calculated as the area of the hysteresis loops. These results show some frequency dependency with stable and repeatable hysteretic behavior. What distinguishes this particular damping system from most of those previously studied is its distinct re-centering capability. Force-deformation relationships of two tests which have approximately the same test velocities but different amplitudes are compared on Figure 2.3. The slight increase in the damper stiffness is due to the fact that elastomer pressure increases as the piston rod is forced into the plunger cavity, further tightening the seal shown in Figure 2.1.

Table 2.1: Specimen Test Results - BC1C

Specimen Test Id.	Testing Frequency, Hz	# of Cycles	Max/Min Stroke, mm	Max/Min Force, kN	Energy kN mm
S1	2	5	5.8/-6.5	9.3/-9.1	275
S2	1.5	5	7.5/-8.3	11.4/-10.3	428
S3	1	5	10.6/-10.6	12.6/-13.7	669
S4	0.5	5	10.6/-10.6	11.7/-12.4	596
S5	1	3	10.5/-10.5	10.6/-11.3	273
S6	0.5	5	10.6/-10.6	10.0/-10.9	456
S7	1	3	10.6/-10.5	11.9/-12.0	339
S8	1	3	10.6/-10.5	11.3/-10.9	318
S9	1	3	10.6/-10.5	12.6/-13.3	344
S10	1	3	10.6/-10.5	12.4/-12.8	308
S11	1	3	10.6/-10.5	10.6/-10.7	262
S12	0.5	5	23.7/-23.3	24.7/-24.2	1423
S13	0.5	5	23.6/-23.2	26.8/-27.2	1839
S14	0.5	5	23.7/-23.3	24.8/-25.3	1560
S15	0.5	4	23.7/-23.2	24.7/-23.7	1305
S16	0.5	5	23.6/-22.9	25.2/-25.5	1599
S17	0.5	5	23.6/-23.1	24.9/-25.3	1509
S18	0.5	5	23.7/-23.2	24.7/-25.2	1475
S19	0.5	5	23.7/-23.2	27.1/-24.2	1906
S20	0.5	5	23.7/-23.2	26.8/-26.5	1765

2.2.2 Prototype Damper - BC5A

Specimen tests of a BC5A type damper which essentially has the prototype damper properties for the shaking table test structure were conducted on an axial loading machine. Specimen test results of this single-acting damper are summarized on Table 2.2. Force-deformation relationships for two different test amplitudes with various testing frequencies are plotted on Figure 2.4.a and 2.4.b. As can be seen from these figures, frequency dependency is more pronounced for this damper. Normalized force-deformation relationships of a BC5A and BC1C damper are compared in Figure 2.5 for the testing frequencies of 1 *Hz* and 2 *Hz* respectively. In general, the post-yield stiffenss can be altered during design by varying the piston rod/plunger cavity volume relationship and elastomer compressibility. In this figure damper displacement is normalized with respect to damper stroke capacity. Nominal stress on elastomer was determined approximately dividing the damper force by the internal area of the plunger.

In the following paragraphs, development of an analytical model of this unique behavior is presented. An alternate analytical model for re-centering devices is described by Tsopelas and Constantinou (1994).

Table 2.2: Specimen Test Results - BC5A

Specimen Test Id.	Testing Frequency, Hz	# of Cycles	Damper Stroke, mm	Damper Force, kN	Energy kN mm
P1	0.025	2	-63.6	-129.1	7339
P2	0.01	1	-59.2	-118.3	4670
P3	0.033	2	-63.6	-125.8	6954
P4	0.1	2	-63.6	-136.1	8182
P5	0.1	2	-25.6	-76.9	2386
P6	1.0	2	-25.2	-90.7	3355
P7	0.3	2	-25.7	-80.0	2842

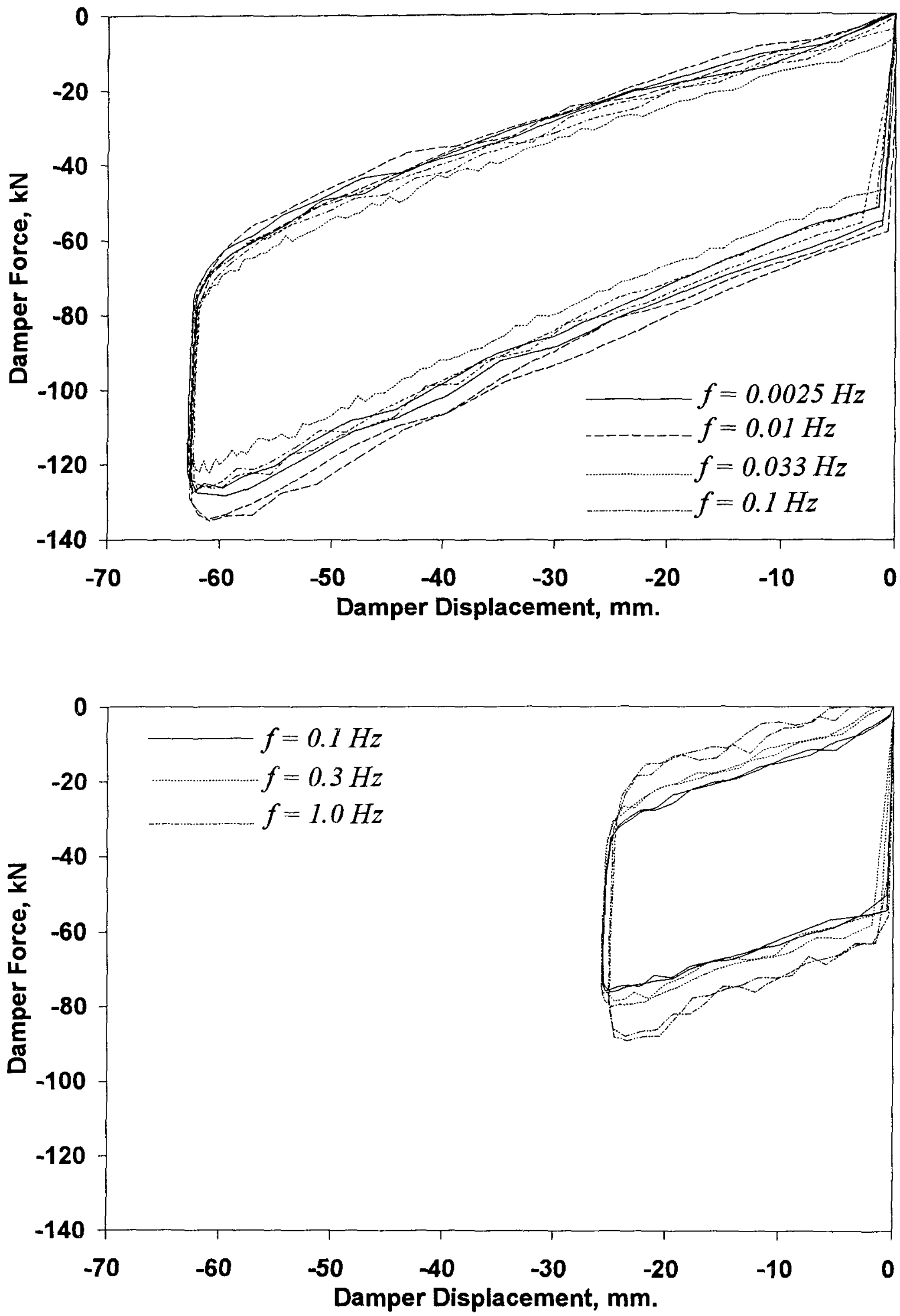

Figure 2.4 Specimen Tests Results of BC5A Prototype Damper

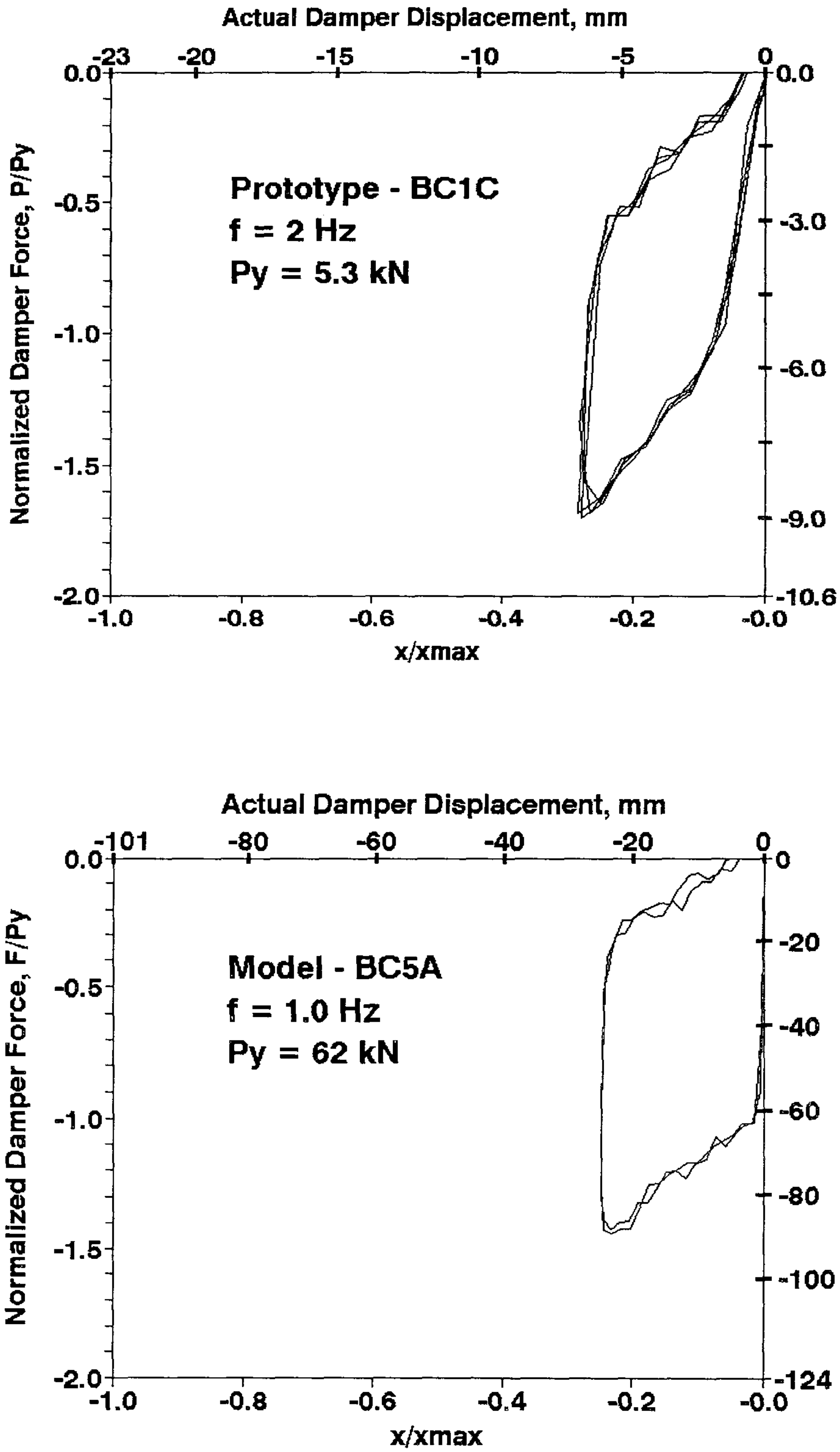

Figure 2.5 Comparison of Prototype and Model Damper Behavior

2.3 Analytical Characterization and Implementation of the Damper Behavior

In this subsection, analytical modeling of the dampers behavior based on the specimen tests is described. The model is verified using damper displacement histories recorded during the shaking table tests. Very good agreement between the experimental and analytical force-deformation relationships was observed. Implementation of this model in the well-known non-linear structural dynamic analysis program DRAIN-2DX (Prakash et al. 1992) is given next.

2.3.1 Analytical Modeling of the Dampers

It was observed from the specimen test results that the dampers exhibit a significant velocity dependency which was expected due to the nature of the elastomeric material and orificing as described above. The total damper force can be calculated as the sum of the spring force F_s and the velocity-dependent (viscous) force F_v:

$$F_D = F_s + F_v \tag{2.1}$$

The spring component has in essence a bilinear relationship and is shown in Figure 2.6. The four-parameter model proposed first by Menegotto and Pinto (1973) may be used to define this skeleton curve as follows:

$$F_S = K_2\, x + \frac{(K_1 - K_2)\, x}{\left[1 + \left|\frac{K_1 x}{P_y}\right|^R\right]^{1/R}} \tag{2.2}$$

in which x = the damper displacement or stroke, K_1 = the initial stiffness when the damper and connecting rod are fully extended, K_2 = elastomeric stiffness that is activated when the prestress has been overcome, P_y = damper static prestress force, and R = curvature shape parameter.

The viscous part of the hysteresis model [Eq. (2.1)] should reflect the self-centering characteristic of the dampers as well as the velocity dependency. Therefore, a non-linear viscous-rate dependent model was modified to include the self-centering characteristics of the damper as follows:

$$F_v = C\ sign(\dot{x})\,|\dot{x}|^{\alpha} \left|\frac{x}{x_{\max}}\right|^{\beta} \tag{2.3}$$

in which C = the damper constant, $\dot{x}$ = the damper velocity, $x_{\max}$ = the damper stroke capacity, and α , β are positive real exponents. It should be noted here that α is the velocity exponent while β is a mechanical configuration exponent. It was found that $\alpha = \beta$ for a double-acting damper modified from a single acting unit as shown in Figure 2.1, otherwise $\beta = 0$. Except for the shape factor R in Eq. (2.4), the spring force parameters can be determined graphically from the experimental damper force-deformation plots. Calibration of test results suggests that a shape factor of $R = 2$ is best to define the skeleton curve.

Thus, for the dampers used in the present investigation the proposed model takes the following form:

$$F_D = K_2\, x + \frac{(K_1 - K_2)\, x}{\sqrt{1 + \left(\dfrac{K_1 x}{P_y}\right)^2}} + C\ sign(\dot{x}) \left|\dot{x}\ \frac{x}{x_{\max}}\right|^{\alpha} \tag{2.4}$$

Having determined these static parameters (K_1, K_2, P_y), the viscous component term is determined from the experimentally observed force-deformation results. Average values of the parameters for the BC1C type damper used subsequently in this study are given in Table 2.2. Also included in the table are the corresponding values for the BC5A damper.

It should be noted here that compression and tension properties differ slightly due to the constraints imposed by the mechanical modification to achieve "similar" force-deformation behavior in two directions.

Figure 2.7 shows the effects of damper parameters (Eq. 2.4) on the shape of the hysteresis loop. One of the advantages of the model developed above is that the model parameterscorrespond to distinct physicals characteristics. It is well-known that orificing in such viscous dampers produces a velocity dependent viscous force proportional to $|\dot{x}|^{\alpha}$.

Table 2.2: Parameters for BC1C and BC5A Dampers

Damper	Loading Direc.	C (kN/mm/sec)	α	β	P_y (kN)	K_1 (kN/mm)	K_2 (kN/mm)	x_{max} (mm)
BC1C	Comp.	0.17	0.2	0.2	3.3	7	0.66	23
	Tension	0.19	0.2	0.2	2.7	5.3	0.79	23
BC5A	Comp.	1.92	0.2	0.15	26.7	62	1.14	101

A desired α coefficient can be achieved by a certain orifice configuration, depending on the type of damper performance needed (Figure 2.7.c). The size of the orifice also controls the amount of the viscous material flow which determines the level of viscous force (Figure 2.7.f). The damper static prestress force is obtained by precharging the elastomer to a certain pressure which acts to bring the device back to its original position. An optimum prestress level can therefore be readily determined for a specified maximum damper force requirement (Figure 2.7.d). β is the mechanical configuration exponent and reflects the self-centering characteristics of the damper as shown in Figure 2.7.g.

Model prediction is given in Figure 2.8 in comparison with the experimentally observed results. It should be noted here that the actual damper displacement histories obtained from the shaking table tests were used in these plots.

2.3.2 Implementation of the Model in DRAIN-2DX

The non-linear time history analysis computer program, DRAIN-2DX, for general inelastic dynamic analysis of structures subjected to earthquake loadings originally developed at University of California at Berkeley (Prakash et al. 1992), was extended to include the force-deformation behavior of the dampers described above.

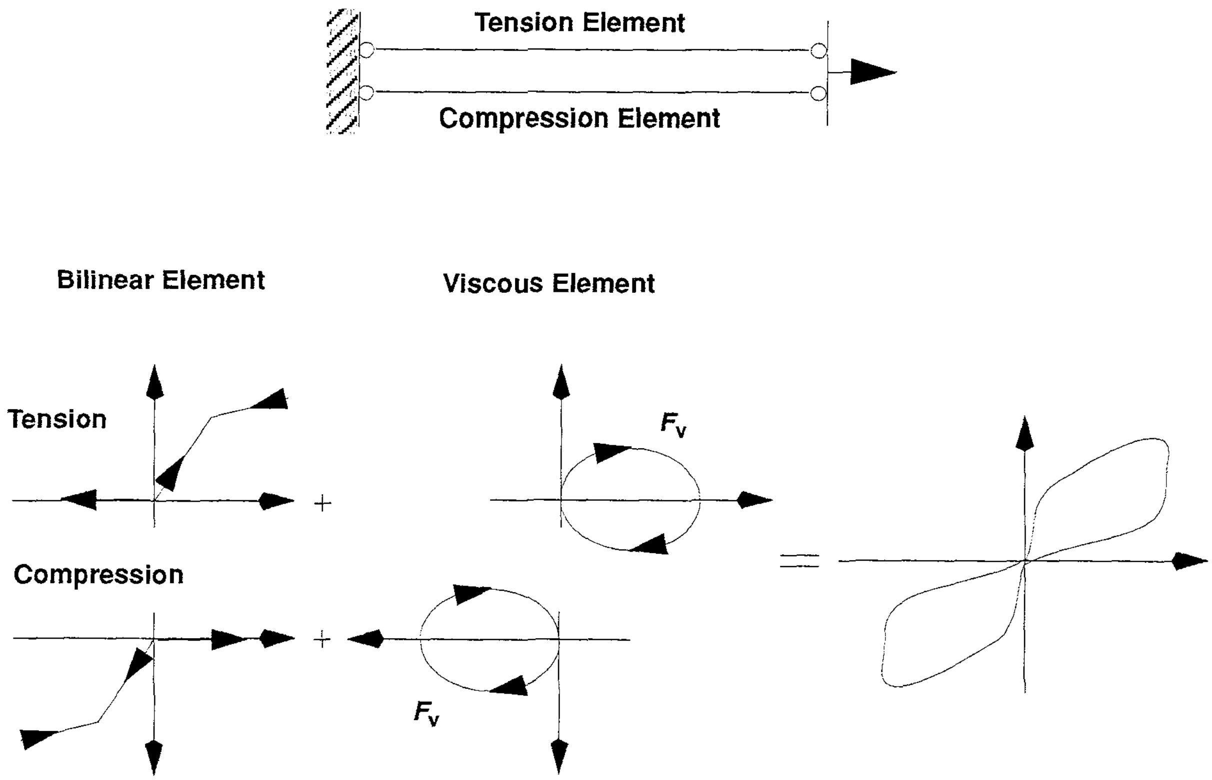

Figure 2.6 Modelling of Dampers

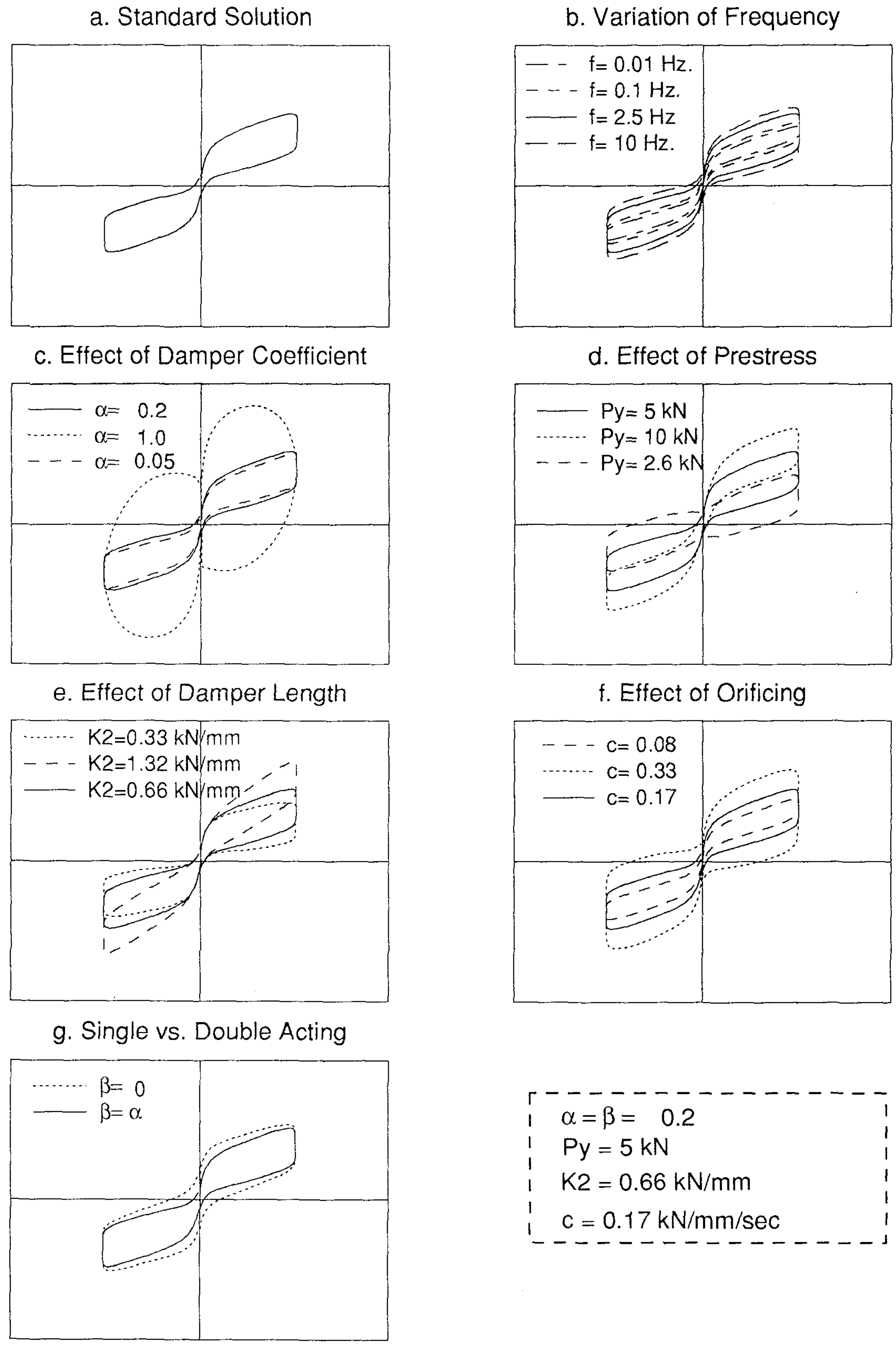

Figure 2.7 Effects of Damper Parameters

The modeling of the dampers consists of using two "damper" elements in parallel, one of which acts in tension (goes slack in compression) while the other acts in compression only (gap opens in tension). This feature enables the assignment of different tension and compression properties for a double-acting damper, as well as allowing modeling single-acting dampers for other possible cases. Hence, the double-acting elastomeric spring dampers used in this study were modeled in the modified DRAIN- 2DX program as depicted in Figure 2.6.

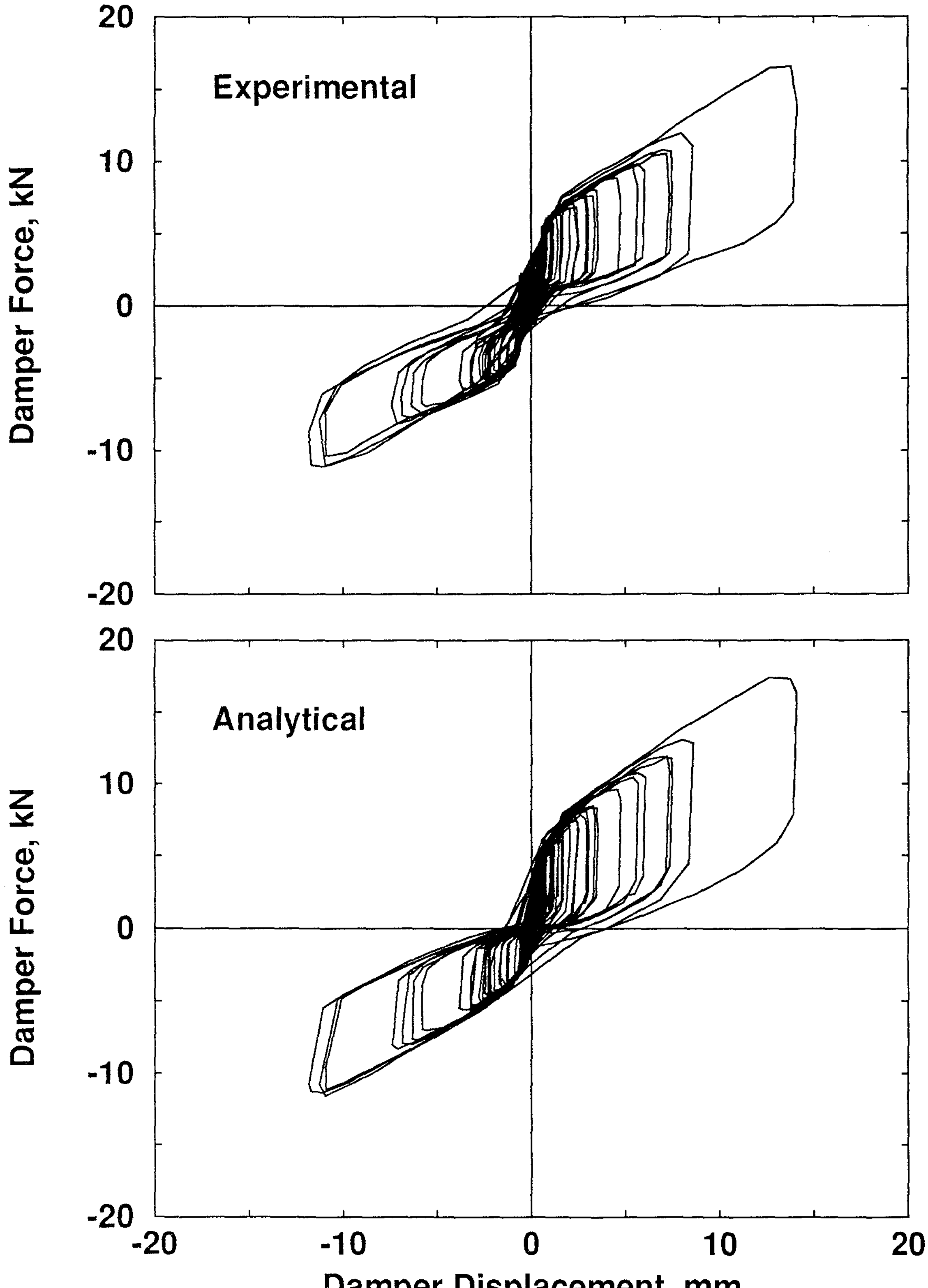

Figure 2.8.a Comparison of Experimental and Analytical Responses - El Centro 0.3g - BC1C

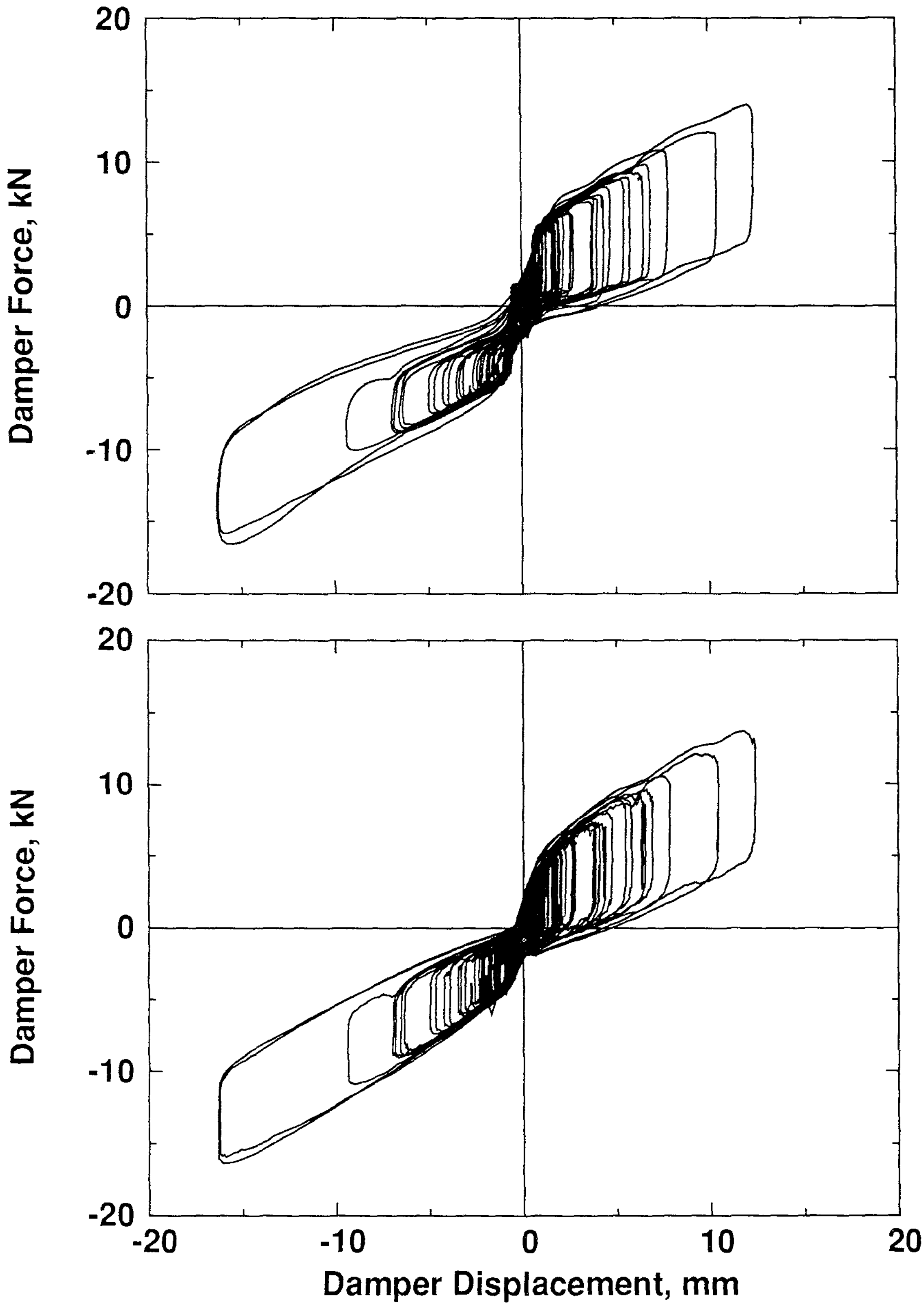

Figure 2.8.b Comparison of Experimental and Analytical Responses - Taft 0.3g - BC1C

SECTION 3

TEST STRUCTURE AND SHAKING TABLE TEST PROGRAM

3.1 Introduction

The model structure tested in this study was a 1/3-scale three-story, three bay by one-bay, lightly reinforced (non-ductile) concrete frame building representing an interior bay of a typical office building. Figure 3.1 shows the principal model dimensions. This structure was constructed and tested under various simulated base motions using the shaking table in the Seismic Laboratory at the State University of New York at Buffalo (Bracci et al. 1992a).

The concrete used in this frame had a target strength of 24 MPa, but the final strength of different components had differences due to variable casting conditions. The concrete specimen test results are summarized in Table 3.1. The slab reinforcing steel was a Gauge 12 (2.8 mm dia.) galvanized, square mesh with a wire pitch of 51 mm. The transverse reinforcing steel was Gauge 11 (3.0 mm dia.) black wire whereas the longitudinal reinforcing steel of beams and columns was annealed D4 (5.7 mm dia.) and D5 (6.4 mm dia.) rebars, respectively. Concrete blocks (8.9 kN, 6 per floor) and lead bricks (0.07 kN, 288 per floor)

Table 3.1: Concrete Properties

Pour # - Location	$f_c^{\prime}$ (MPa)	E_c (MPa)	ε_{co}	ε_{spall}
1- Lower 1st Story Columns	23	20,100	0.0020	0.011
2- Upper 1st Story Columns	30	27,000	0.0020	0.017
3- 1st Story Slab	34	27,000	0.0021	0.009
4- Lower 2nd Story Columns	30	27,000	0.0026	0.014
5- Upper 2nd Story Columns	26	23,200	0.0022	0.020
6- 2nd Story Slab	20	20,200	0.0015	0.020
7- 3rd Story Columns	23	26,200	0.0019	0.020
8- 3rd Story Slab	28	23,200	0.0021	0.012

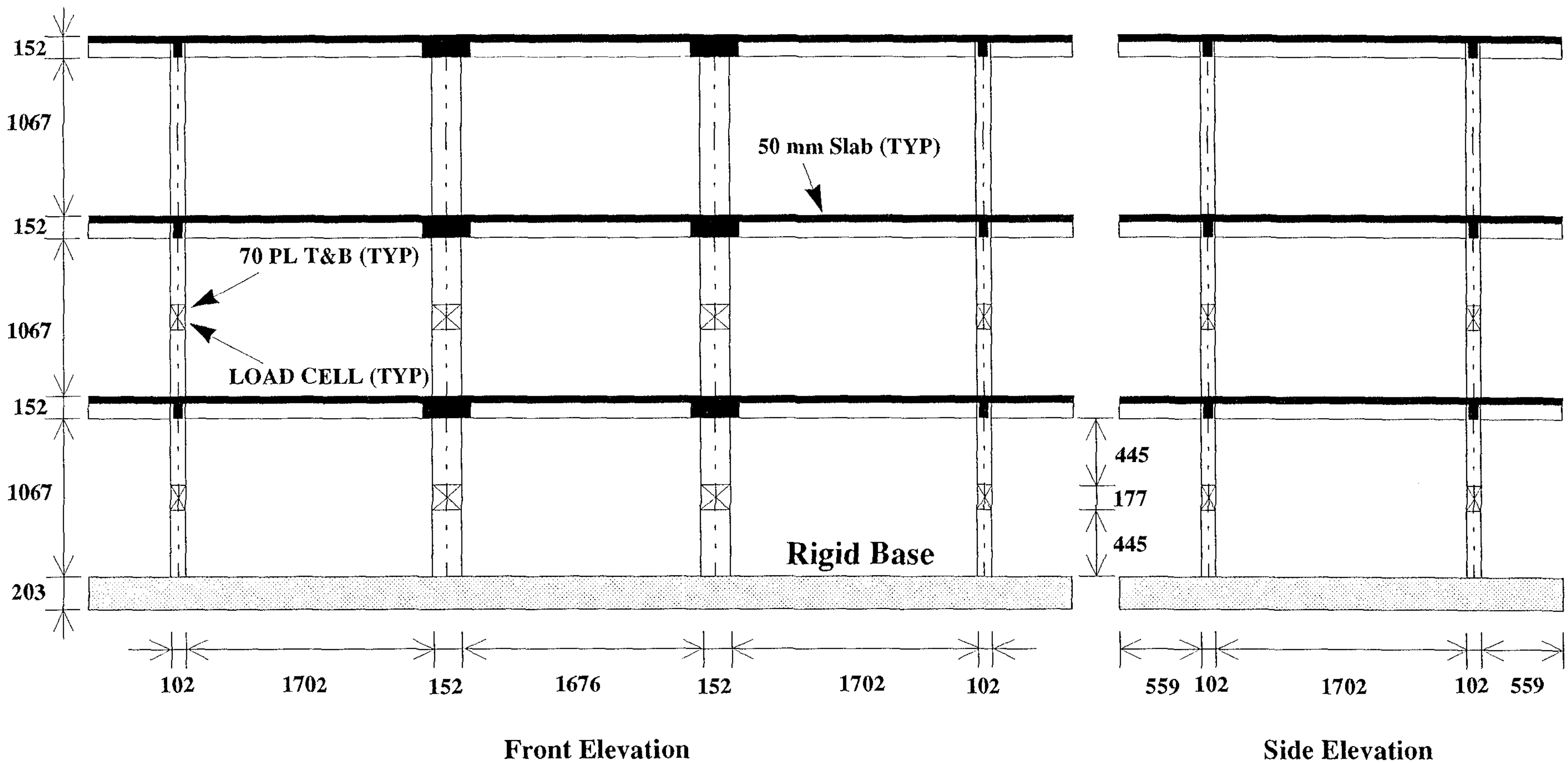

* All dimensions are in millimeters

Figure 3.1 Test Structure - Front and Side Elevations were used to comply with the mass similitude requirements of the shaking test building. Further details of the test structure can be found in Bracci et al. (1992a).

The structure was first tested under simulated base motions which had a peak acceleration of 0.3 g (Bracci et al. 1992b). Considerable non-linear behavior was observed; hence the structure was damaged such that an incipient column sidesway mechanism was apparent. Subsequently, the damaged building was retrofitted by strengthening the interior columns of the building using concrete jacketing method. Complete details of the retrofitted structure is shown in Figures 3.2 and 3.3. First, the existing columns were encased in a concrete jacket with additional longitudinal and transverse reinforcement. Then longitudinal high strength column reinforcing bars were post-tensioned. The beam-column joints were also strengthened with a reinforcing concrete fillet (Figure 3.3). Later, the retrofitted structure was again subjected to various base motions (Bracci et al. 1992c).

This damaged building provided the setting for the further studies of retrofits using various types of dampers such as viscoelastic, friction dampers and viscous wall systems. In this study, elastomeric spring dampers were installed on the diagonal bracings as shown in Figure 3.4.a and in the photograph of Figure 3.4.b.

3.2 Shaking Table Test Setup and Instrumentation

A total of 88 data channels were used to monitor the model structure response. A complete list of these channels and corresponding descriptions are given in Table 3.2. After the test structure was fixed to the shaking table platform, a set of transducers and accelerometers were installed as shown in Figure 3.5.

Linear sonic transducers were used to measure the absolute response displacements in the longitudinal (N-S) direction of the base and each story level of the model during the shaking table tests. The displacement transducers had a global displacement range of ± 25 mm, ± 20 mm and ± 15 mm, respectively and were conditioned by a generic power supply and manufacturer amplifier-decoders. The same type of transducers were also installed on the dampers as shown in Figure 3.4.b, in order to record the damper displacement history during the shaking table tests along with the built-in axial load cells.

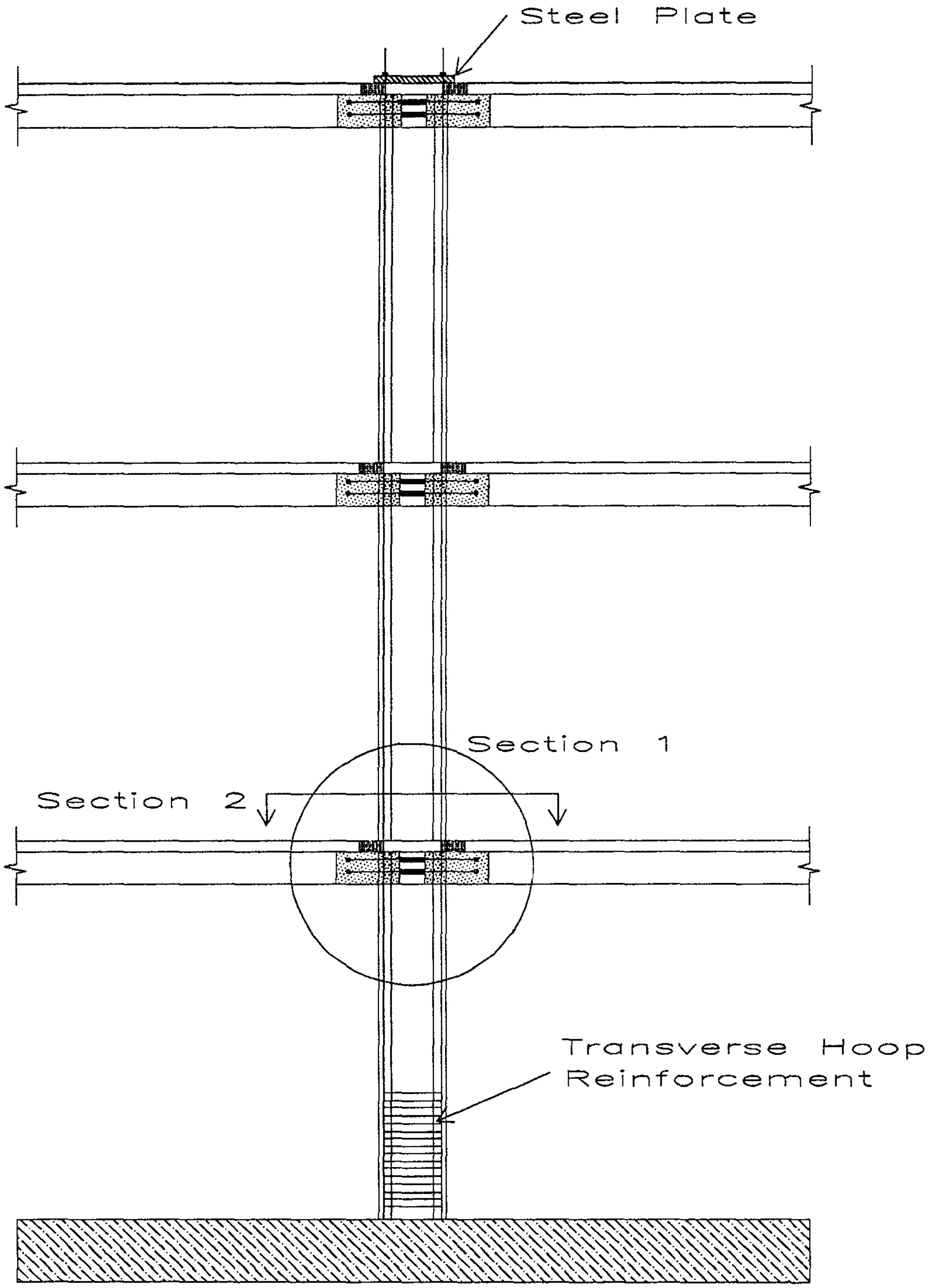

Figure 3.2 Retrofitted Columns

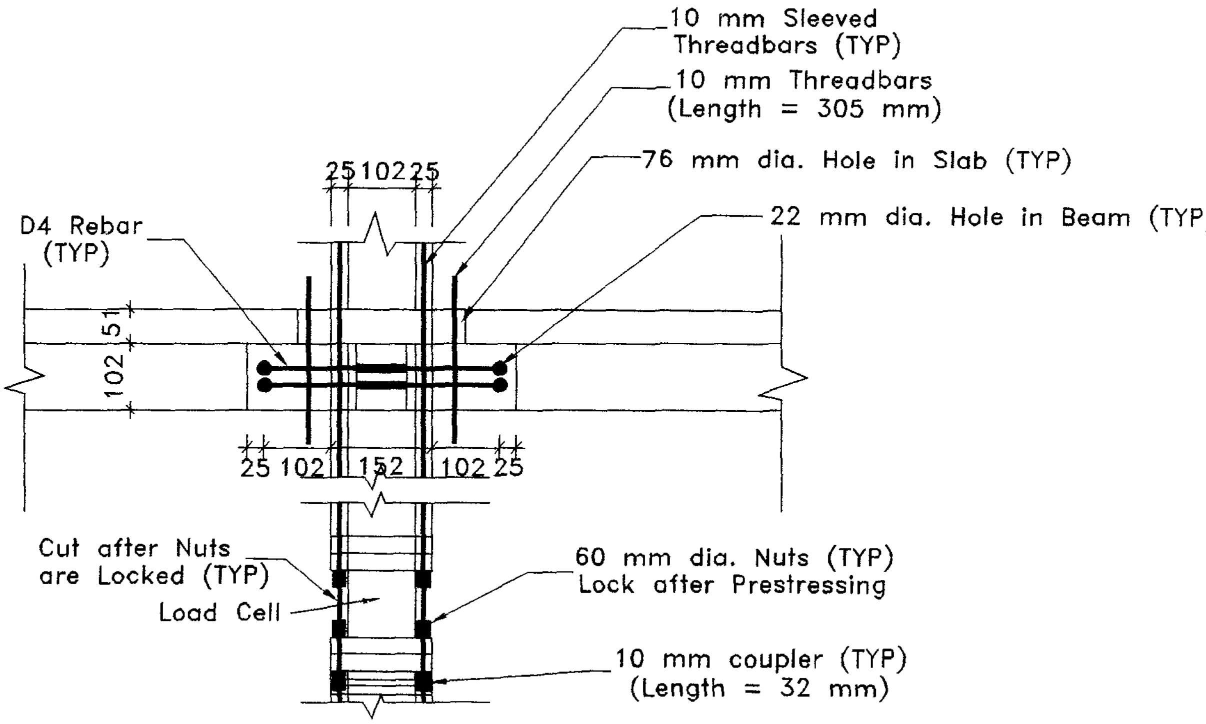

Section 1

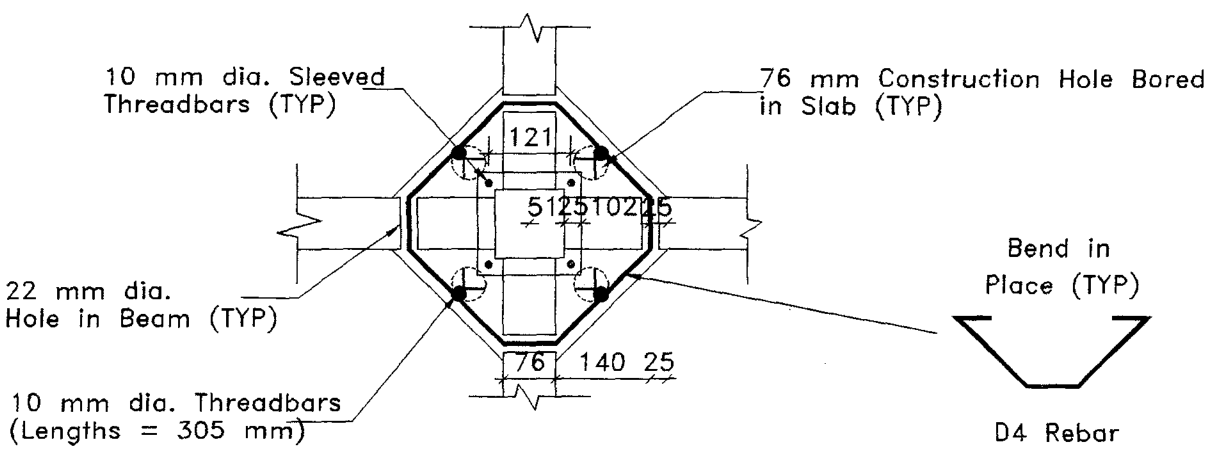

Section 2

Figure 3.3 Details of Column Retrofit

Table 3.2: Description of Monitored Channels

Channel Name	Full Scale	Units	Channel Description
AH# (1-8)	10.2	G's	Horizontal acceleration at the floor levels - two on each level
AV# (1-8)	4.1	G's	Vertical acceleration at the floor levels - two on each level
AT# (1-8)	4.1	G's	Transverse acceleration at the floor levels - two on each level
D# (1-8)	260	mm	Horizontal displacement of the floor levels - two on each level
N# (1-8)	182.2	kN	Column axial force - first and second stories only
MX# (1-8)	666.4	kN m	Column x-axis (NS) moment - first and second stories only
MY# (1-8)	666.4	kN m	Column y-axis (EW) moment - first and second stories only
SX# (1-8)	22.8	kN	Column x-axis shear force - first and second stories only
SY# (1-8)	22.8	kN	Column y-axis shear force - first and second stories only
DDE# (1-3)	52	mm	East side dampers' displacement
DDW# (1-3)	52	mm	West side dampers' displacement
FDE# (1-3)	91.1	kN	East side dampers' force
FDW# (1-3)	91.1	kN	West side dampers' force
DLAT	156	mm	Shaking table horizontal displacement
ALAT	2.0	G's	Shaking table horizontal acceleration
DVRT	126	mm	Shaking table vertical displacement
AVRT	4.1	G's	Shaking table vertical acceleration

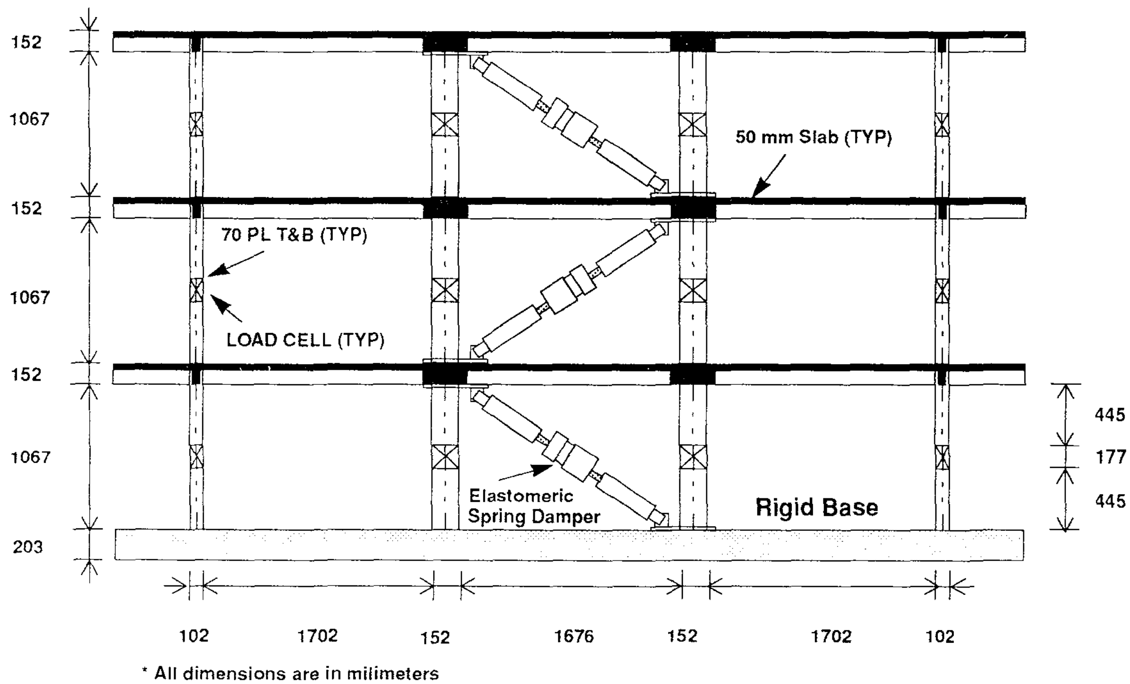

(a) Test Structure

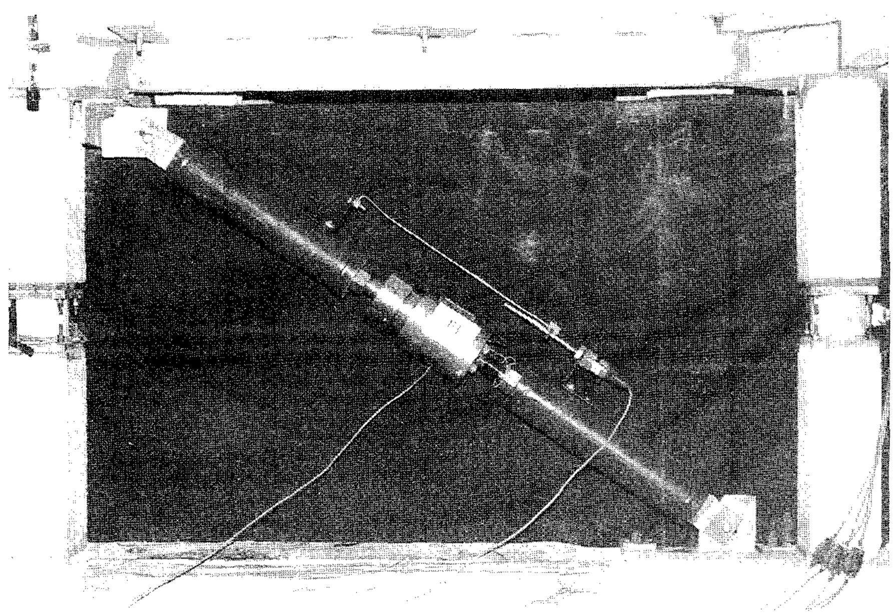

(b) Elastomeric Spring Damper in Place

Figure 3.4 Test Structure with Elastomeric Spring Dampers

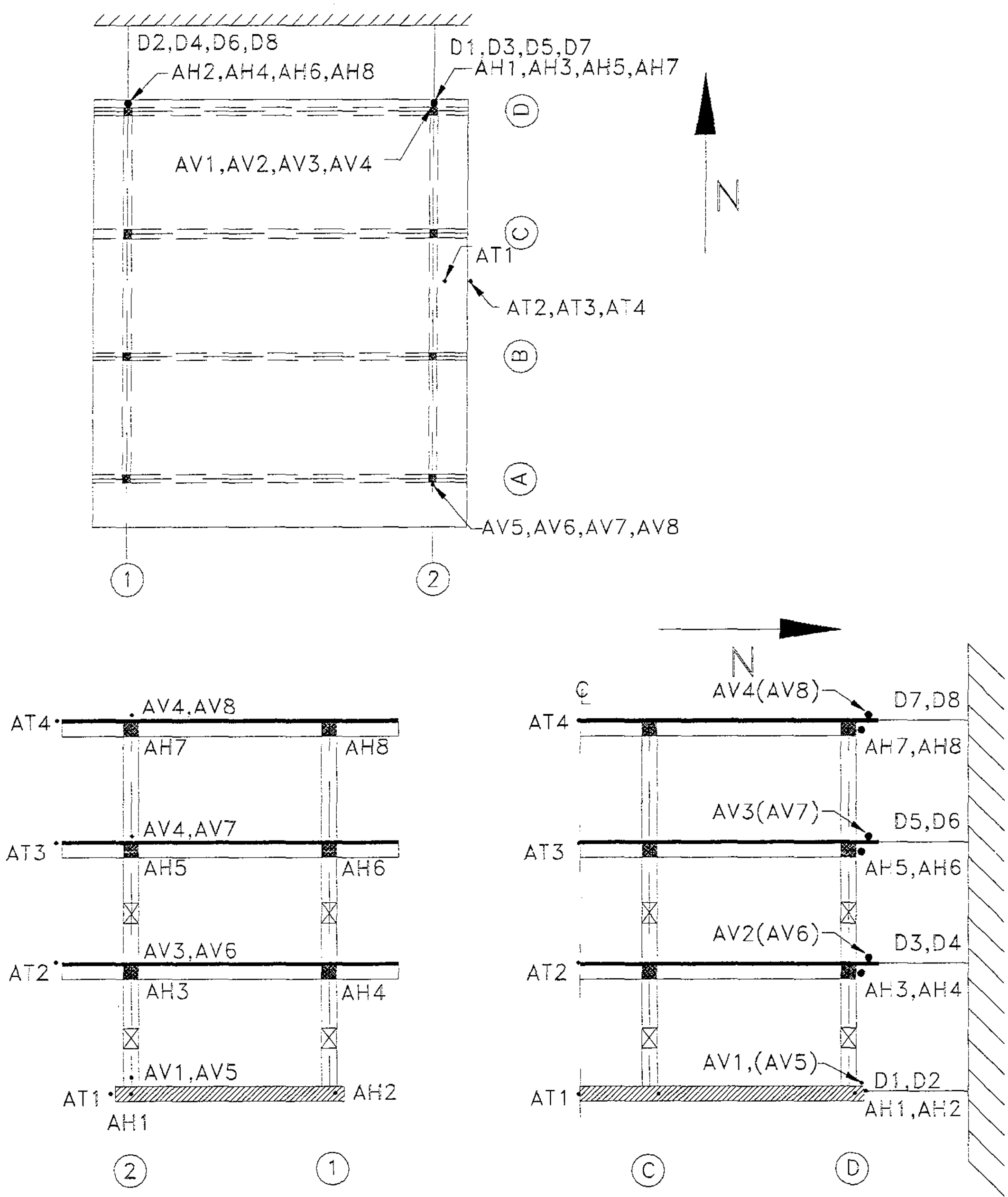

Figure 3.5 Instrumentation of the Test Structure

Resistive accelerometers were used to measure the story level accelerations. They were positioned as shown in Figure 3.5, to record the accelerations in the direction of the motion (AH#), transverse to the motion (AT#) and vertical motion (AV#). The longitudinal accelerometers were placed on both east and west sides of the structure to detect any torsional response. The accelerometers were conditioned with 2310 Vishay Signal Conditioners, which filtered the frequencies above 25 Hz. during the tests. Accelerometers were calibrated for an acceleration range of $\pm 2\ g$ per 10 $volts$.

Special load cells to measure the internal force response of the model, which included axial load, shear forces and bending moments were installed at the mid-height of first and second story columns. A more detailed description of the load cells can be found in Bracci et al. (1992a).

3.3 Test Program

Prior to installation of the elastomeric spring dampers one quick release test was conducted to generate free vibrations on the structure by pulling the structure from the roof level. Hence, the initial dynamic characteristics were identified from Fourier Transforms of the story level acceleration time histories. In order to make a "before and after" damper installation comparison, two simulated minor ground motion tests followed this identification test, namely Elcentro 0.3 g and Taft 0.2 g. After the dampers were mounted on all three levels, one more quick release test was conducted to investigate the preliminary effect of the dampers on the structural dynamic properties.

In this experimental study, seventeen shaking table tests were conducted using four different ground motions, namely Taft 1952 N21E, El Centro 1940 NS, Pacoima Dam 1971 S16E, and Hachinohe1968 NS at various peak ground acceleration (PGA) levels (0.2 g to 0.4 g). Ground motions were time scaled (by a factor of $1/\sqrt{3}$) in order to meet the similitude requirements. Sample acceleration-time histories for these ground motions are given in Figure 3.6.

Three different damper configurations were tested removing one set of dampers each time from one story level to study the effects of damper configuration on the seismic response. Preliminary analyses showed that the bare structure could withstand Taft and El Centro ground motions at 0.2 g and 0.3 g PGAs, respectively, without a catastrophic structural failure. Hence, these ground motions formed the basis for a comparison of seismic responses with different damper configurations.

A wide banded (0 to 50 Hz) white noise base excitation applied by the shaking table, was used for determining the dynamic characteristics of the model after each simulated earthquake test. The peak acceleration was scaled to 0.05 g to provide enough excitation such that the modes of vibration could be identified. A complete list of the ground motions used in the study and test program is given in Table 3.3.

Table 3.3: Test Log of Model Structure with Elastomeric Spring Dampers

Test Id.	Test Date	Table Motion	Nominal PGA (g)
QUIKREL	6.13.1994	Quick Release (13.3 kN at roof level)	-
DBFWH05	"	White Noise	0.05
DBFEC30	"	El Centro NS (86%) - Imperial Valley, May 18 1940	0.30
EBFWH05	"	White Noise	0.05
EBFTA20	"	Taft N21E (128%) - Kern County, July 21 1952	0.20
FBFWH05	"	White Noise	0.05
JQCKREL[1]	6.16.1994	Quick Release (13.3 kN at roof level)	-
AWN005B	6.17.1994	White Noise	0.05
ATA020	"	Taft N21E (128%)	0.20
AWN005A	"	White Noise	0.05
BEL030	"	El Centro NS (86%)	0.30
BWN005A	"	White Noise	0.05
CTA030	6.20.1994	Taft N21E (192%)	0.30
CWN005A	"	White Noise	0.05
DPA020	"	Pacoima Dam S16E (17%) - San Fernando, February 9 1971	0.20
DWN005A	"	White Noise	0.05
EPA040	"	Pacoima Dam S16E (34%)	0.40
EWN005A	"	White Noise	0.05
FTA040	"	Taft N21E (256%)	0.40

Table 3.3: Cont'd

Test Id.	Test Date	Table Motion	Nominal PGA (g)
FWN005A	"	White Noise	0.05
GEL040	6.23.1994	El Centro NS (114%)	0.40
GWN005A	"	White Noise	0.05
HHA020	"	Hachinohe NS (87%) - Tokachi, May 16 1968	0.20
HWN005A	"	White Noise	0.05
IHA030	"	Hachinohe (131%)	0.30
IWN005A	"	White Noise	0.05
JWN005B[2]	"	White Noise	0.05
JTA005	"	Taft N21E (32%)	0.05
JWN005A	6.23.1994	White Noise	0.05
KTA020	"	Taft N21E (128%)	0.20
KWN005A	"	White Noise	0.05
LEL030	"	El Centro NS (86%)	0.30
LWN005A	"	White Noise	0.05
MWN005B[3]	6.24.1994	White Noise	0.05
MTA005	"	Taft N21E (32%)	0.05
MWN005A	"	White Noise	0.05
NTA020	"	Taft N21E (128%)	0.20
NWN005A	"	White Noise	0.05
OEL030	"	El Centro NS (86%)	0.30
OWN005A	"	White Noise	0.05
PWN005B[4]	"	White Noise	0.05
PTA005	"	Taft N21E (32%)	0.05
PWN005A	"	White Noise	0.05
QTA020	"	Taft N21E (128%)	0.20
QWN005A	"	White Noise	0.05
REL030	"	El Centro NS (86%)	0.30
RWN005A	"	White Noise	0.05

[1] Dampers on all levels installed
[2] Dampers removed from third story level
[3] Dampers removed from second story level
[4] Dampers removed from first story level: bare frame

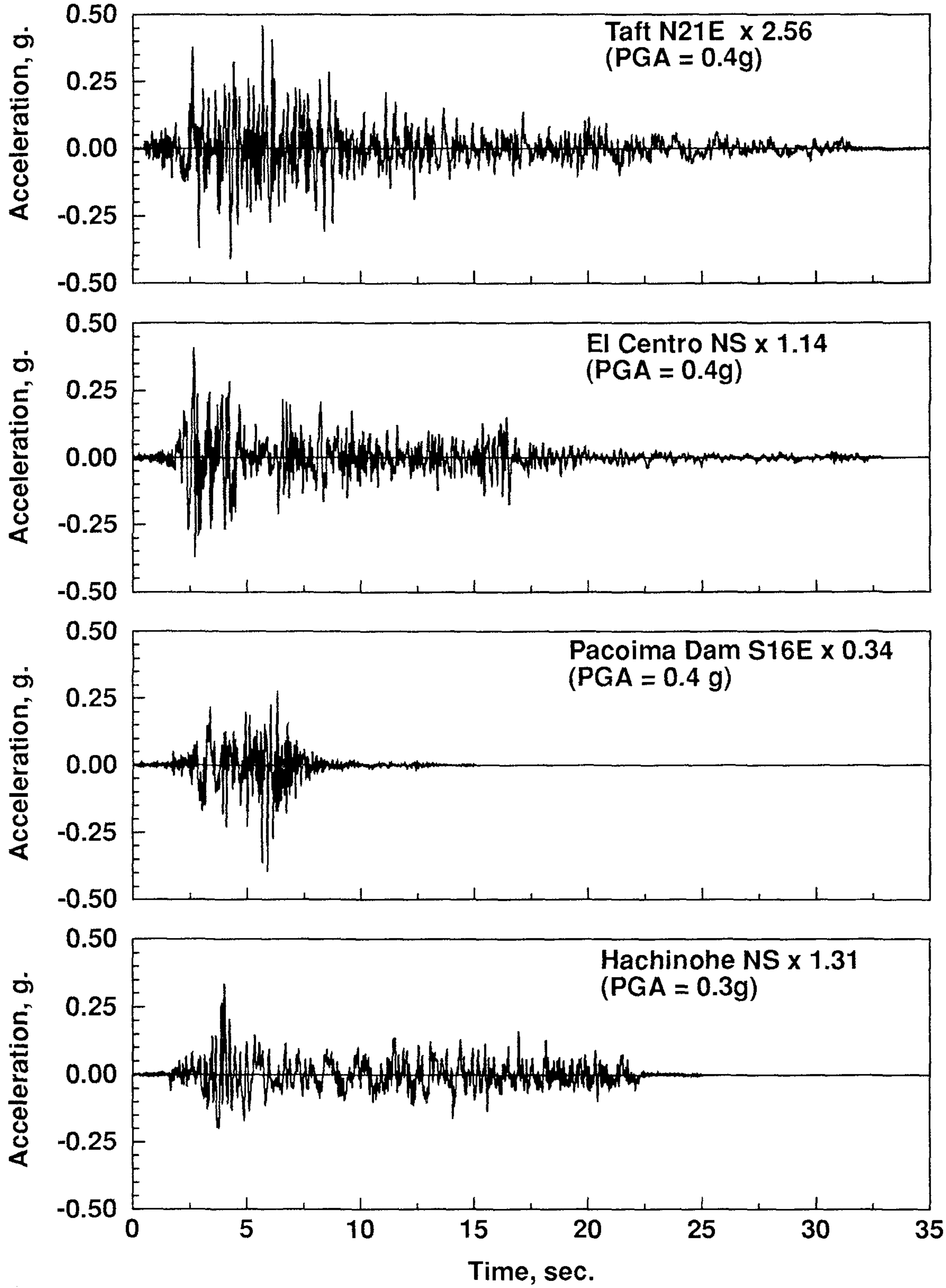

Figure 3.6 Sample Scaled Acceleration Records

SECTION 4

SHAKING TABLE TEST RESULTS

4.1 Introduction

In this section experimental results are presented along with the analytical predictions obtained from the enhanced DRAIN-2DX computational model described in Section 2. These results are further discussed in Section 5. Effects of supplemental damping on the structural response are identified from the shaking table tests in terms of the following response types: story displacement, story shear/base shear and energy dissipation. Experimental results are given in the following paragraphs and are summarized in tables. Story displacement time histories, interstory displacement-story shear, damper force-displacement relationships and energy time histories are plotted for the test cases; (a) without dampers, (b) dampers on all stories, (c) dampers on first two stories, and (d) dampers on the first story only. Energy time histories are plotted in terms of input energy, kinetic energy and energy dissipated by the dampers. It was assumed that the rest of the energy input was dissipated by hysteretic and/or other means of energy dissipation inherent to the model test structure as given in the following equation (Uang 1990):

$$E_I = E_K + E_S + E_H + E_\xi + E_D \tag{4-1}$$

in which, E_K = the kinetic energy, E_S = the strain energy stored, E_H = the hysteretic energy dissipated by the inelastic action of the structural members, and E_ξ = the viscous damped energy, and E_D = the energy dissipated by the dampers. The latter is defined as the sum of the areas within the force-deformation loops of each damper.

In presenting the shaking table test results, major emphases are placed on the overall response of the test structure subjected to simulated ground motions as well as the corresponding response of the dampers themselves. As with most of the supplemental damping systems, stiffening of the structure due to installation of the damping devices is also a major concern, since increase in stiffness leads to an increase in the seismic energy input. This input energy must be dissipated by the damping devices and/or inelastic action of the structural members. While the damping devices might perform merely as energy dissipators or drift limiters for virgin structures (none or a few yielded structural elements), self-centering characteristics (if any) of such devices would be more beneficial in retrofit applications of already damaged structures. Hence, from this point of view, the advantage of using self-centering elastomeric spring dampers will be noted in the forthcoming sections.

4.2 Preliminary Tests on the Undamped Structure

4.2.1 Initial Dynamic Properties of the Test Structure

One quick release test (QUIKREL) was conducted to identify the natural frequencies and the first mode equivalent viscous damping characteristics of the model structure. The pull force at the time of release was 13.3 kN. Fourier transforms of the free vibration-story level acceleration records were used to determine the natural frequencies. Half Power (Band-Width) Method (Clough and Penzien, 1993) was applied as the kth mode damping ratio was determined from the frequencies for which the response at the kth natural frequency is reduced by $1/\sqrt{2}$. Hence, the natural frequencies of the structure were 1.50, 5.96 and 11.80 Hz for the three modes of the undamped structure. Corresponding first mode equivalent viscous damping ratios were 8.0, 3.5 and 4.5%. Story level accelerations and corresponding Fourier transforms are shown in Figure 4.1.

Following the quick release test, the model structure was subjected to a white noise shaking table excitation with a peak table acceleration of $0.05\,g$ (DBFWH05) in order to characterize the dynamic structural properties more thoroughly. Story level transfer functions were again used to determine the dynamic properties, namely, natural frequencies, mode shapes, stiffness matrices and equivalent viscous damping ratios. Hence, the natural frequencies were 1.42, 5.59 and 11.89 Hz with the equivalent viscous damping ratios of 8.9,

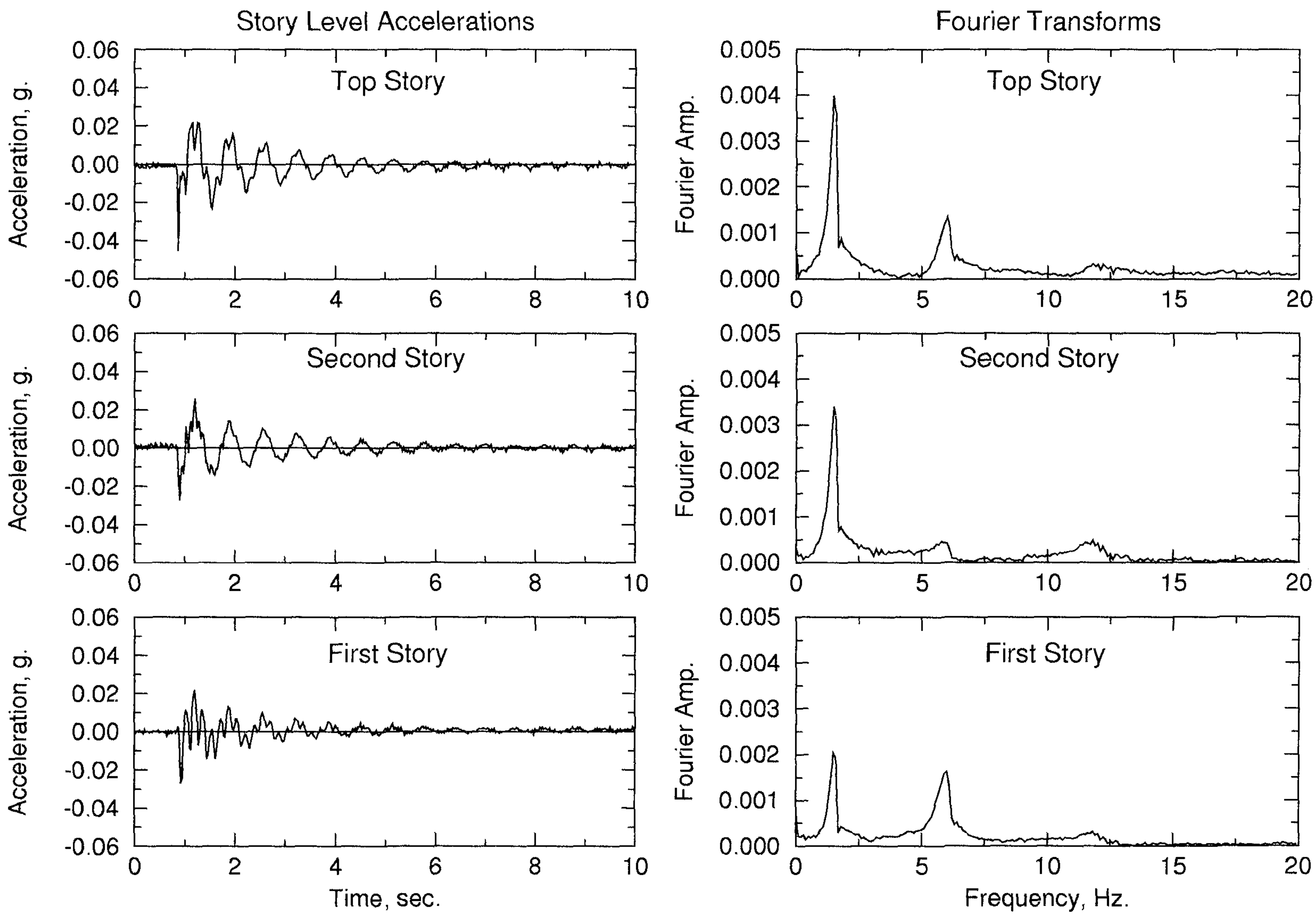

Figure 4.1 Quick Release Test Results (QUIKREL)

5.4, 1.9%, respectively, for the three modes of vibration. Selected story level transfer functions are plotted on Figure 4.4.

This test together with the quick release test also served to assess the level of damage imposed on the structure by the previous shaking table tests as noted in Section 3. These experimental results were used to calibrate the analytical model accordingly. Preliminary analyses therefore showed that the model structure could withstand El Centro and Taft ground motions at PGA levels of 0.3 and 0.2 g without collapse. These ground motions were also used to generate the benchmarks for response comparisons of different damper configurations.

4.2.2 Simulated Ground Motion Test Results

The test structure was subjected to two simulated ground motions, namely Taft 0.2 g and El Centro 0.3 g, before the dampers were installed (Table 3.3). White noise tests were conducted after each ground motion test to identify the changes in the dynamic properties of the structure. Table 4.1 summarizes the maximum response of the structure to these ground motions in terms of base and story level acceleration, velocity, interstory displacement (normalized with respect to story height), story shear (normalized with respect to story weight) and column axial force. Experimentally obtained story displacement time histories, story shear vs interstory displacement and energy time histories are plotted on Figures 4.2 and 4.3.

The measured maximum base acceleration was 0.29 g where the observed maximum interstory drift was 2.4% for the El Centro 0.3 g (DBFEL30) test. Corresponding values for the Taft 0.2 g test (EBFTA20) were 0.21 g and 1.5%. The maximum story velocities occurring in the third story level were 321 and 303 mm/sec for the DBFEL30 and EBFTA20 tests, respectively. Normalized story shears were 17.6, 18.3% for the first story and 12.9, 2.1% of the story weight for the second story, respectively. As it was expected, interior column axial forces were higher than those of exterior columns for the undamped structure due to stiffer interior columns.

Table 4.1: Summary of Maximum Response - Bare Frame

STORY/ TEST ID[3]	PEAK ACCELERATION g.				VELOCITY mm/sec			Interstory Displ. / Story Height[1]			Story Shear / Story Weight[2]		Column Axial Force kN			
													Exterior		Interior	
	BASE	1st	2nd	3rd	1st	2nd	3rd	1st	2nd	3rd	1st	2nd	1st	2nd	1st	2nd
BEFORE DAMPER INSTALLATION																
DBFEL30	0.293	0.285	0.186	0.268	223	289	321	0.024	0.011	0.005	0.176	0.129	7.8	6.5	12.4	9.8
EBFTA20	0.210	0.231	0.196	0.259	129	209	303	0.015	0.009	0.005	0.183	0.021	9.0	6.6	11.1	9.0
AFTER DAMPER REMOVAL																
PTA005	0.063	0.064	0.053	0.075	43	51	77	0.004	0.002	0.002	0.049	0.036	2.3	2.2	2.8	2.4
QTA020	0.205	0.313	0.145	0.260	157	203	239	0.019	0.008	0.004	0.144	0.101	8.9	6.2	8.7	7.7
REL030	0.287	0.315	0.196	0.300	237	298	343	0.027	0.012	0.006	0.174	0.077	8.5	7.2	13.3	10.9

[1] 1.22 m
[2] 360 kN
[3] See Table 3.3

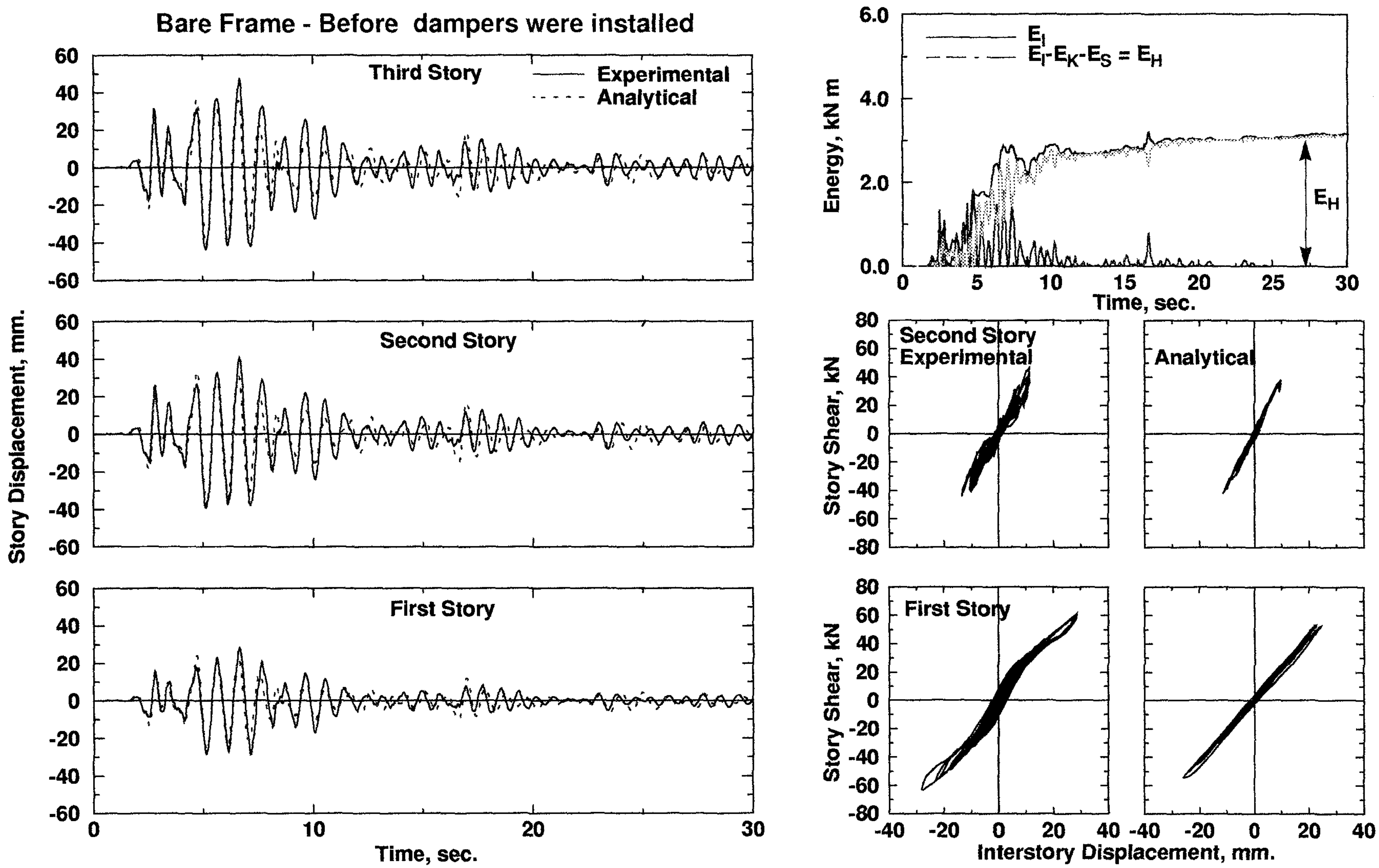

Figure 4.2 Experimental Results - EL CENTRO 0.3g (DBFEL30)

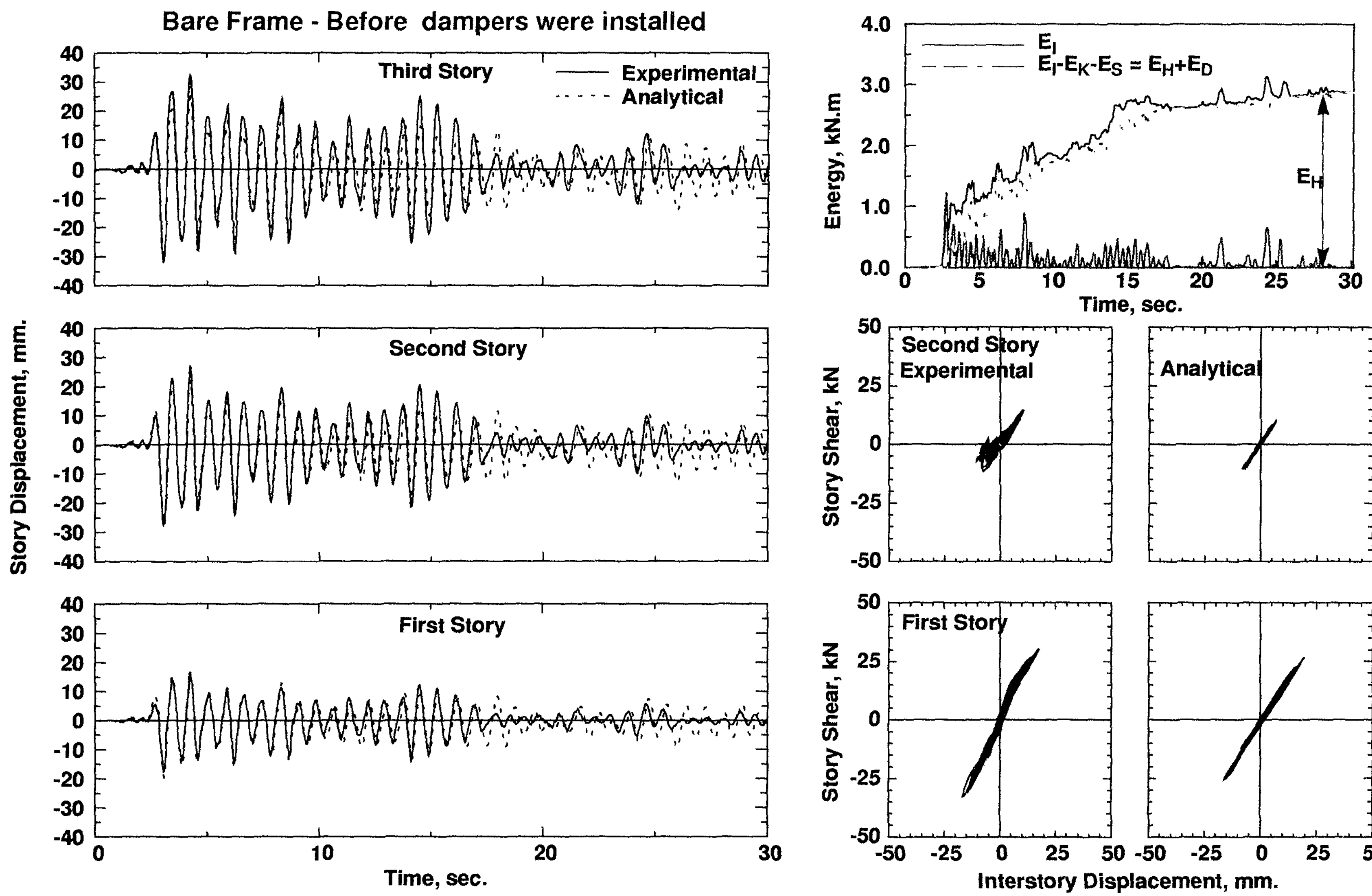

Figure 4.3 Experimental Results - TAFT 0.2g (EBFTA020)

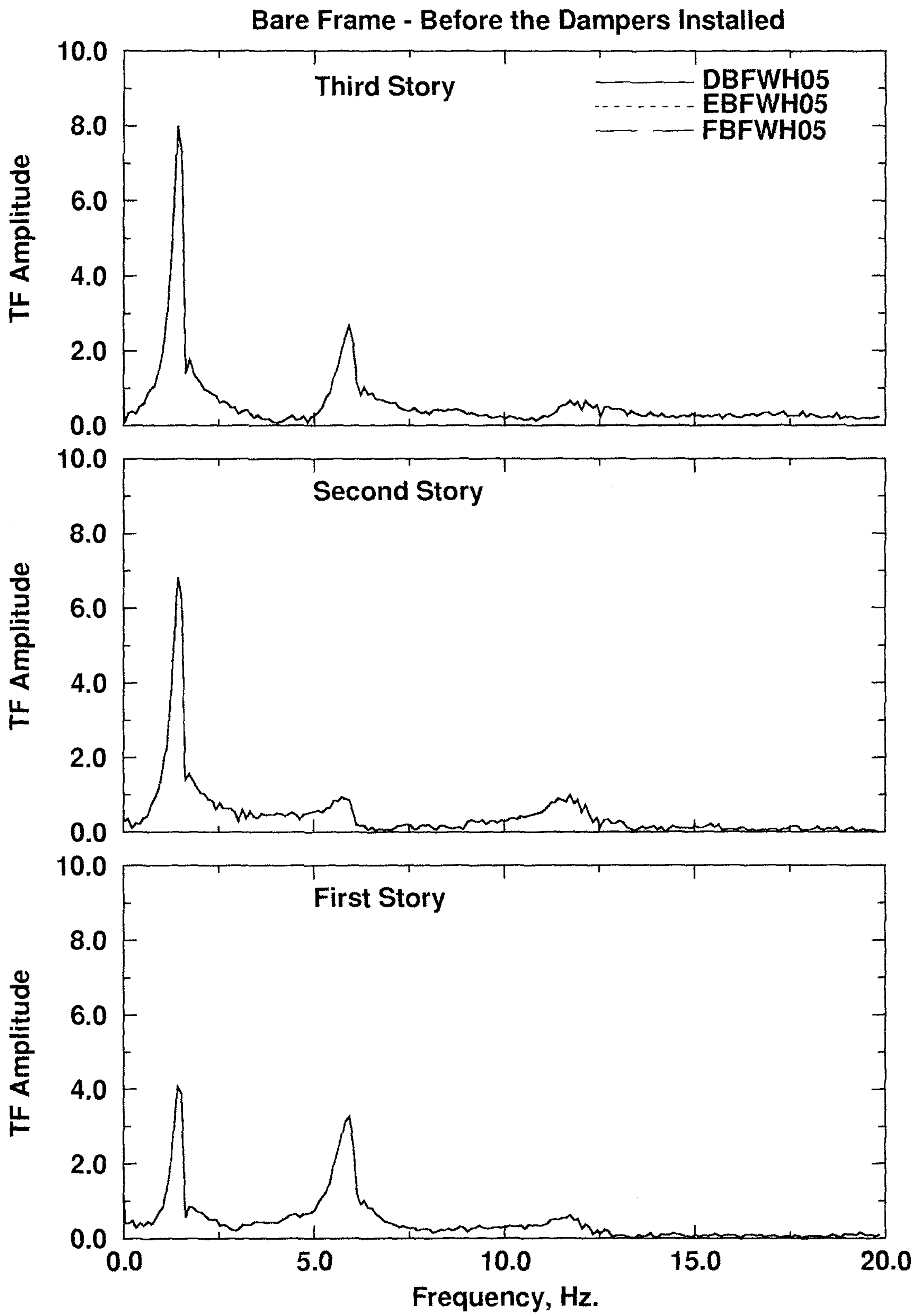

Figure 4.4 Story Transfer Functions
Bare Frame - Before the Dampers Installed

Natural frequencies of the undamped test structure for the 3 modes determined from the white noise tests conducted after each ground motion test were 1.42, 5.59, and 11.89 Hz. Corresponding equivalent viscous damping ratios were found to be 8.9, 5.4, and 1.9%. These were the same for both tests, namely, EBFWH05 and FBFWH05, whose story level transfer functions are plotted on Figure 4.4.

4.3 Tests on the Structure with Dampers on All Stories

4.3.1 Initial Dynamic Properties of the Test Structure

After the dampers were installed on all stories, one quick release test (JQCKREL) was conducted. Maximum pulling force at the time of release was 13.3 kN. Fourier transforms of the free vibration-story level acceleration records were used to determine the first mode of natural frequency and corresponding equivalent viscous damping ratio. Higher mode frequencies could not be identified due to the fact that the test structure was highly damped. Hence, the higher modes could not be excited. Therefore, the first mode natural frequency and equivalent viscous damping ratio were 2.25 Hz and 40%, respectively. Story level accelerations and corresponding Fourier transforms are plotted on Figure 4.5.

One white noise test was conducted prior to ground motion tests in order to identify the dynamic properties of the test structure accurately. Hence, the natural frequencies were 2.76, 11.18, 15.97 Hz, respectively, for the three modes of vibration. Corresponding equivalent viscous damping ratios were found to be 23.0, 18.0 and 4.3%. Story level transfer functions are shown on Figure 4.24.

4.3.2 Simulated Ground Motion Test Results

The test structure was subjected to four different simulated ground motions at various peak ground accelerations (a total of nine tests; see Table 3.3) after the dampers were installed in the bracings at each level. For each ground motion, the maximum PGA

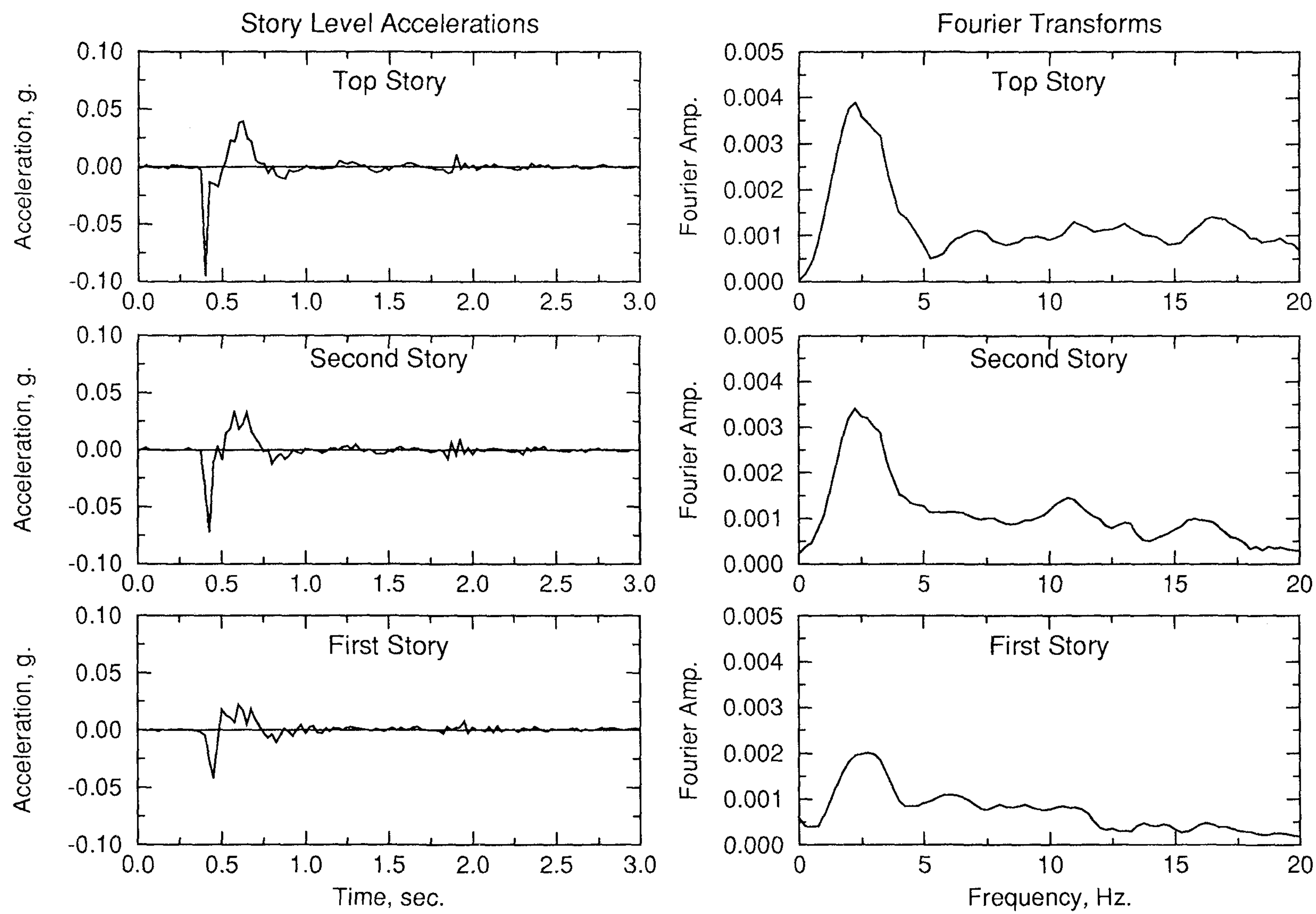

Figure 4.5 Quick Release Test Results (JQCKREL) - Dampers on All Stories

Table 4.2: Summary of Maximum Response - Dampers on All Stories

STORY/ TEST ID[3]	PEAK ACCELERATION g.				VELOCITY mm/sec			Interstory Displ. / Story Height[1]			Story Shear / Story Weight[2]		Column Axial Force kN			
													Exterior		Interior	
	BASE	1st	2nd	3rd	1st	2nd	3rd	1st	2nd	3rd	1st	2nd	1st	2nd	1st	2nd
ATA020	0.225	0.153	0.168	0.237	124	170	189	0.007	0.006	0.003	0.093	0.090	17.7	12.9	7.0	5.1
BEL030	0.316	0.222	0.231	0.281	170	274	319	0.017	0.008	0.003	0.141	0.093	20.5	15.9	9.6	7.7
CTA030	0.330	0.259	0.225	0.326	210	271	340	0.018	0.009	0.004	0.119	0.109	21.8	16.7	9.5	8.1
DPA020	0.195	0.147	0.159	0.195	188	175	200	0.011	0.006	0.02	0.105	0.063	15.1	12.3	6.3	4.6
EPA040	0.395	0.304	0.338	0.385	273	370	415	0.028	0.013	0.006	0.191	0.150	27.0	17.4	14.9	11.4
FTA040	0.459	0.313	0.324	0.415	287	374	444	0.028	0.012	0.005	0.188	0.149	29.8	18.2	12.8	11.4
GEL040	0.409	0.241	0.246	0.289	201	315	373	0.022	0.010	0.004	0.148	0.114	22.5	15.6	11.7	8.5
HHA020	0.205	0.213	0.205	0.281	191	258	302	0.016	0.017	0.004	0.127	0.098	21.7	15.7	8.2	8.2
IHA030	0.335	0.362	0.322	0.415	268	380	427	0.025	0.011	0.006	0.170	0.154	28.1	18.1	11.3	12.0

[1] 1.22 m
[2] 360 kN
[3] See Table 3.3

level that the structure could withstand without collapse was predetermined based on the analytical model introduced in Section 2 and further described in Section 5. According to this analytical study, it was concluded that the ground accelerations higher than 0.4 g for the ground motions Taft N21E, El Centro 1940 NS, Pacoima Dam S16E and higher than 0.3 g for Hachinohe NS, would likely cause a catastrophic failure of the structure. Therefore, using these ground motions, PGA levels were so chosen that one moderate and one severe ground motion test could be conducted for each.

Table 4.2 summarizes the maximum response of the structure to these ground motions in terms of base and story level acceleration, velocity, interstory displacement (normalized with respect to story height), story shear (normalized with respect to story weight) and column axial force. Experimentally obtained story displacement time histories, story shear vs interstory displacement, damper force-displacement and energy time histories are plotted on Figures 4.6 to 4.23.

Natural frequencies of the structure were determined from white noise test results conducted after each test. Selected story level transfer functions are plotted on Figure 4.24. According to these results, frequencies and corresponding equivalent viscous damping ratios did not change, i.e. they were 1.42, 5.59, and 11.89 Hz, with equivalent viscous damping ratios 8.9, 5.4, and 1.9%.

4.3.2.1 Test Results - Taft N21E

Three tests were conducted using Taft N21E at nominal 0.2 g, 0.3 g and 0.4 g PGAs (ATA020, CTA030, FTA040). However, measured base accelerations were 0.23 g, 0.33 g and 0.46 g, respectively. Results are shown in Figures 4.6 and 4.7, 4.10 and 4.11, and 4.16 and 4.17. The maximum recorded interstory drifts were 0.8, 1.8 and 2.8% covering the range of minor-moderate to severe ground motion for the test structure. A similar trend can be observed in comparing the third story velocities which were 189, 340 and 444 mm/sec, respectively. Normalized second story shears were 9.3, 10.9 and 14.9%

where that of the first story were 14.1, 11.9 and 18.8% of the story weight. It should be noted here that although the story level accelerations were almost doubled, increase in the story shears were compansated by the dampers. Maximum column axial forces were recorded during the Taft 0.4 g test, as 29.8 kN and 12.8 kN for the first floor exterior and interior columns, respectively.

Finally, total seismic input energy increased from 3.3 kNm to 10.1 kNm for Taft 0.2 g and Taft 0.4 g tests, respectively. 87% of the input energy was dissipated by the dampers during Taft 0.2 g test, where this ratio dropped down to 73% for Taft 0.3 g and to 71% for Taft 0.4 g tests.

4.3.2.2 Test Results - El Centro NS

The test structure was subjected to El Centro ground motion at nominal 0.3 g and 0.4 g PGAs. The measured maximum base acceleration was 0.32 g where the observed maximum interstory drift was 1.5% for the El Centro 0.3 g (BEL030) test. Corresponding values for El Centro 0.4 g (GEL040) test were 0.41 g and 2.2%. The maximum story velocity occurring in the third story was 319 and 373 mm/sec for the BEL030 and GEL040 tests, respectively. Normalized story shears were 14.1, 14.8% for the first story and 9.3, 11.4% for the second story, respectively. The maximum column axial forces measured during the GEL040 test were 22.5 kN and 11.7 kN in the first floor exterior and interior columns, respectively. Results are shown in Figures 4.8, 4.9, 4.18 and 4.19.

Total seismic input energy increased from 5.0 kN m to 7.4 kN m for El Centro 0.3 g and El Centro 0.4 g tests, respectively. Some 75% of the input energy was dissipated by the dampers during the El Centro 0.3 g test; this ratio is similar to the 74% observerd for El Centro 0.4 g test.

4.3.2.3 Test Results - Pacoima Dam S16E

Two tests were conducted using Pacoima S16E at nominal 0.2 g and 0.4 g PGAs (DPA020, FPA040). The characteristics of this ground motion that distinguish it from the other ground motions are its short duration and its impulse nature. The measured base accelerations were 0.20 g and 0.40 g, respectively. The maximum recorded interstory drifts were 1.1 and 2.8% covering the range of moderate to severe ground motion for the test structure. Similar observation can be made in comparing the third story velocities which were 200 and 415 mm/sec, respectively. Normalized second story shears were 6.3 and 15.0% where that of the first story were 10.5 and 19.1% of the story weight. Results are shown in Figures 4.12, 4.13, 4.14 and 4.15.

Finally, total seismic input energy increased from 1.1 kNm to 6.4 kNm for Pacoima 0.2 g and Pacoima 0.4 g tests, respectively. Some 73% of the input energy was dissipated by the dampers during the Pacoima 0.2 g test; this ratio dropped down to to 60% for the Pacoima 0.4 g test - the difference is presumably due to hysteretic energy absorption (inelastic action) by the structural elements.

4.3.2.4 Test Results - Hachinohe NS

The test structure was subjected to Hachinohe ground motion at nominal 0.2 g and 0.3 g PGAs. The measured maximum base acceleration was 0.21 g where the observed maximum interstory drift was 1.6% for the Hachinohe 0.2 g (HHA020) test. Corresponding values for the Hachinohe 0.3 g (IHA030) test were 0.34 g and 2.5%. The maximum story velocity occurring in the third story was 302 and 427 mm/sec for HHA020 and IHA030 tests, respectively. Normalized story shears were 12.7, 17.0% for the first story and 9.8, 15.4% of the story weight for the second story, respectively. The maximum column axial forces measured during IHA020 test were 28.1 kN and 11.3 kN in the first floor exterior and interior columns, respectively. Reults are shown in Figures

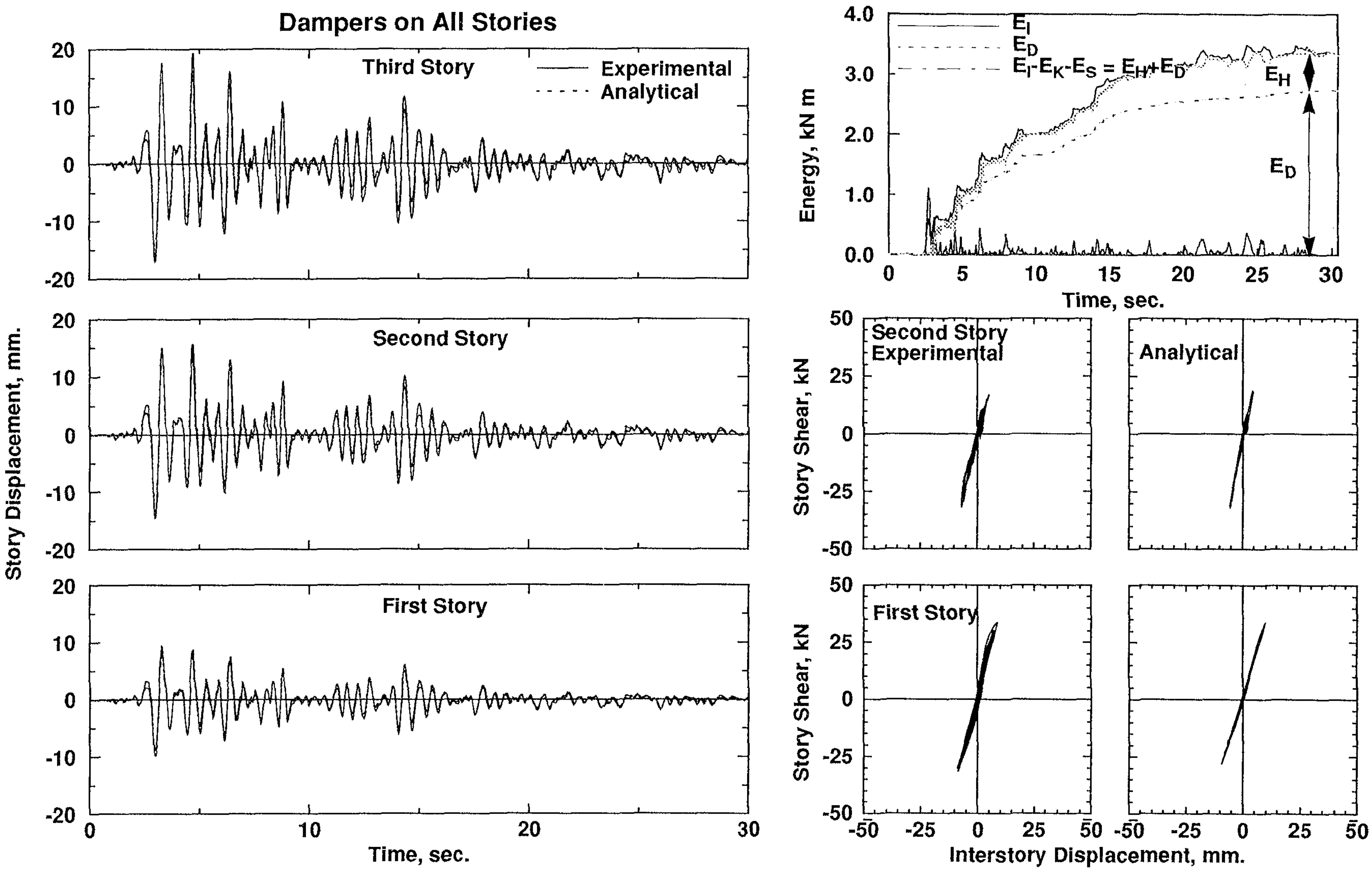

Figure 4.6 Experimental Results - TAFT 0.2g (ATA020)

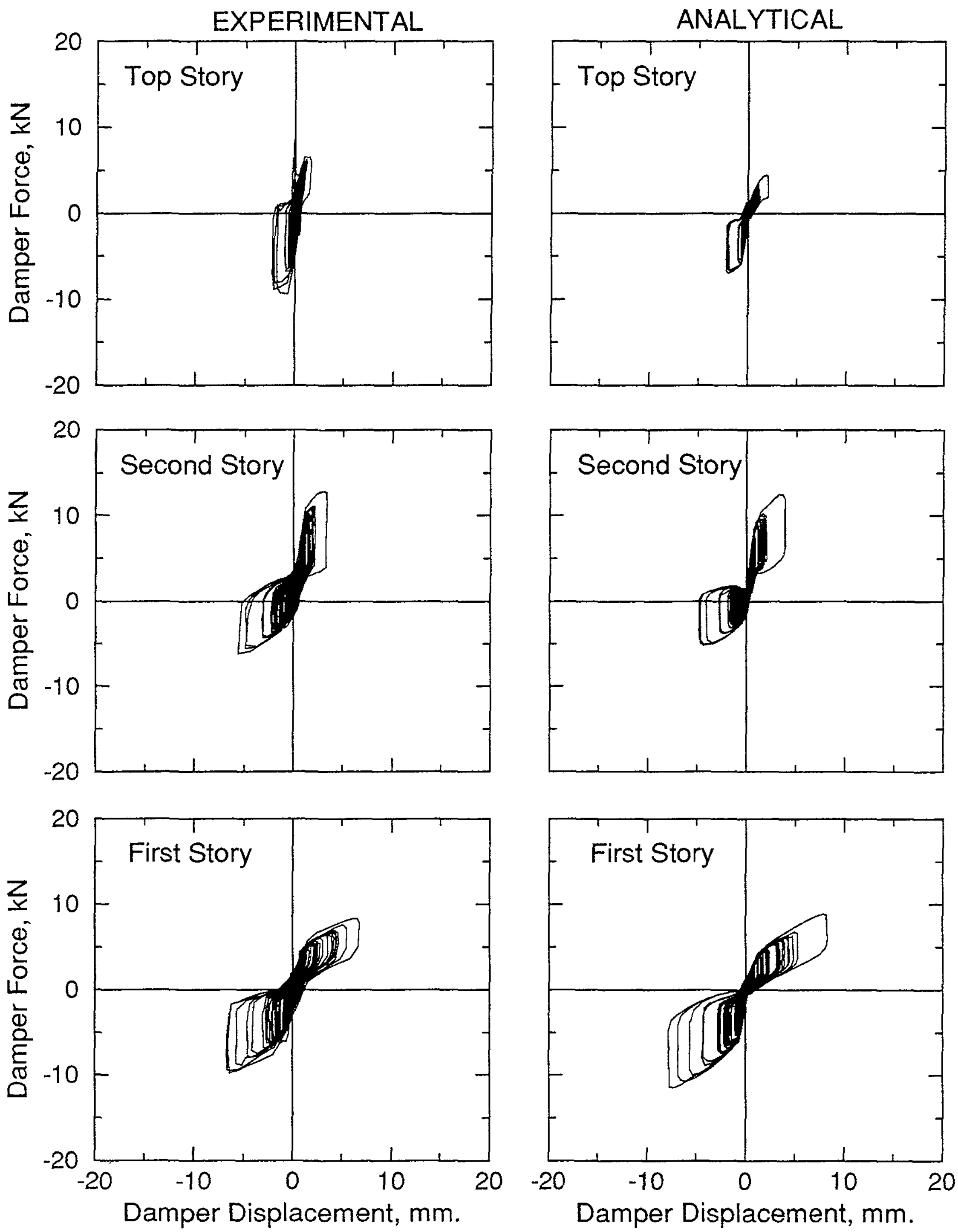

Figure 4.7 Damper Force-Deformation Behavior - TAFT 0.2g (ATA020)

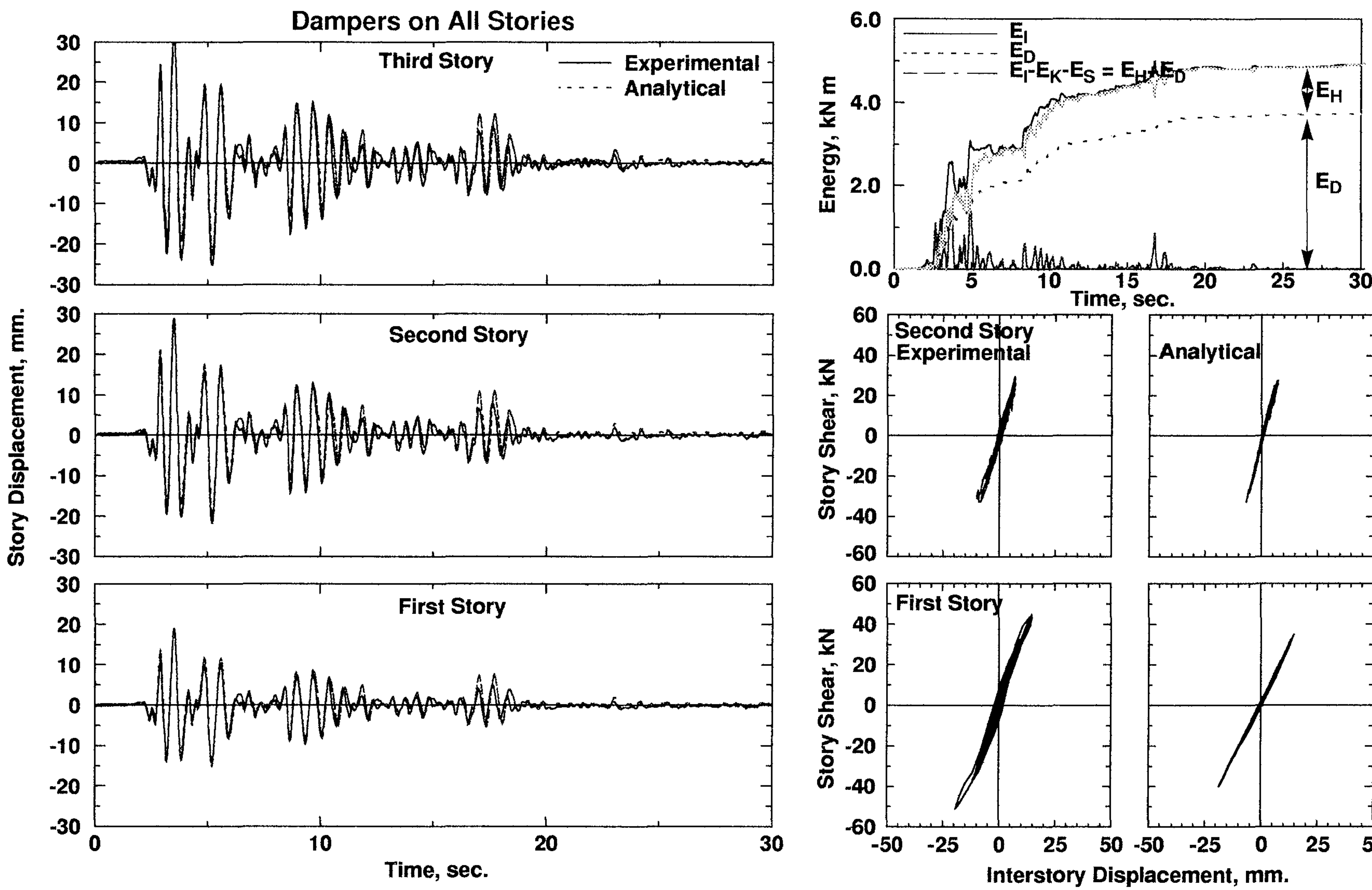

Figure 4.8 Experimental Results - EL CENTRO 0.3g (BEL030)

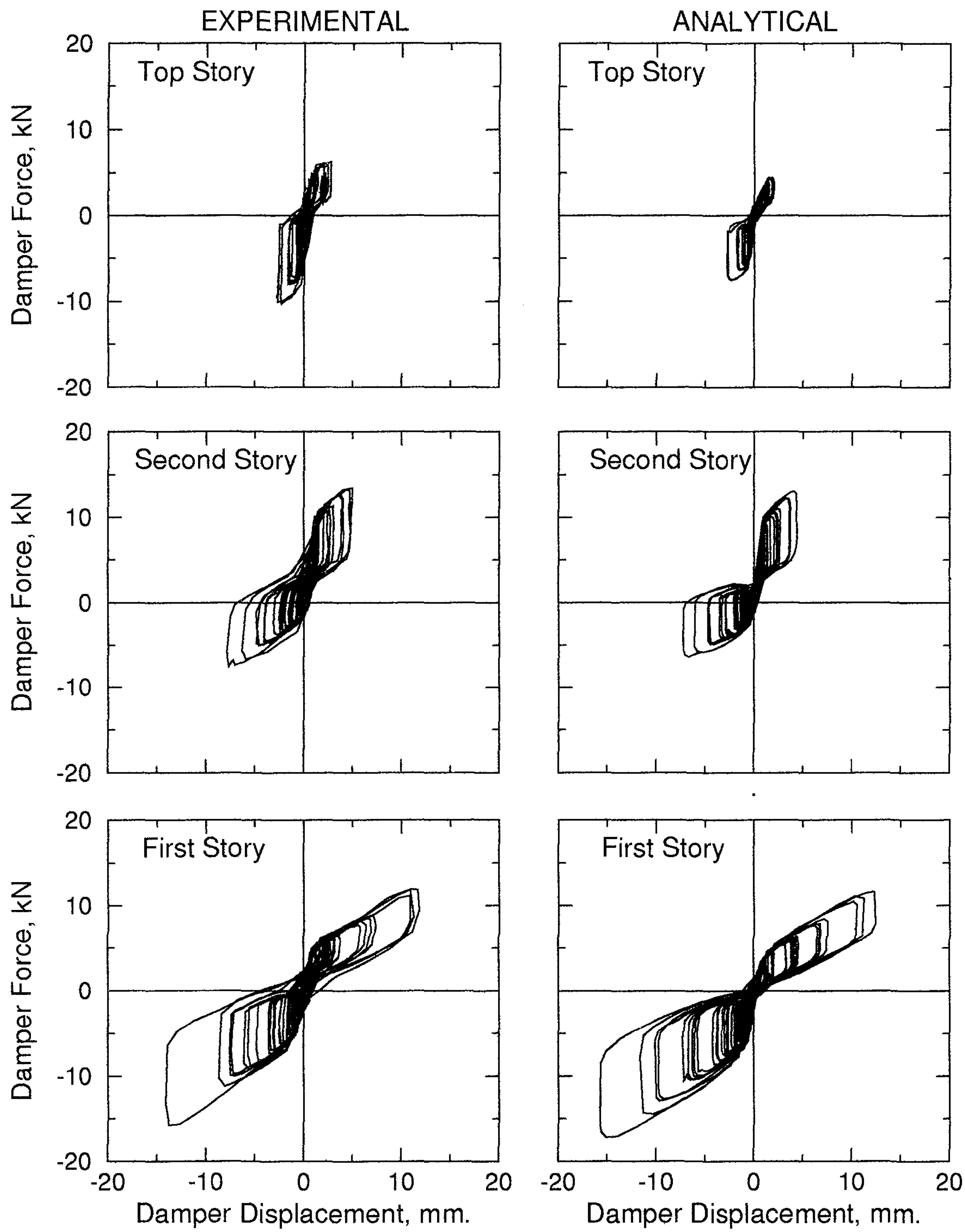

Figure 4.9 Damper Force-Deformation Behavior - EL CENTRO 0.3g (BEL030)

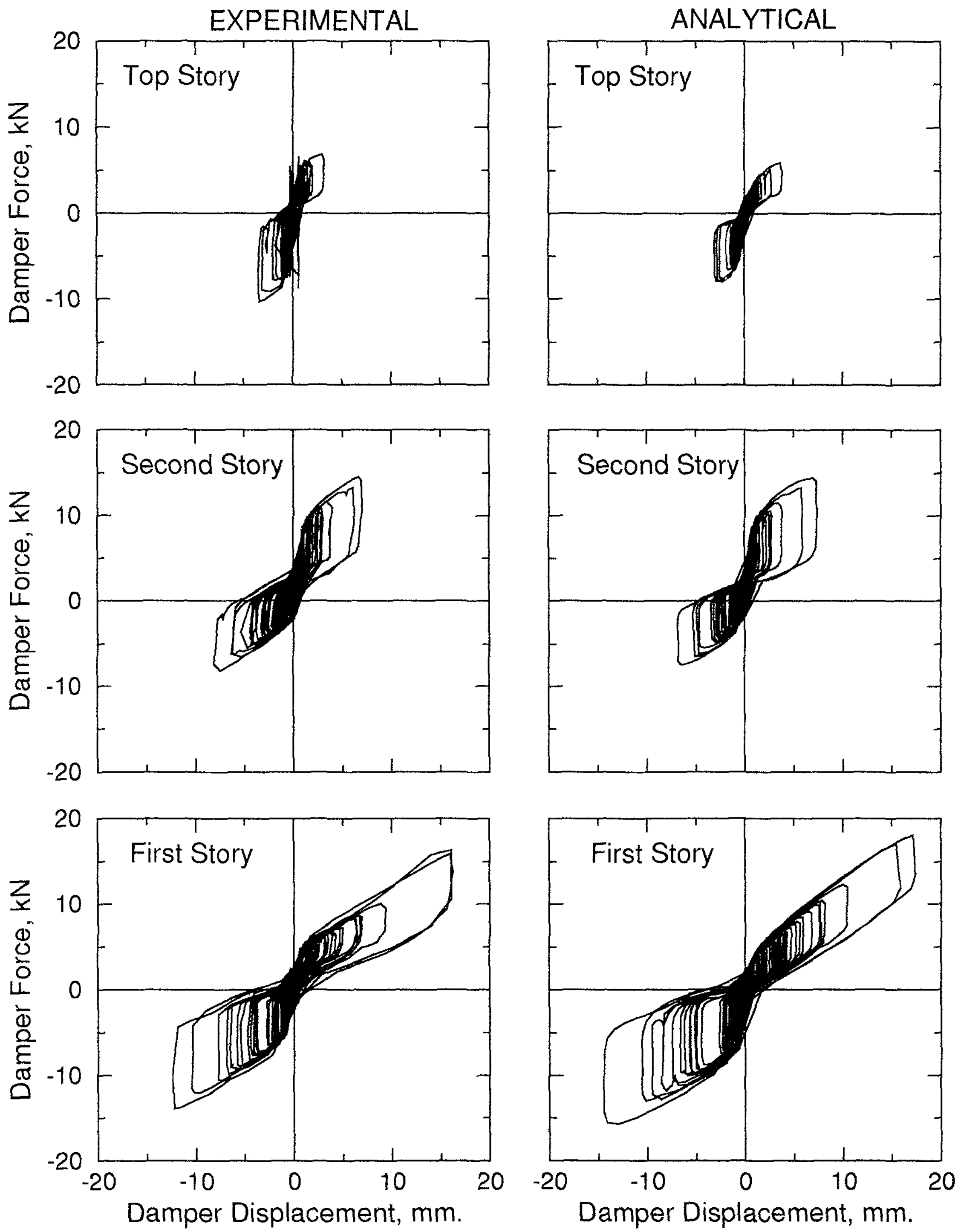

Figure 4.11 Damper Force-Deformation Behavior - TAFT 0.3g (CTA030)

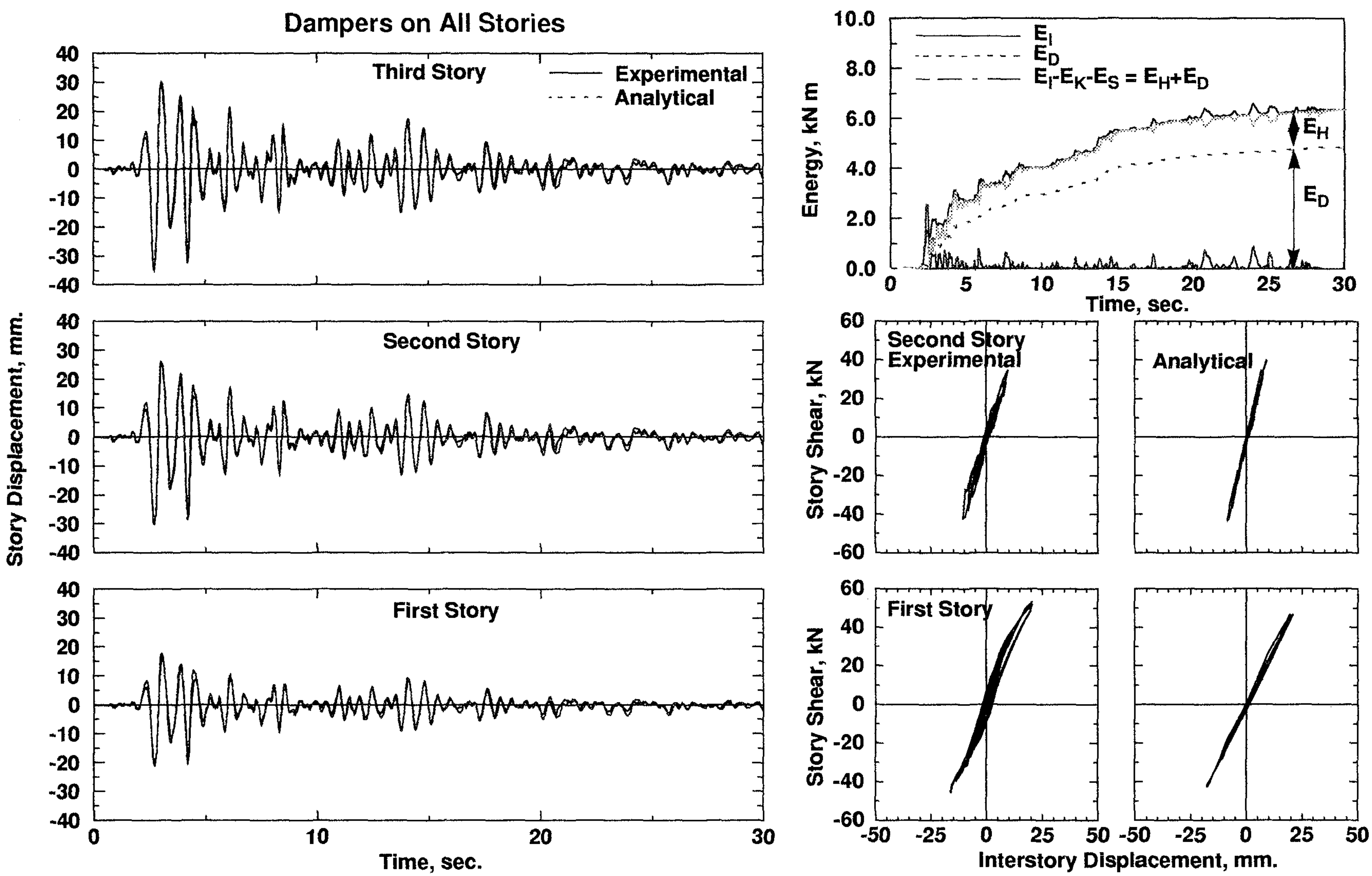

Figure 4.10 Experimental Results - TAFT 0.3g (CTA030)

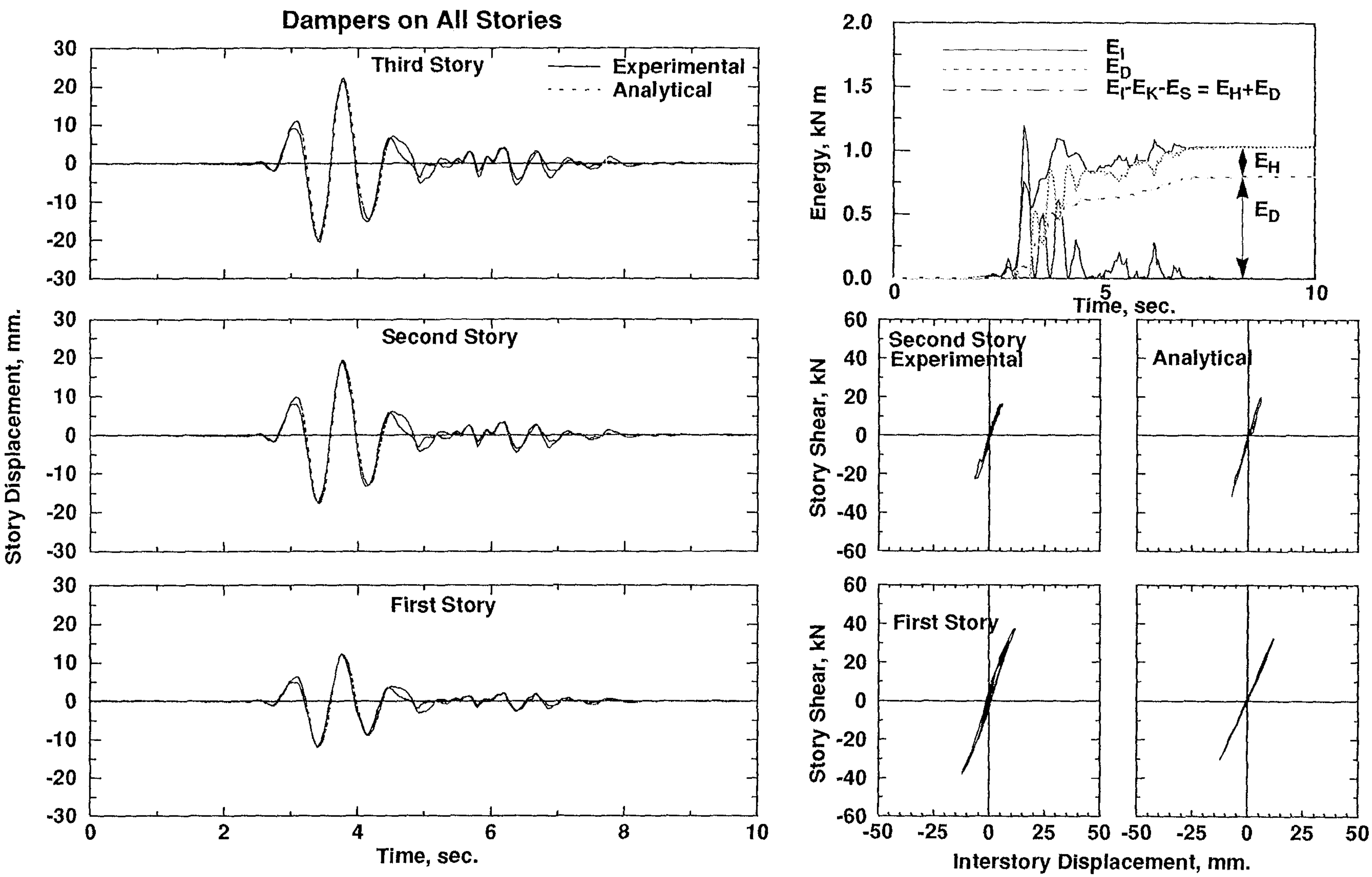

Figure 4.12 Experimental Results - PACOIMA 0.2g (DPA020)

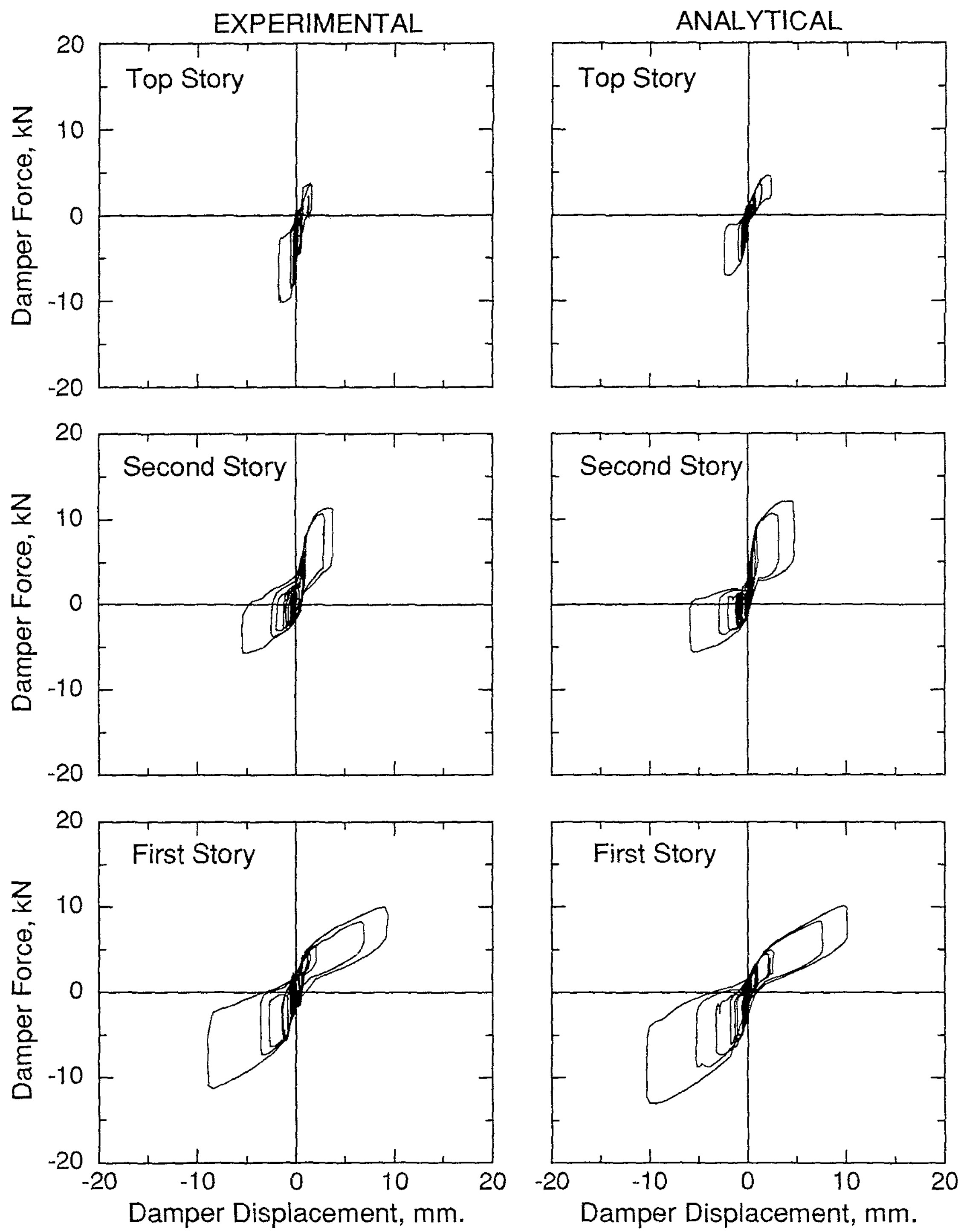

Figure 4.13 Damper Force-Deformation Behavior - PACOIMA 0.2g (DPA020)

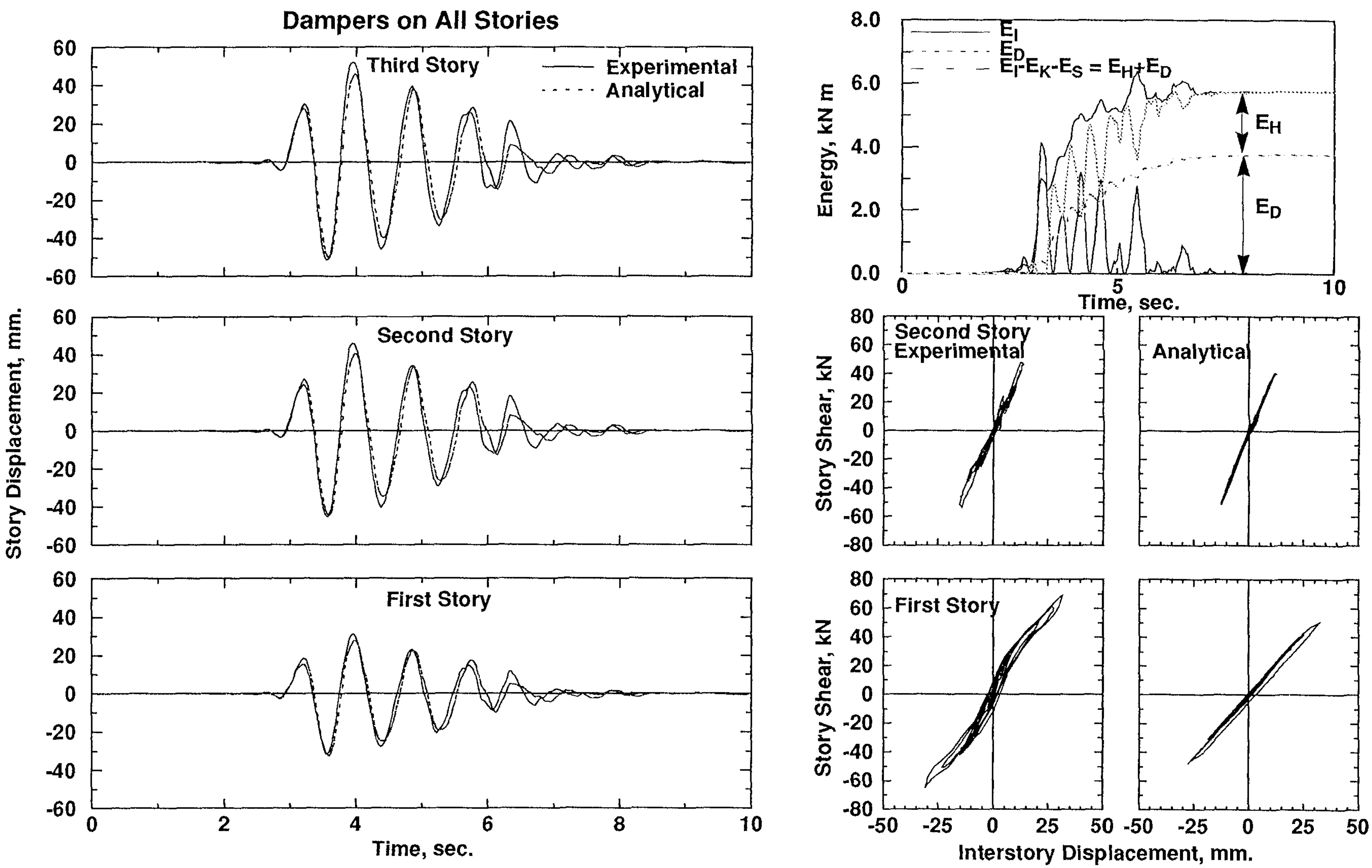

Figure 4.14 Experimental Results - PACOIMA 0.4g (EPA040)

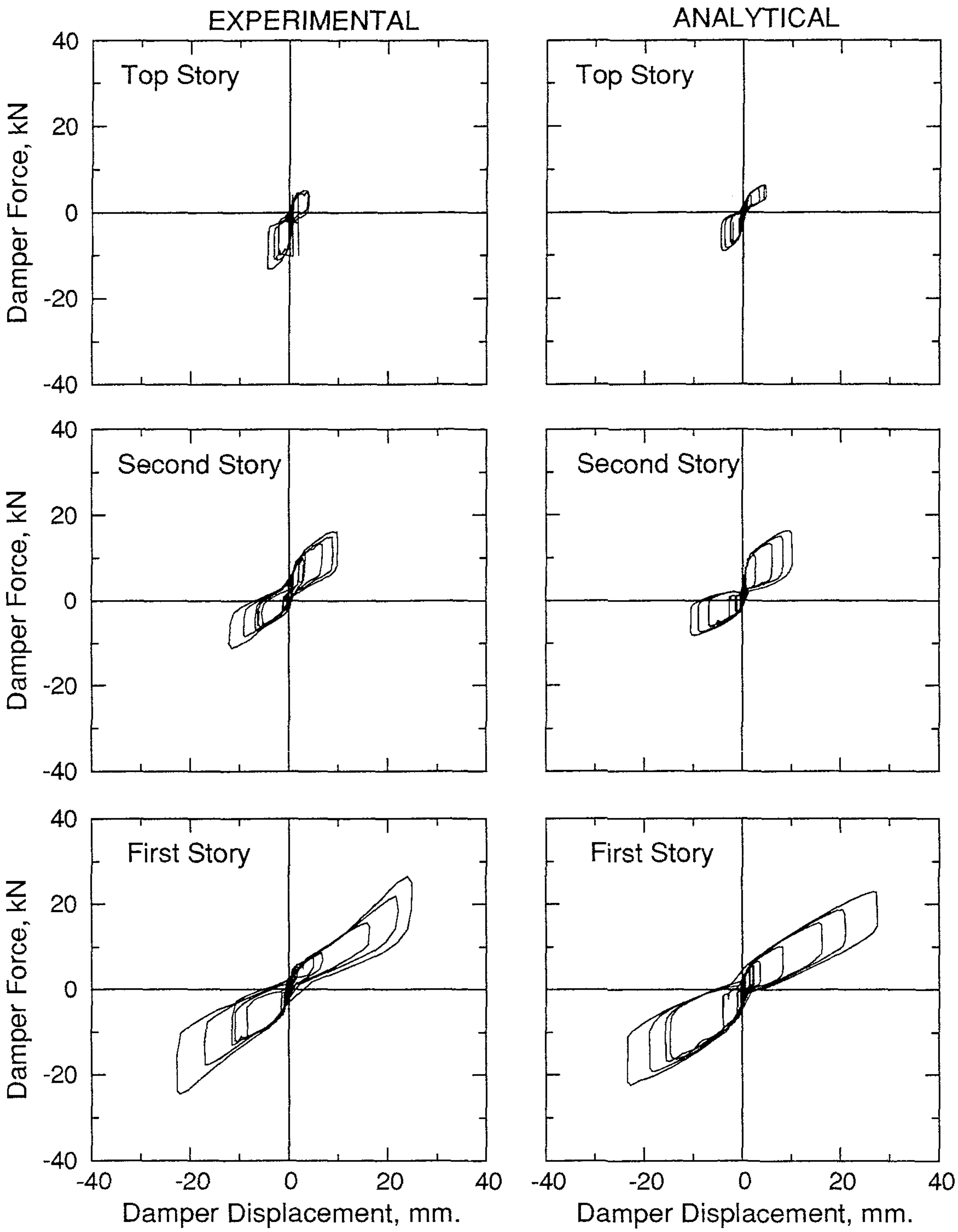

Figure 4.15 Damper Force-Deformation Behavior - PACOIMA 0.4g (EPA040)

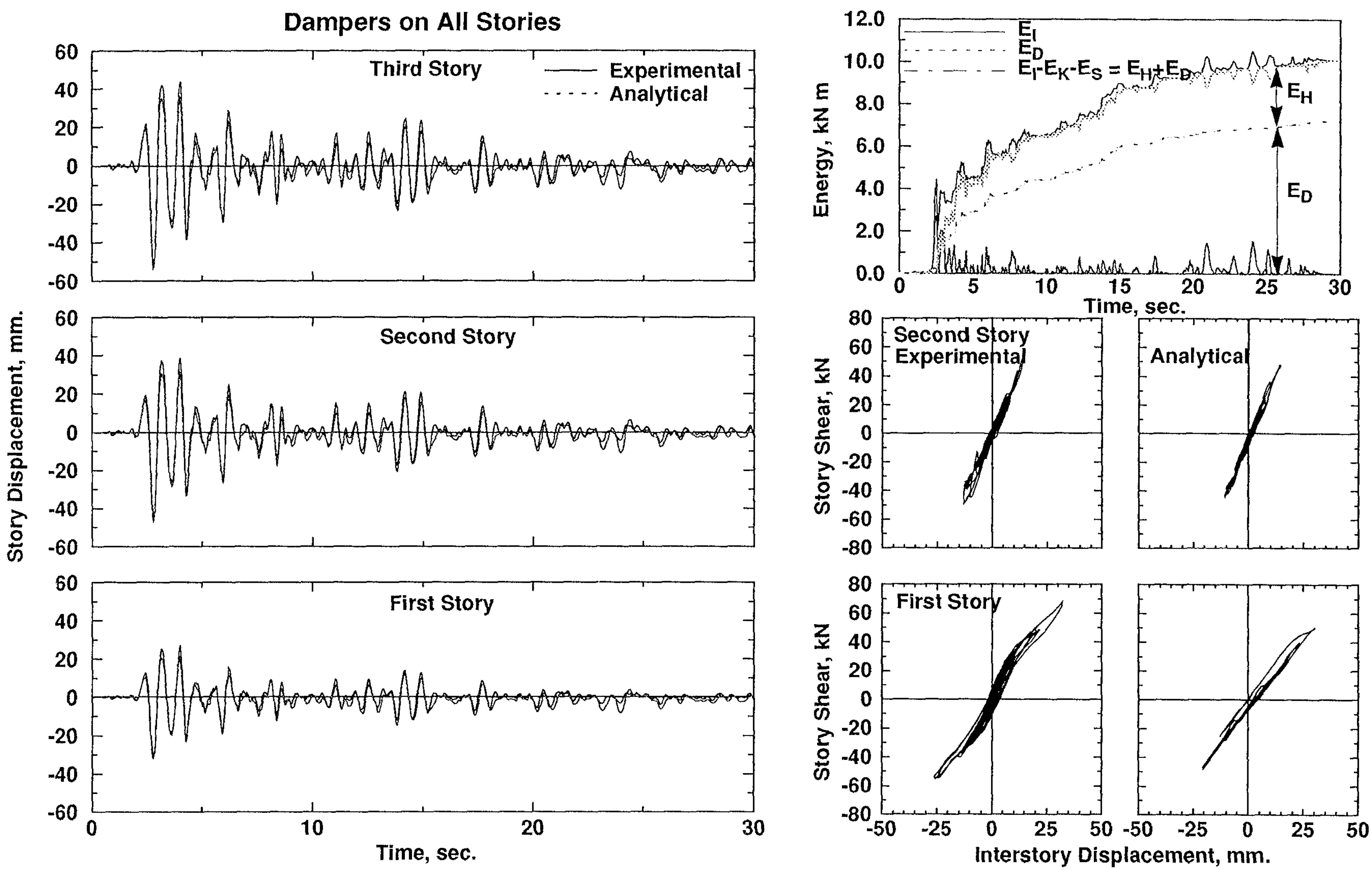

Figure 4.16 Experimental Results - TAFT 0.4g (FTA040)

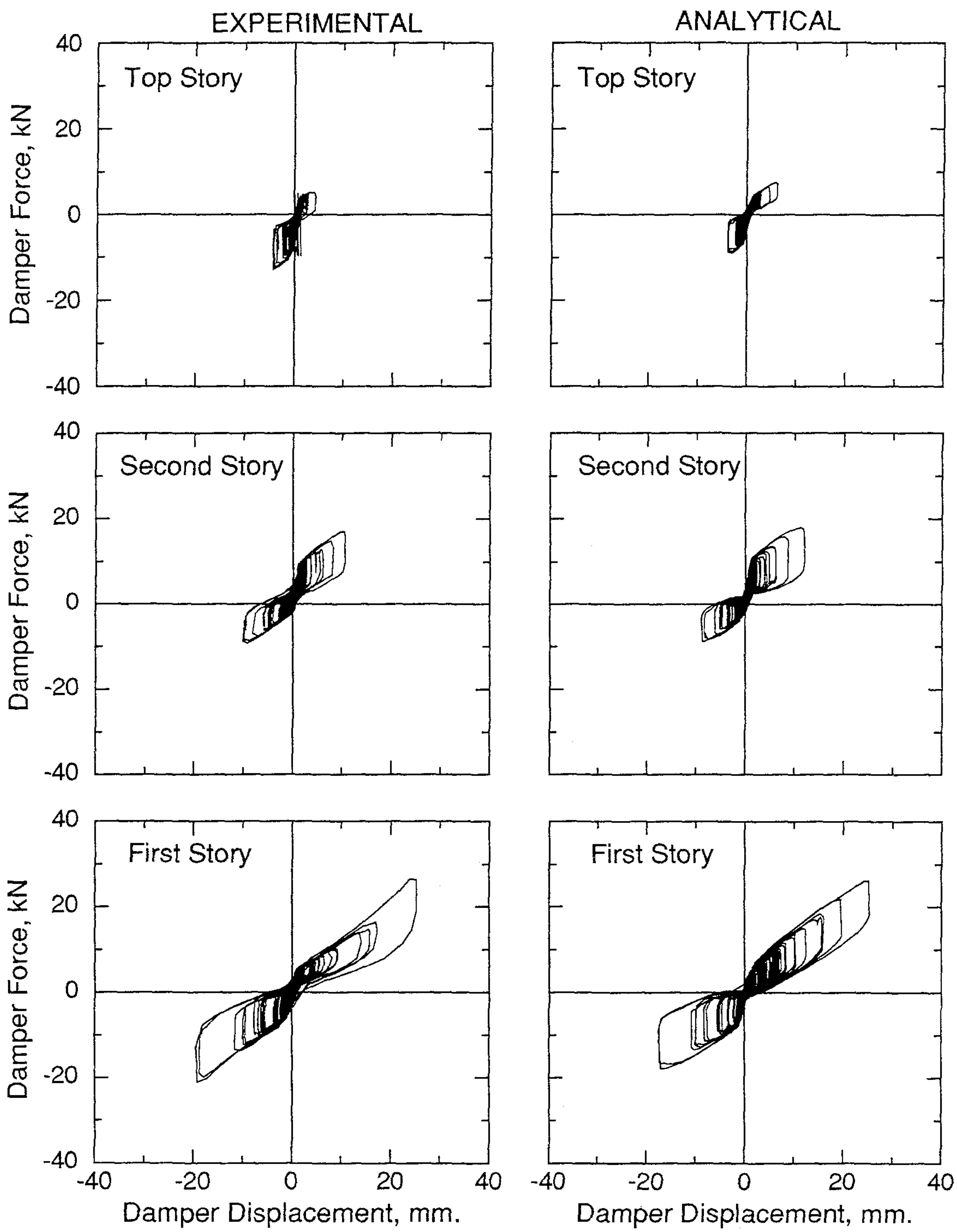

Figure 4.17 Damper Force-Deformation Behavior - TAFT 0.4g (FTA040)

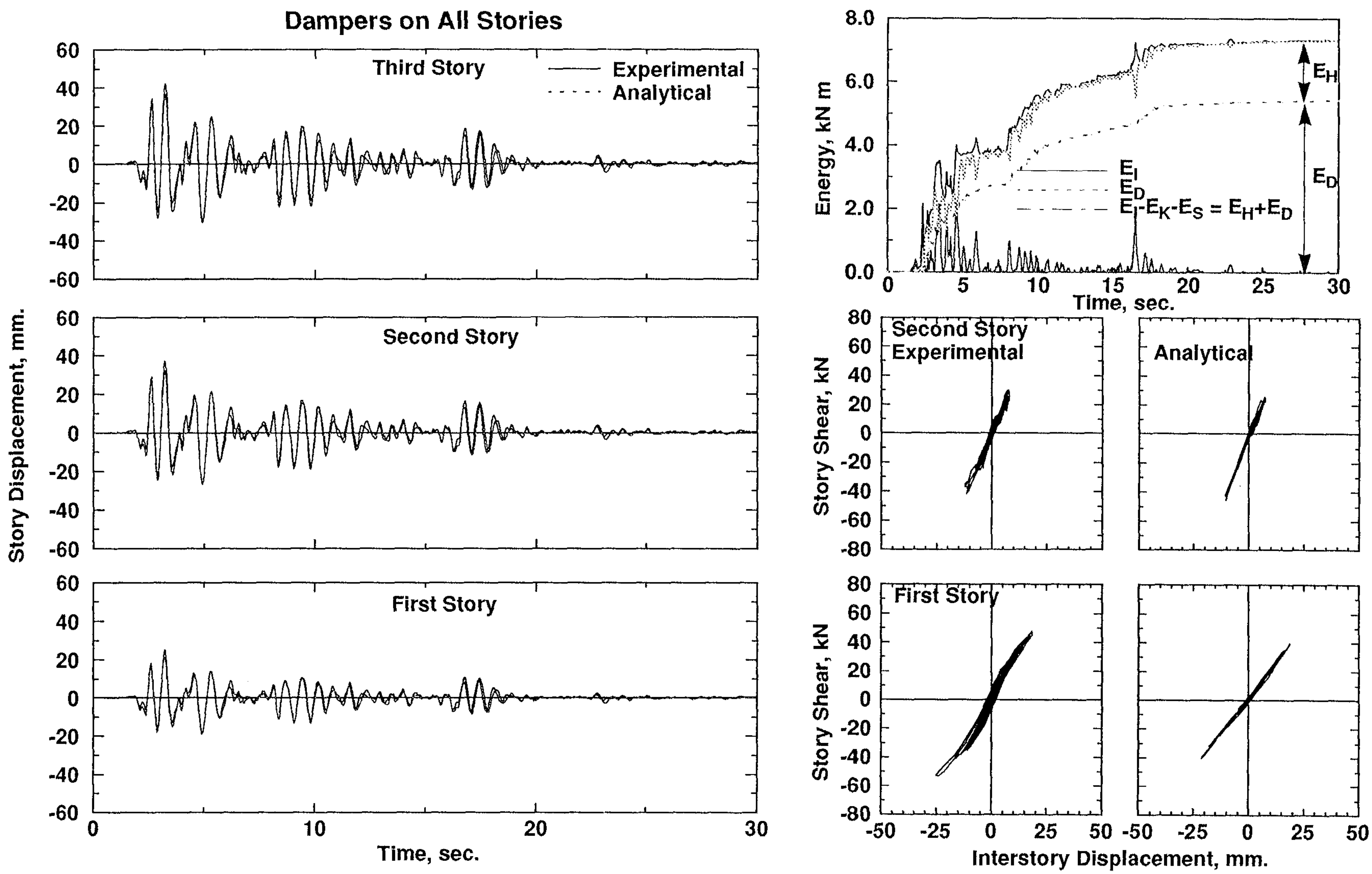

Figure 4.18 Experimental Results - EL CENTRO 0.4g (GEL040)

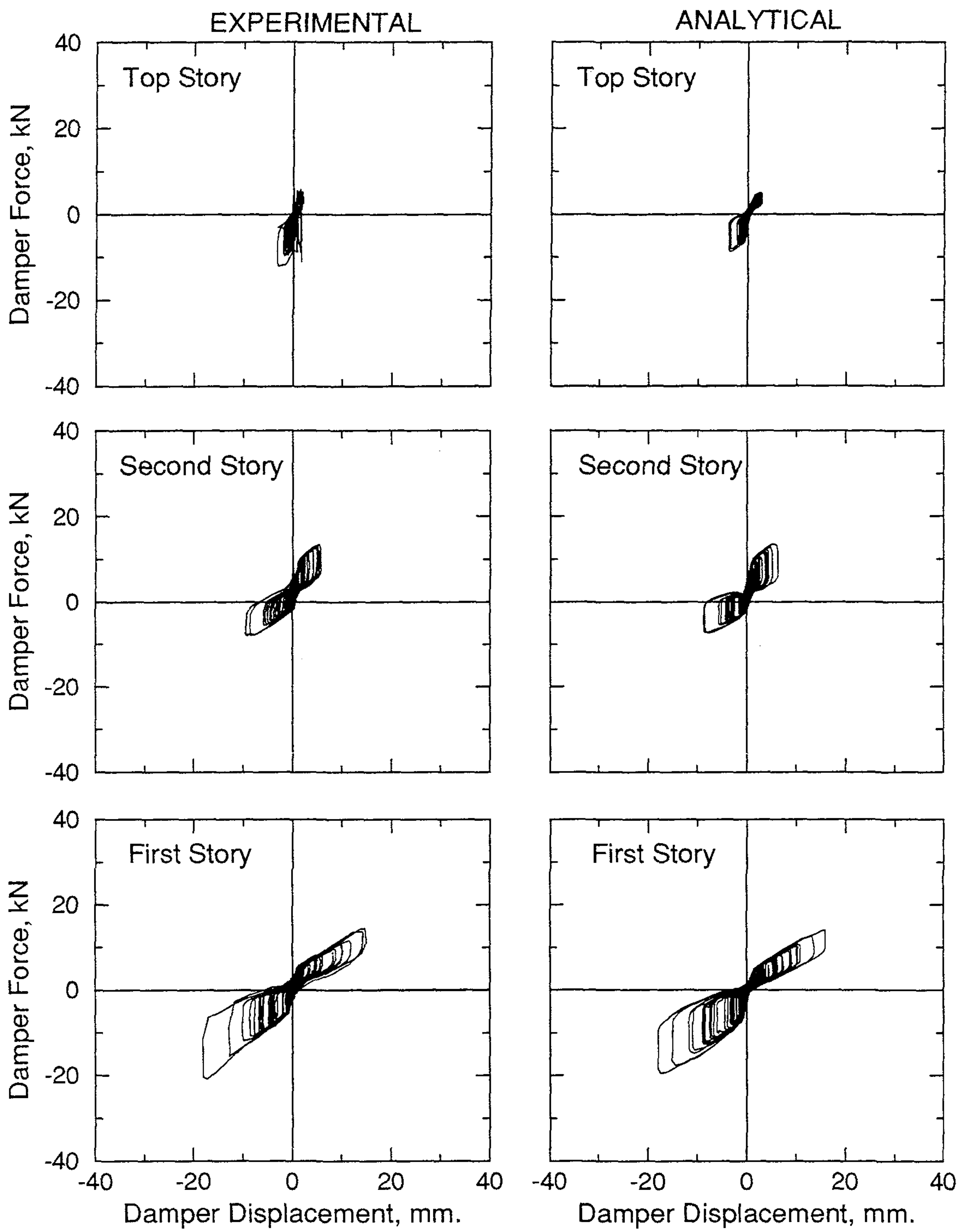

Figure 4.19 Damper Force-Deformation Behavior
EL CENTRO 0.4g (GEL040)

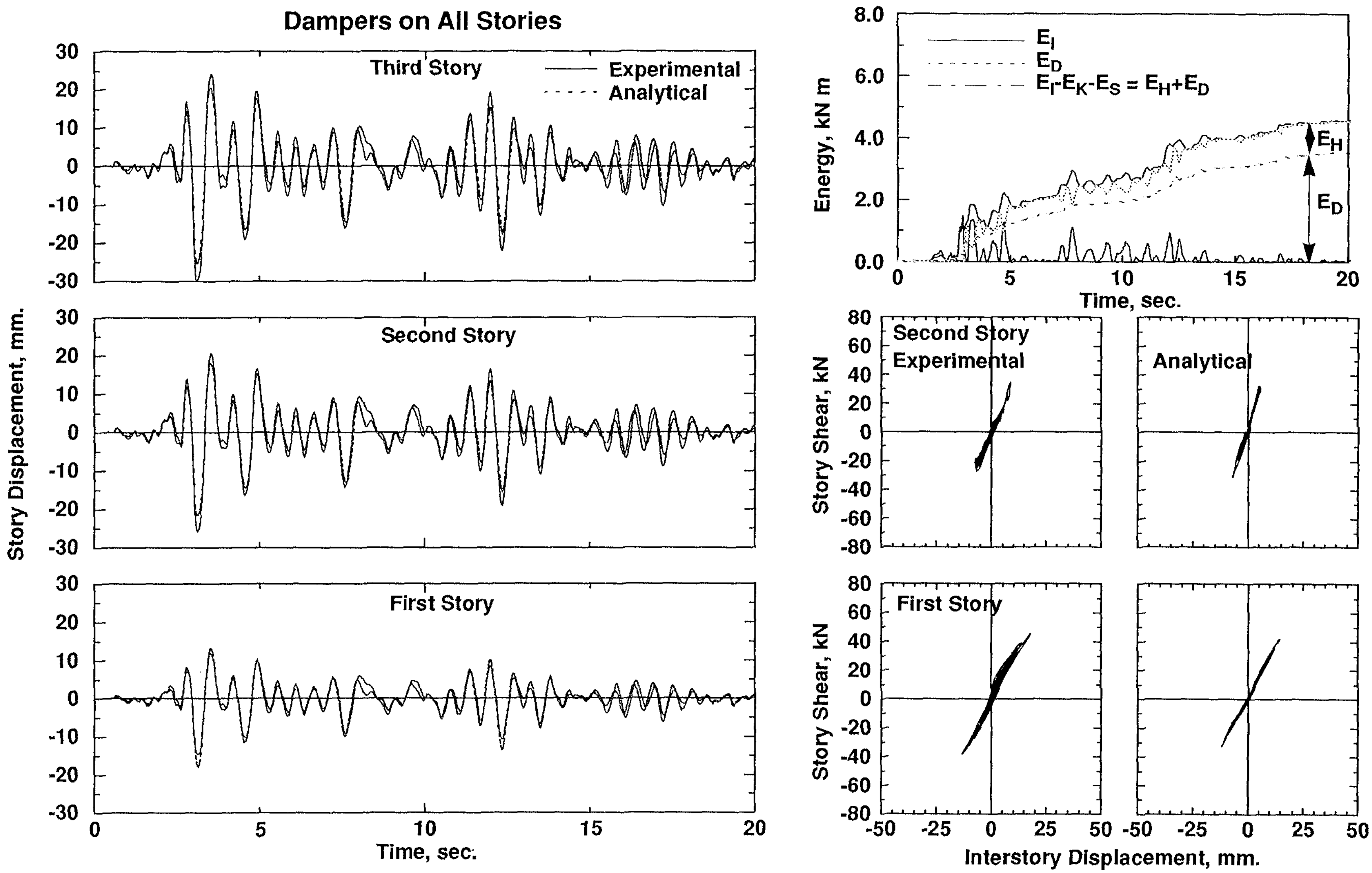

Figure 4.20 Experimental Results - HACHINOHE 0.2g (HHA020)

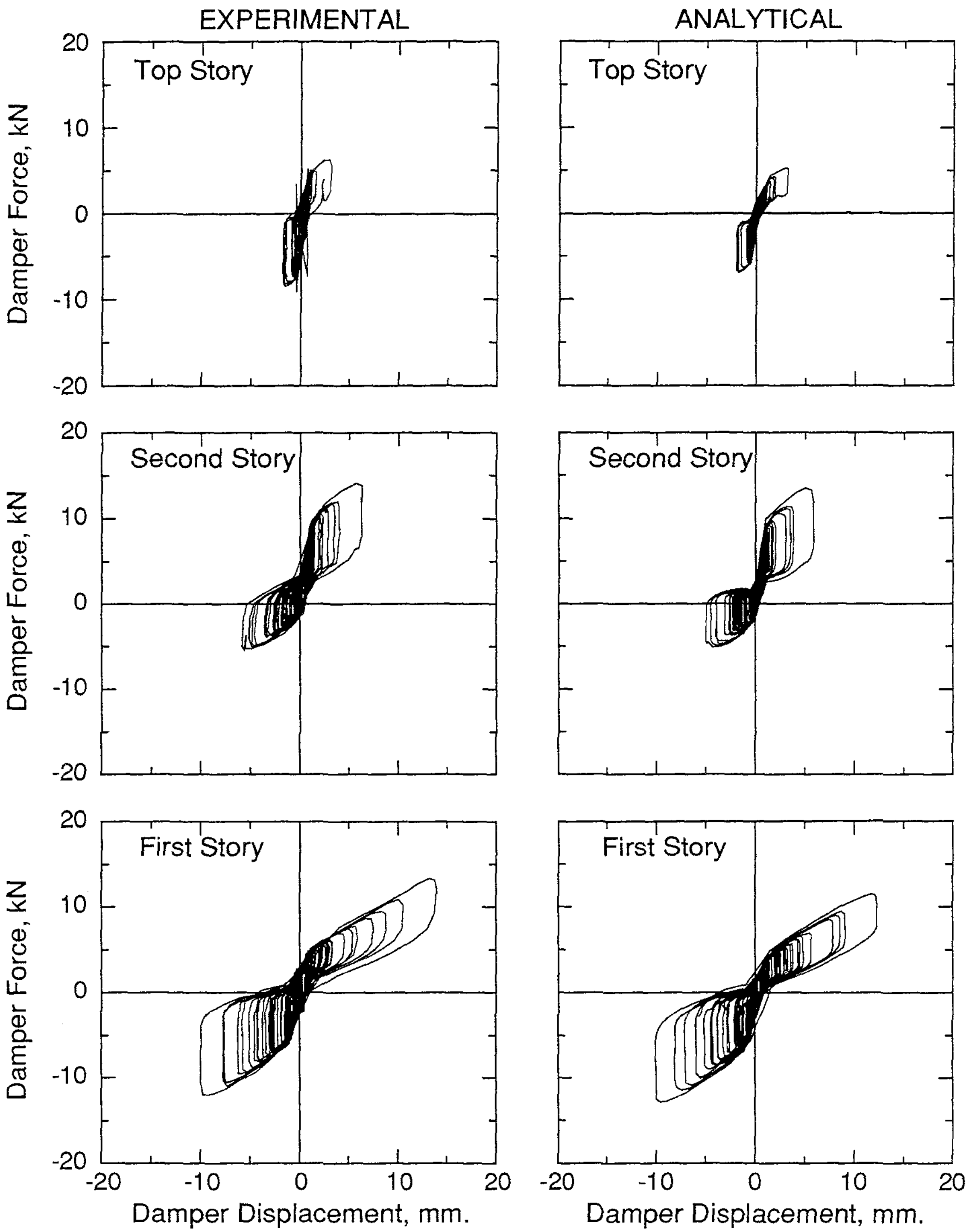

Figure 4.21 Damper Force-Deformation Behavior - HACHINOHE 0.2g (HHA020)

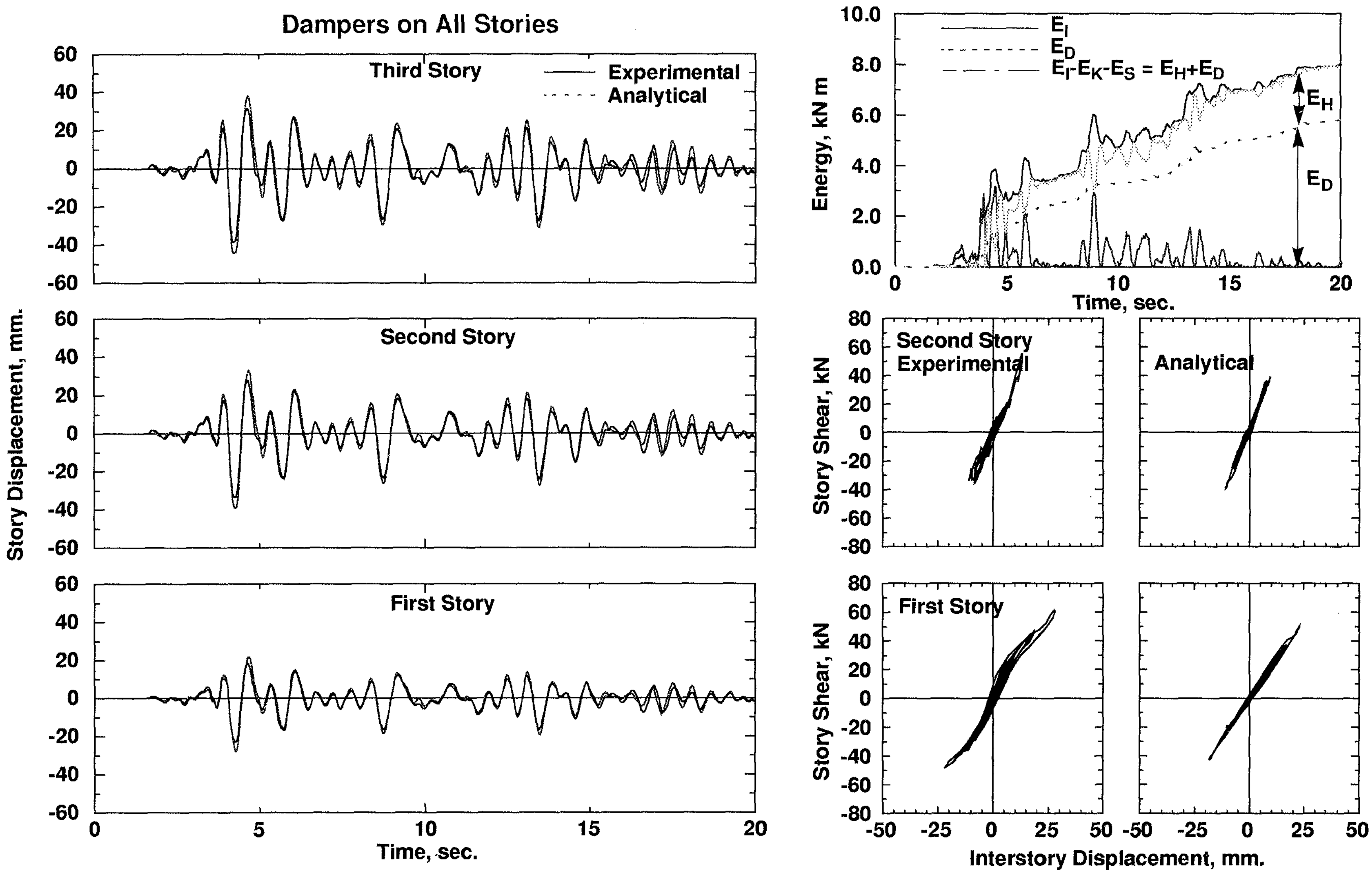

Figure 4.22 Experimental Results - HACHINOHE 0.3g (IHA030)

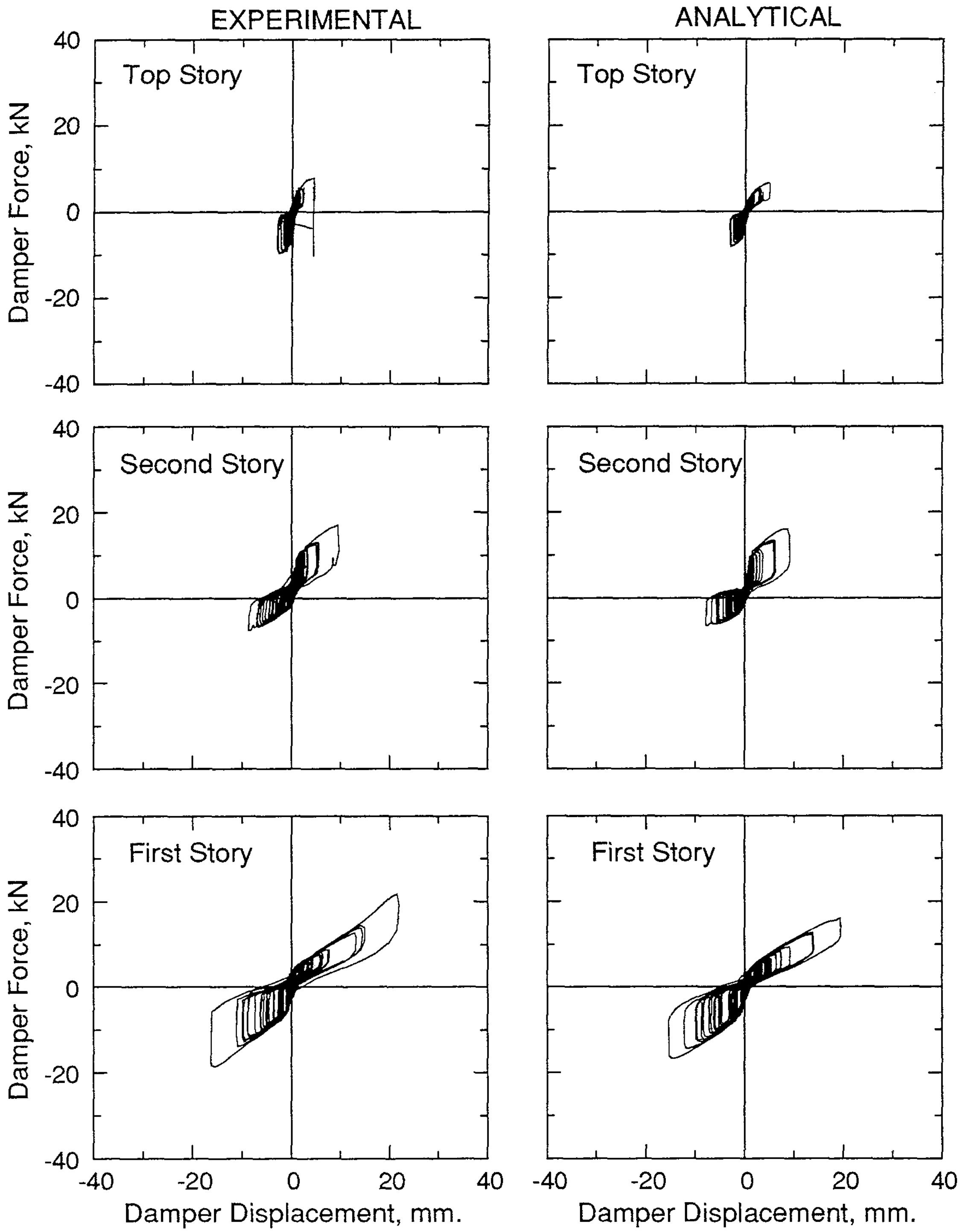

Figure 4.23 Damper Force-Deformation Behavior - HACHINOHE 0.3g (IHA030)

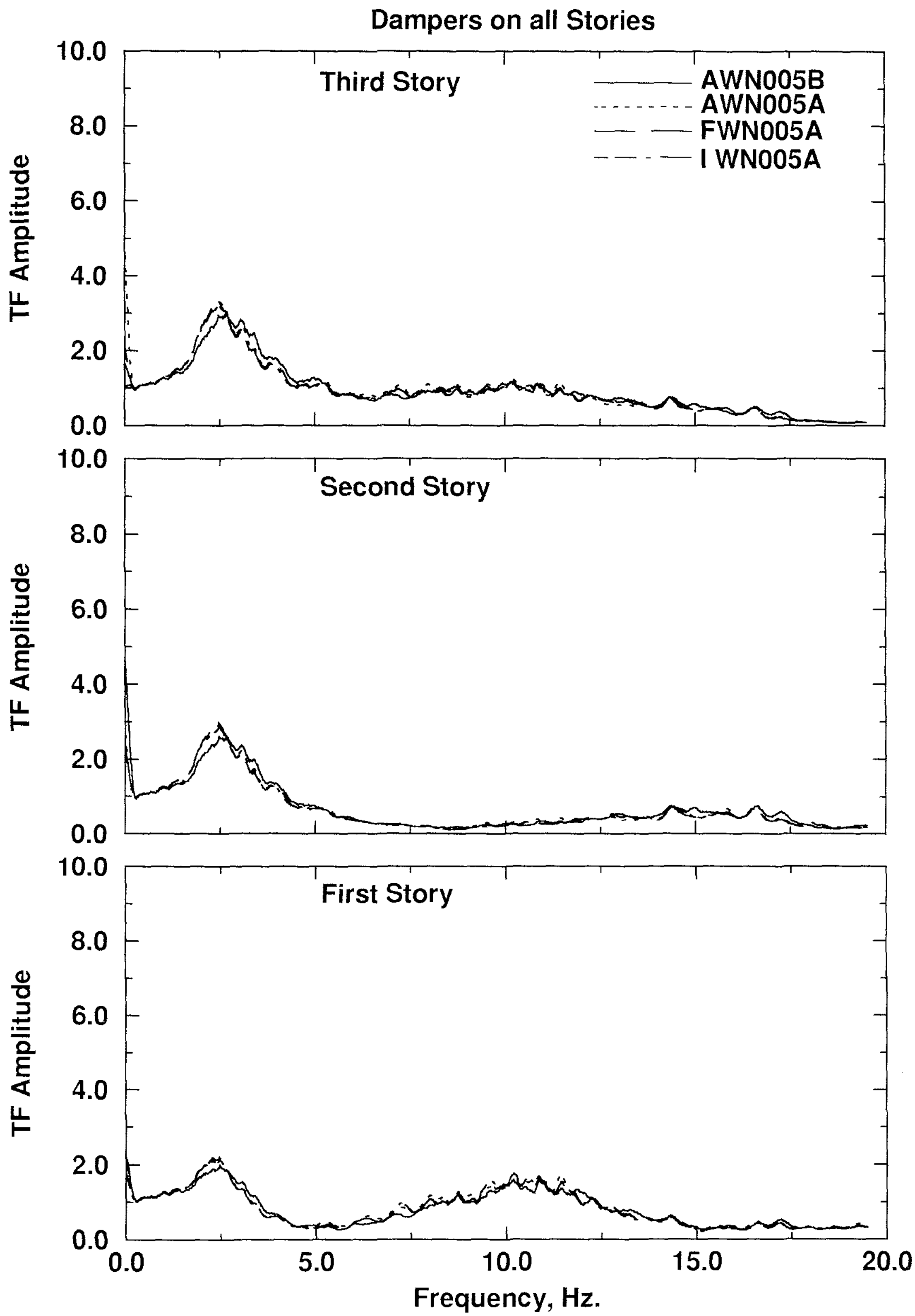

Figure 4.24 Story Transfer Functions
Dampers on all Stories

4.20, 4.21, 4.22 and 4.23.

Total seismic input energy increased from 4.6 kN m to 8.2 kN m for the Hachinohe 0.2 g and Hachinohe 0.3 g tests, respectively. A total of 77% of the input energy was dissipated by the dampers during the Hachinohe 0.2 g test; this ratio was 72% for the Hachinohe 0.3 g test.

4.4 Tests on the Structure with Dampers on the First Two Stories Only

4.4.1 Initial Dynamic Properties of the Test Structure

After the third story dampers were removed, one white noise test was conducted in order to identify the structural dynamic properties of the test structure with dampers only on the first two stories. Story level transfer functions were used to determine the natural frequencies, equivalent viscous damping ratios, mode shapes and story stiffnesses. The natural frequencies were found to be 2.71, 7.96 and 14.43 Hz with corresponding equivalent viscous damping ratios of 22, 6.9, and 4.6%. Story level transfer functions for this test are plotted on Figure 4.29.

4.4.2 Simulated Ground Motion Test Results

The test structure was subjected to three simulated ground motions, namely Taft 0.05 g, Taft 0.2 g and El Centro 0.3 g (Table 3.3). Since the first of these tests led to minor response, only the results of the latter two will be discussed. White noise tests were conducted after each ground motion test to identify the changes in the dynamic properties of the structure. The white noise test results show that the natural frequencies, equivalent viscous damping ratios and mode shapes did not change after these tests. Selected story level transfer functions are plotted on Figure 4.29. Table 4.3 summarizes the maximum

Table 4.3: Summary of Maximum Response - Dampers on the First Two Stories Only

STORY/ TEST ID[3]	PEAK ACCELERATION g.				VELOCITY mm/sec			Interstory Displ. / Story Height[1]			Story Shear / Story Weight[2]		Column Axial Force kN			
													Exterior		Interior	
	BASE	1st	2nd	3rd	1st	2nd	3rd	1st	2nd	3rd	1st	2nd	1st	2nd	1st	2nd
JTA005	0.056	0.053	0.065	0.077	35	41	44	0.001	0.001	0.001	0.023	0.019	7.2	3.5	2.4	1.7
KTA020	0.221	0.200	0.158	0.293	136	176	212	0.009	0.006	0.003	0.090	0.097	14.8	10.4	7.9	6.7
LEL030	0.327	0.201	0.232	0.237	152	243	302	0.015	0.008	0.004	0.120	0.096	17.1	11.5	9.3	7.3

[1] 1.22 m
[2] 360 kN
[3] See Table 3.3

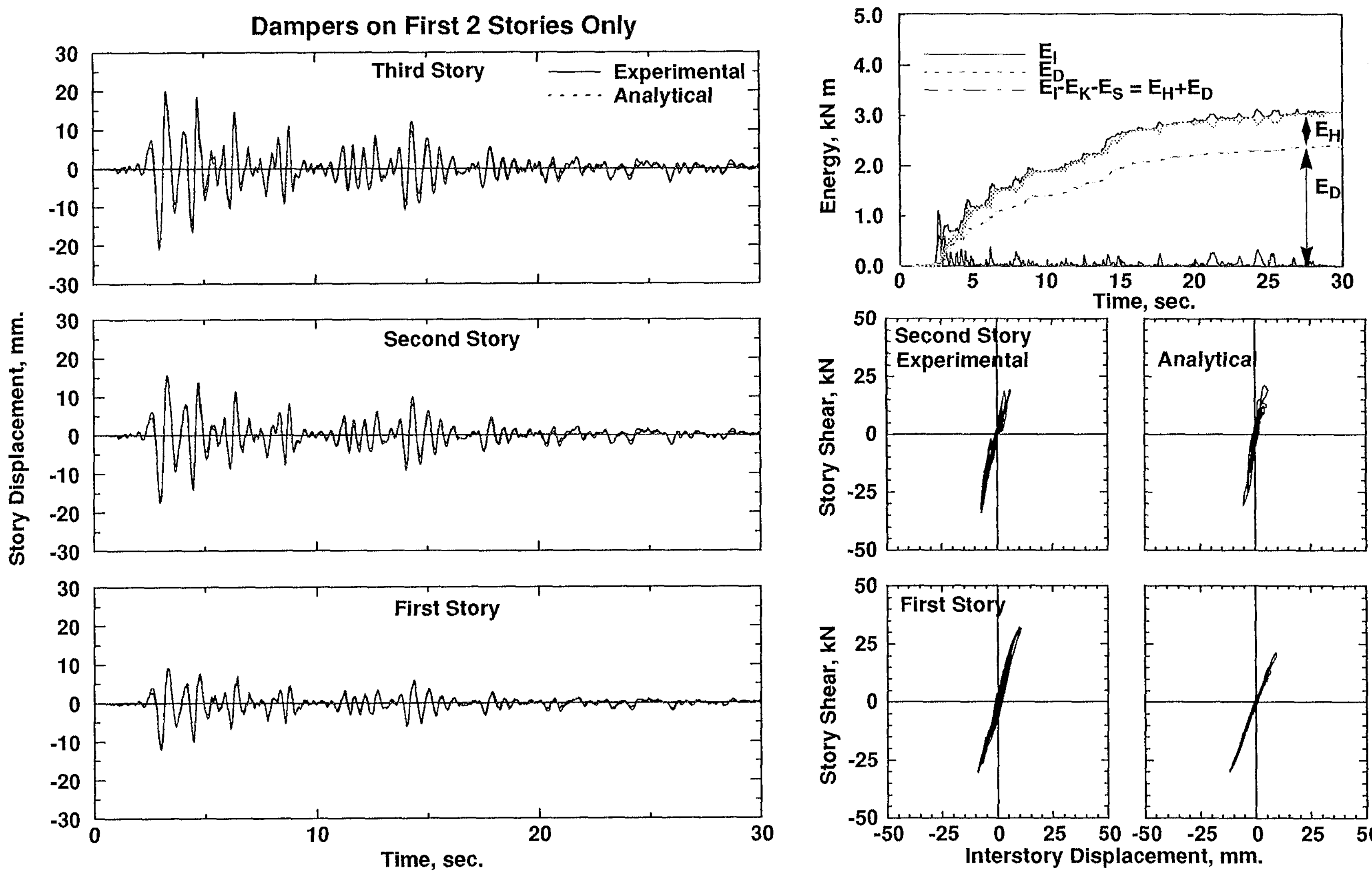

Figure 4.25 Experimental Results - TAFT 0.2g (KTA020)

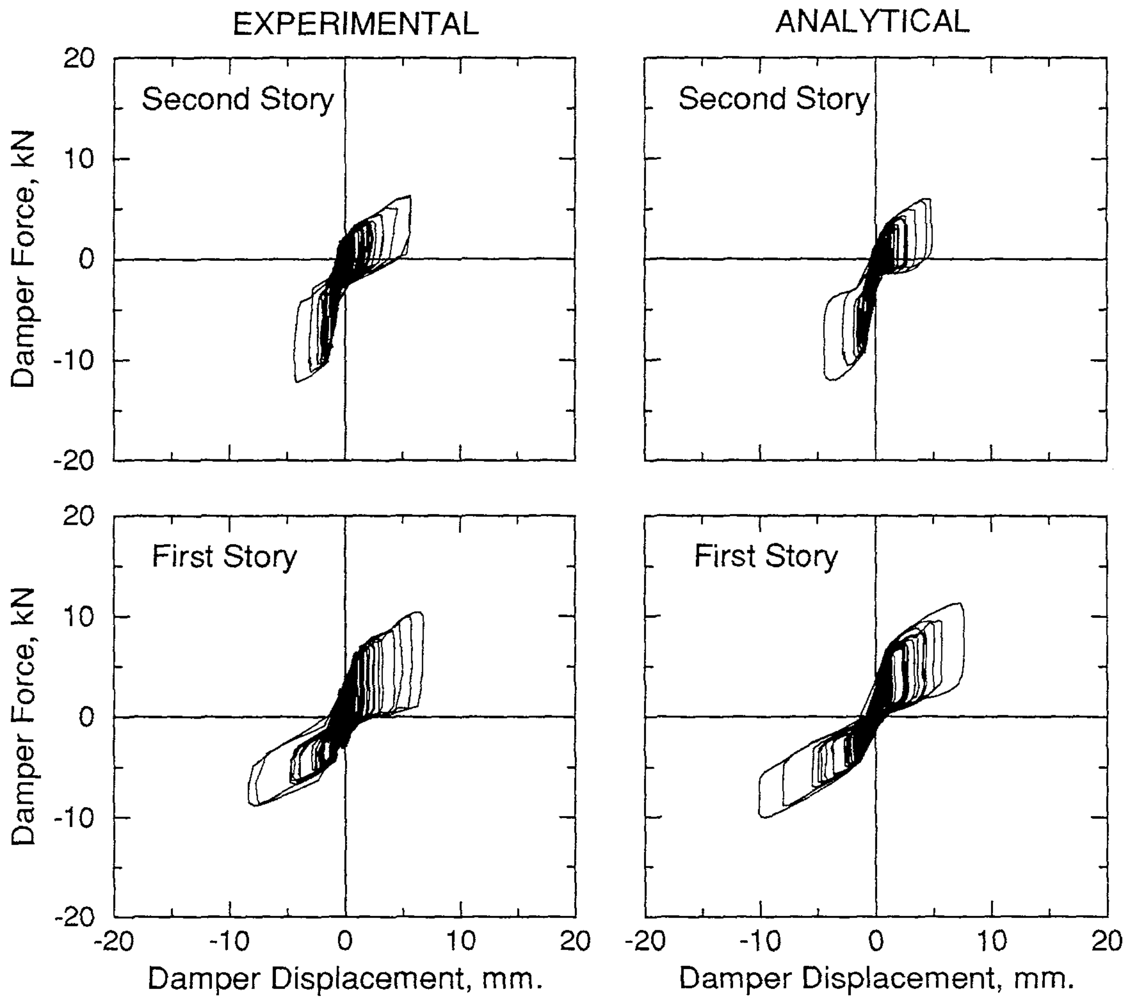

Figure 4.26 Damper Force-Deformation Behavior - TAFT 0.2g (KTA020)

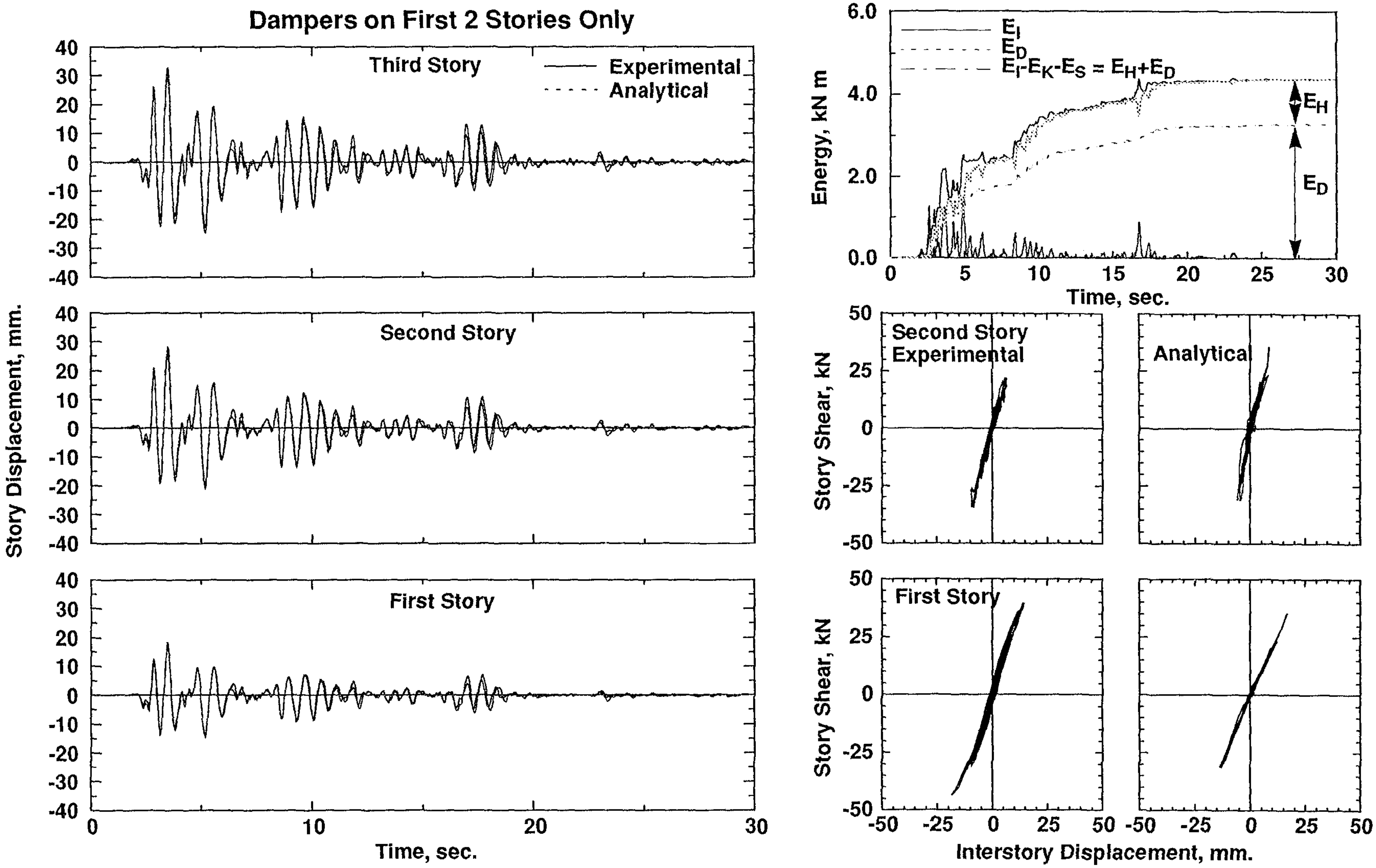

Figure 4.27 Experimental Results - EL CENTRO 0.3g (LEL030)

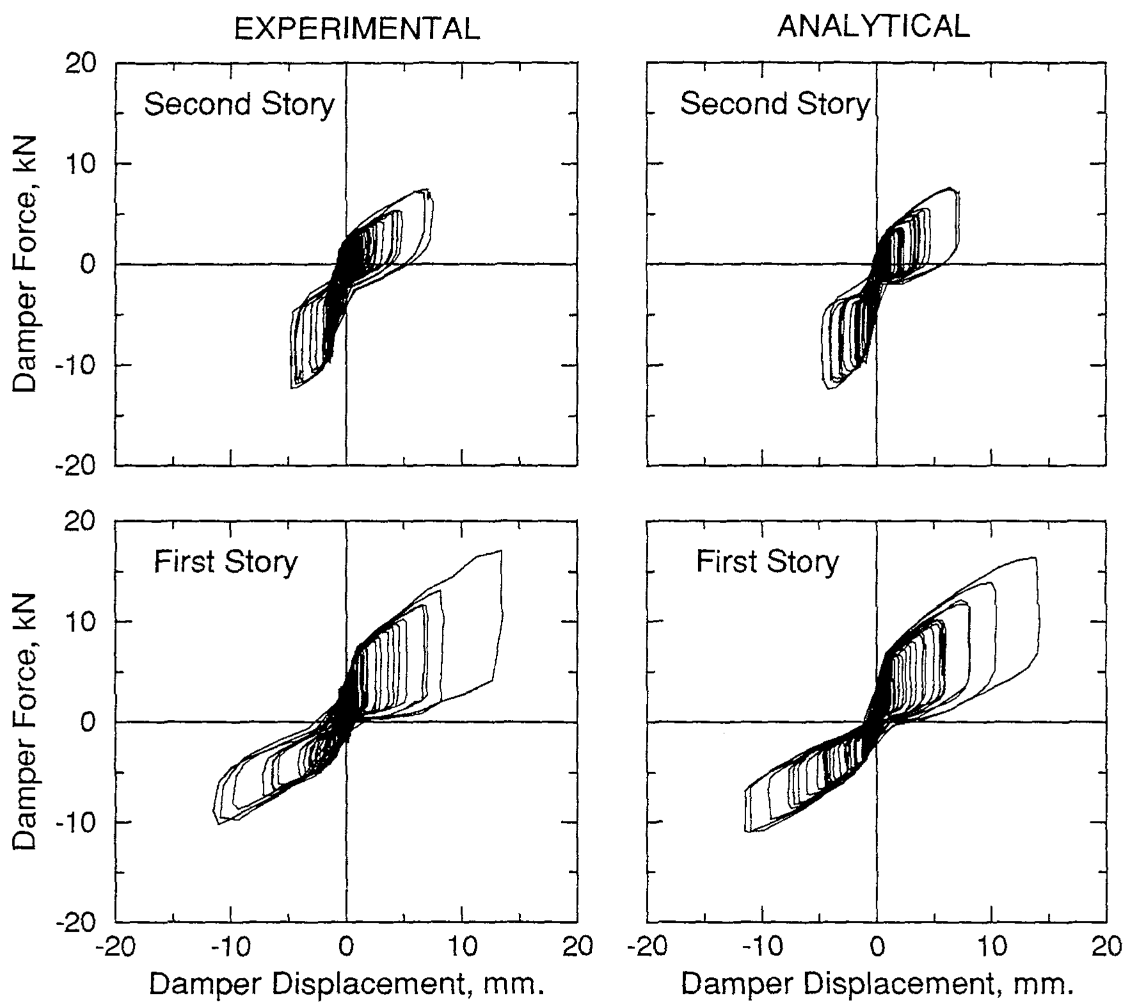

Figure 4.28 Damper Force-Deformation Behavior - EL CENTRO 0.3g (LEL030)

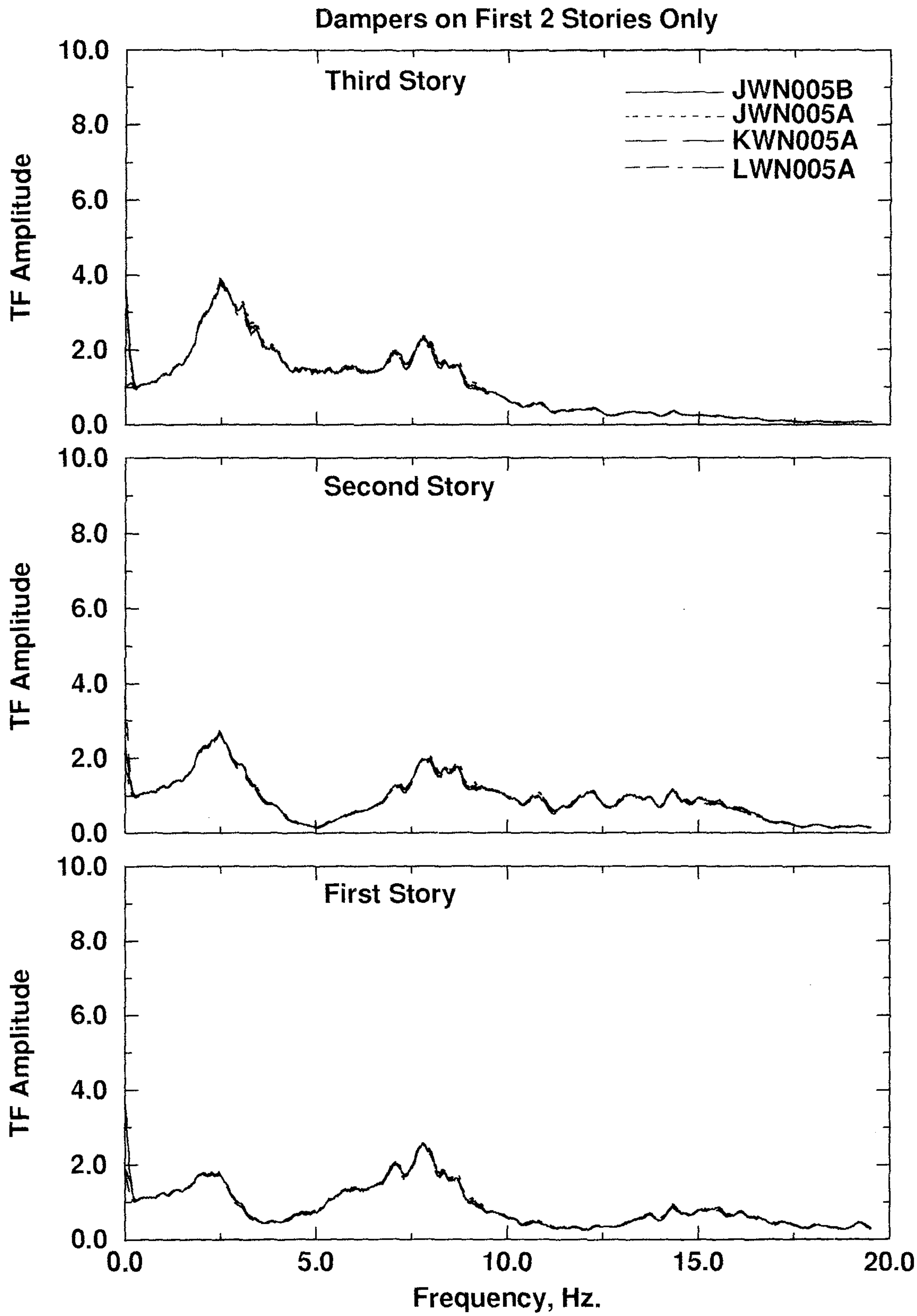

**Figure 4.29 Story Transfer Functions
Dampers on First 2 Stories Only**

response of the structure to the ground motions in terms of base and story level acceleration, velocity, interstory displacement (normalized with respect to story height), story shear (normalized with respect to story weight) and column axial force. Experimentally obtained story displacement time histories, story shear vs interstory displacement, damper force-displacement and energy time histories are plotted on Figures 4.25 to 4.28.

The measured maximum base acceleration was 0.33 g where the observed maximum interstory drift was 1.5% for El Centro 0.3 g (LEL030) test. Corresponding values for Taft 0.2 g test (KTA020) were 0.22 g and 0.9%. The maximum story velocity occurring in the third story level was 302 and 212 mm/sec for LEL030 and KTA020 tests, respectively. Normalized story shears were 12.0, 9.0% for the first story and 9.6, 9.7% of the story weight for the second story, respectively. Maximum column axial forces recorded during the EL Centro 0.3 g test were 17.1 kN and 9.3 kN for the first floor exterior and interior columns, respectively. Corresponding values for the Taft 0.2 g test were 14.8 kN and 7.9 kN. Total seismic input energy was 4.4 kNm for El Centro 0.3 g and 3.1 kNm for Taft 0.2 g. A total of 75% of the input energy was dissipated by the dampers during the El Centro 0.3 g test; this ratio was 78% for Taft 0.2 g test.

4.5 Test on the Structure with Dampers on the First Story Only

4.5.1 Initial Dynamic Properties of the Structure

After the second story dampers were removed, one white noise test was conducted in order to identify the structural dynamic properties of the test structure. Story level transfer functions were used to determine the natural frequencies, equivalent viscous damping ratios, mode shapes and story stiffnesses. The natural frequencies were found to be 2.02, 7.18 and 12.30 Hz with corresponding equivalent viscous damping ratios of 17, 6.1, and 3.1%. Story level transfer functions for this test were plotted on Figure 4.34.

Table 4.4: Summary of Maximum Response - Dampers on the First Story Only

STORY/ TEST ID[3]	PEAK ACCELERATION g.				VELOCITY mm/sec			Interstory Displ. / Story Height[1]			Story Shear / Story Weight[2]		Column Axial Force kN			
													Exterior		Interior	
	BASE	1st	2nd	3rd	1st	2nd	3rd	1st	2nd	3rd	1st	2nd	1st	2nd	1st	2nd
MTA005	0.052	0.060	0.067	0.079	32	33	45	0.001	0.002	0.001	0.019	0.038	6.1	2.0	2.4	1.9
NTA020	0.209	0.254	0.195	0.264	144	199	255	0.012	0.008	0.005	0.105	0.124	12.6	5.5	8.4	8.0
OEL030	0.319	0.192	0.191	0.247	154	225	262	0.013	0.009	0.005	0.108	0.130	13.3	6.1	10.6	7.8

[1] 1.22 m
[2] 360 kN
[3] See Table 3.3

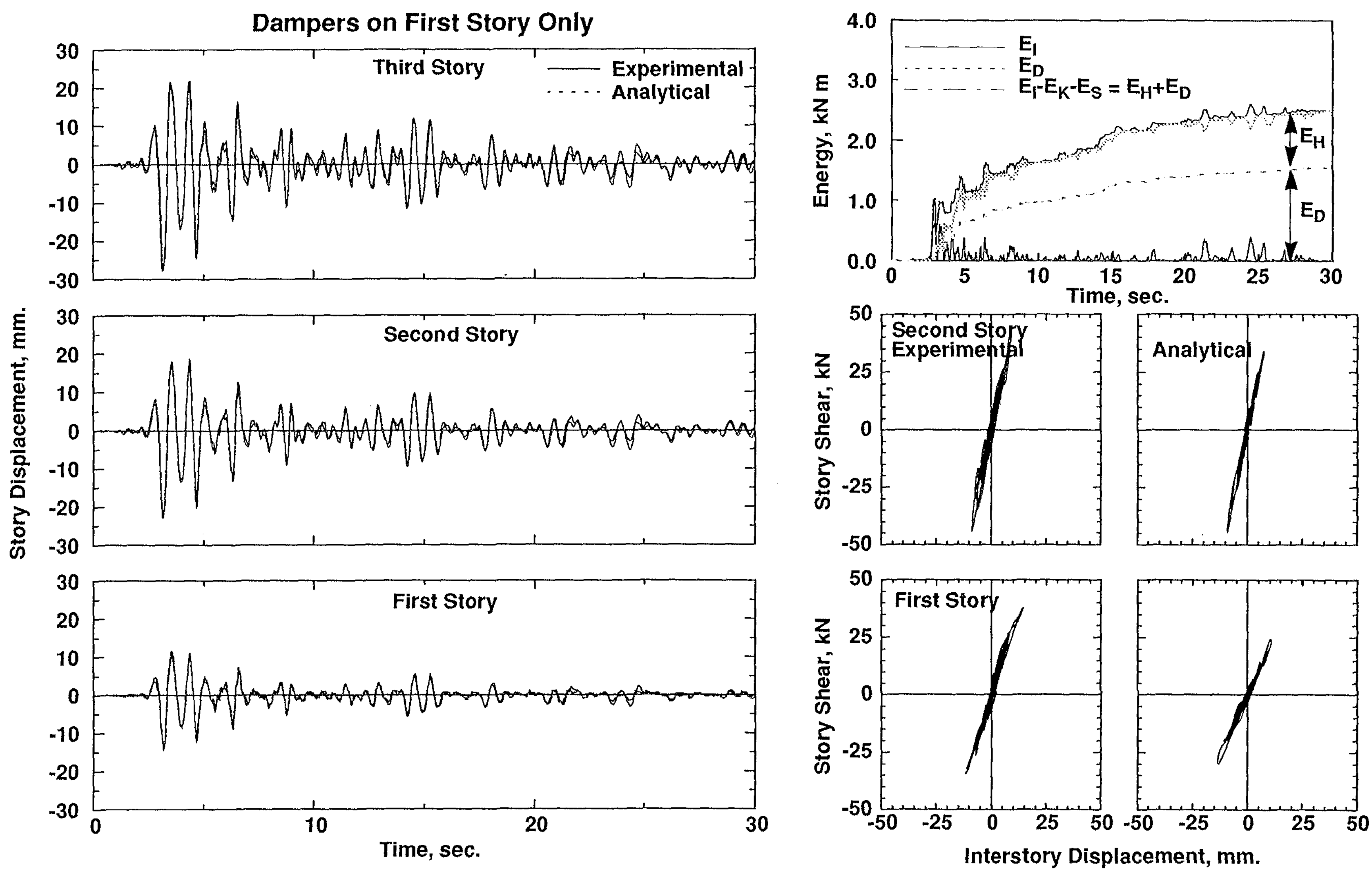

Figure 4.30 Experimental Results - TAFT 0.2g (NTA020)

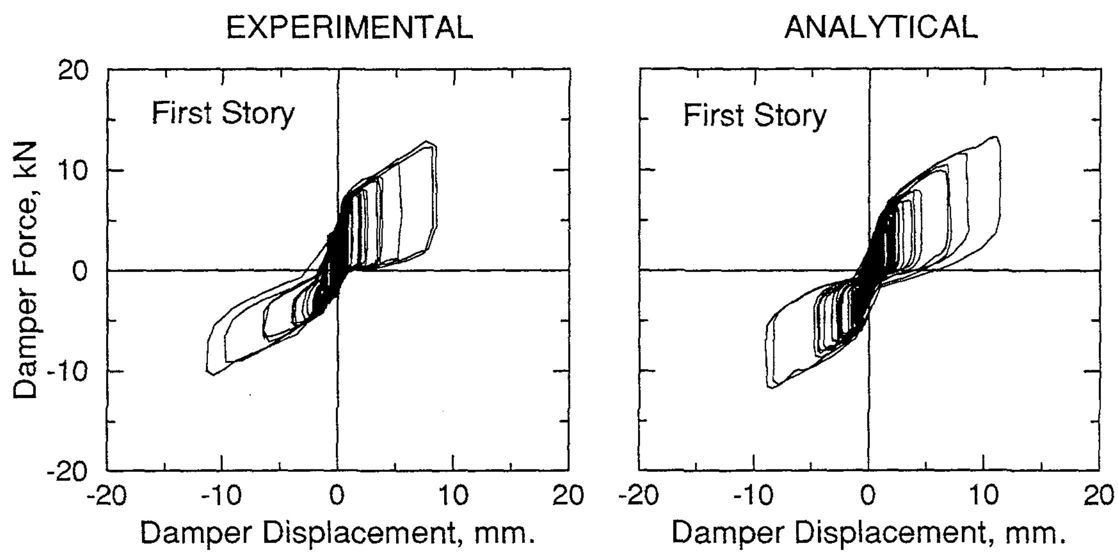

Figure 4.31 Damper Force-Deformation Behavior - TAFT 0.2g (NTA020)

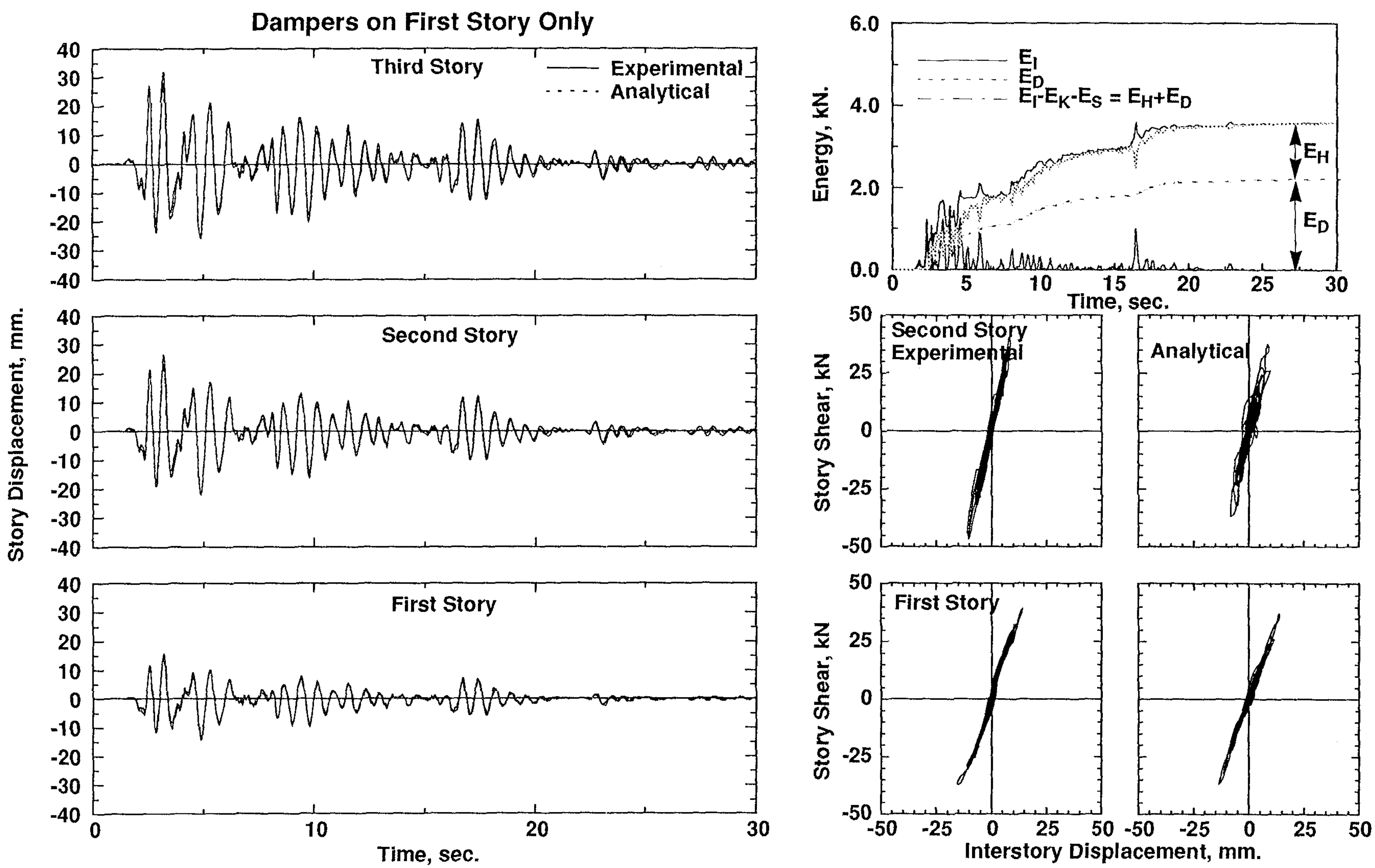

Figure 4.32 Experimental Results - EL CENTRO 0.3g (OEL030)

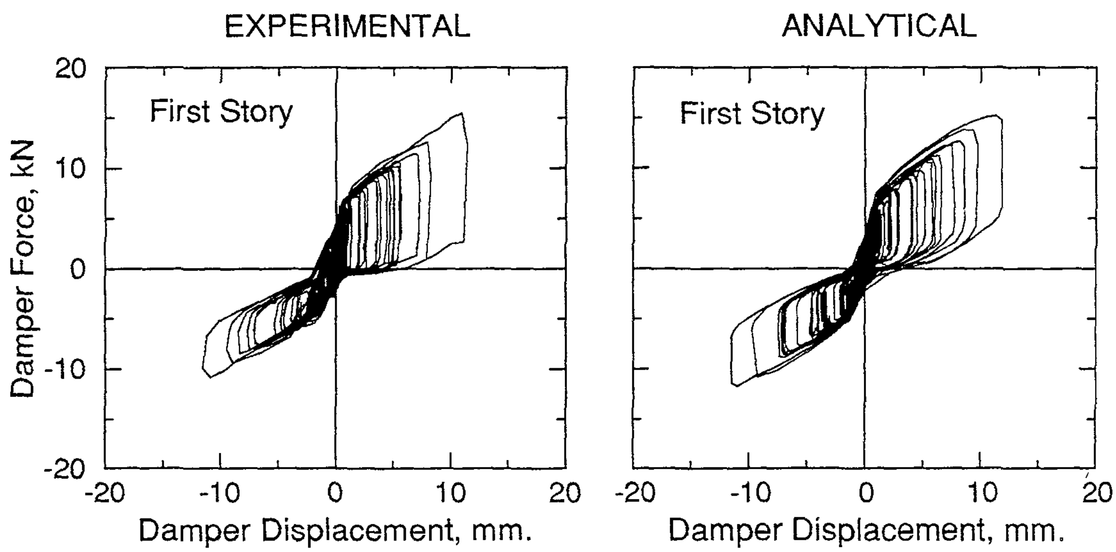

Figure 4.33 Damper Force-Deformation Behavior - EL CENTRO 0.3g (OEL030)

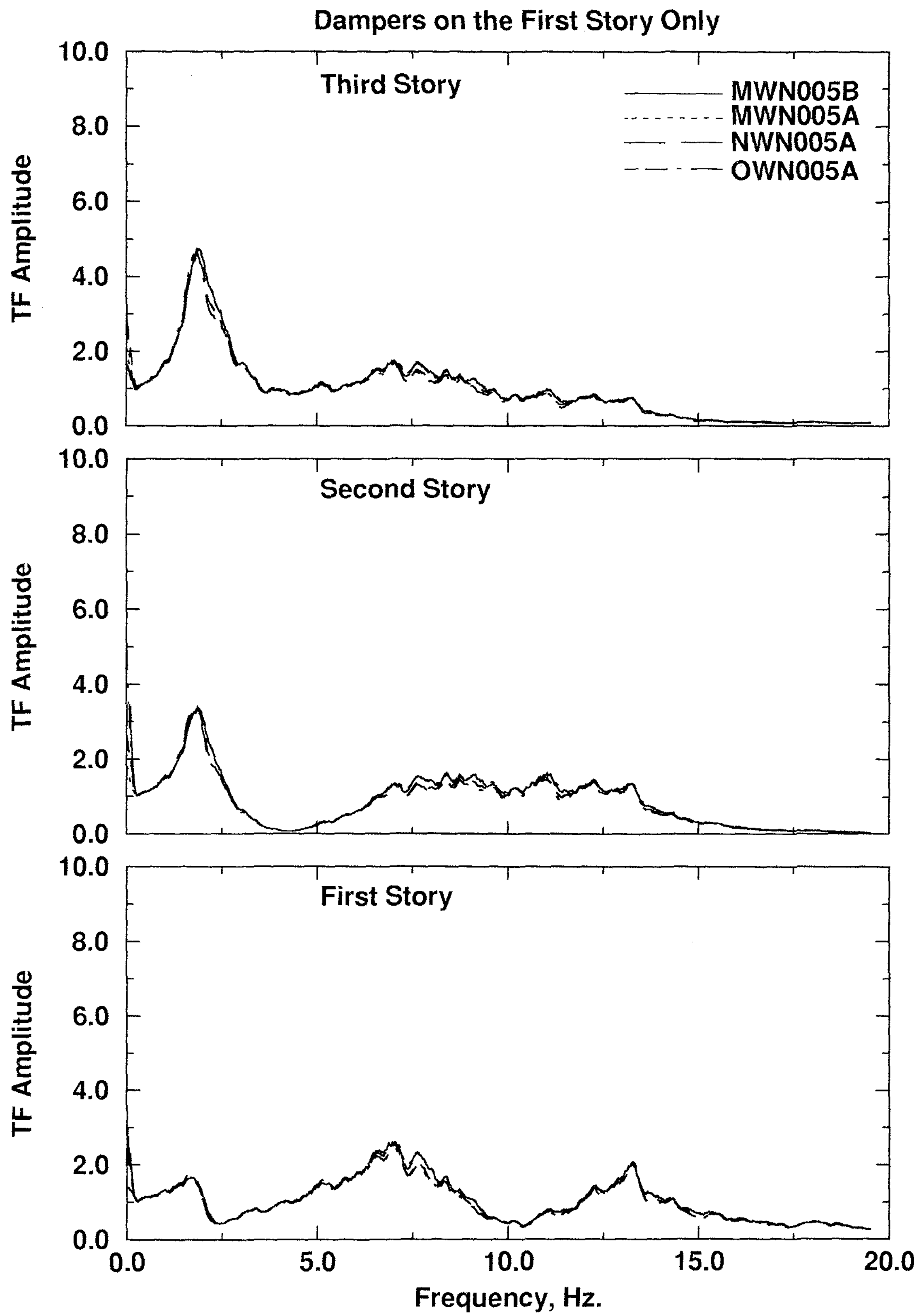

Figure 4.34 Story Transfer Functions
Dampers on the First Story Only

4.5.2 Simulated Ground Motion Test Results

The test structure was subjected to three simulated ground motions, namely Taft 0.05 g, Taft 0.2 g and El Centro 0.3 g. White noise tests were conducted after each ground motion test to identify the changes in the dynamic properties of the structure. As in the previous cases, the white noise test results have shown that the natural frequencies, equivalent viscous damping ratios and mode shapes did not change after these tests. Selected story level transfer functions are plotted on Figure 4.34. Table 4.4 summarizes the maximum response of the structure to the ground motions in terms of base and story level acceleration, velocity, interstory displacement (normalized with respect to story height), story shear (normalized with respect to story weight) and column axial force. Experimentally obtained story displacement time histories, story shear vs interstory displacement, damper force-displacement and energy time histories are plotted on Figures 4.30 to 4.33.

The measured maximum base acceleration was 0.32g where the observed maximum interstory drift was 1.3% for the El Centro 0.3g (OEL030) test. Corresponding values for the Taft 0.2 g test (NTA020) were 0.21 g and 0.8%. The maximum story velocity occurring in the third story level was 262 and 255 mm/sec for OEL030 and NTA020 tests, respectively. Normalized story shears were 10.8, 10.5% for the first story and 13.0, 12.4% of the story weight for the second story, respectively. Maximum column axial forces recorded during the El Centro 0.3 g test were 13.3 kN and 10.6 kN for the first floor exterior and interior columns, respectively. Corresponding values for Taft 0.2 g test were 12.6 kN and 8.4 kN. Total seismic input energy was 3.6 kNm for El Centro 0.3 g and 2.5 kNm for Taft 0.2 g. Some 62% of the input energy was dissipated by the dampers during both the El Centro 0.3 g and Taft 0.2 g tests.

4.6 Test on Bare Structure After All the Dampers were Removed

The purpose for retesting the structure after all dampers were removed was to obtain an indication as to the level of structural deterioration that took place due to the numerous tests conducted with dampers. Frequency shifts and changes in apparent viscous damping are indicators of structural (hysteretic) damage.

4.6.1 Initial Dynamic Properties of the Test Structure

After the first story dampers were removed, one white noise test was conducted inorder to identify the overall damage to the structure. Story level transfer functions were used to determine the natural frequencies, equivalent viscous damping ratios, mode shapes and story stiffnesses. The natural frequencies were found to be 1.42, 5.86 and 12.72 Hz with corresponding equivalent viscous damping ratios of 7.8, 3.1, and 2.4%. Story level transfer functions for this test were plotted on Figure 4.37.

4.6.2 Simulated Ground Motion Test Results

The test structure was subjected to three simulated ground motions, namely Taft 0.05 g, Taft 0.2 g and El Centro 0.3 g (Table 3.3). White noise tests were conducted after each ground motion test to identify the changes in the dynamic properties of the structure. As in the previous cases, the white noise test results show that the natural frequencies, equivalent viscous damping ratios and mode shapes did not change considerably, after these tests. Selected story level transfer functions are plotted on Figure 4.37. Table 4.1 summarizes the maximum response of the structure to the ground motions in terms of base and story level acceleration, velocity, interstory displacement (normalized with respect to story height), story shear (normalized with respect to story weight) and column axial force. Experimentally obtained story displacement time histories, story shear vs interstory displacement and energy time histories are plotted on Figures 4.35 and 4.36.

The measured maximum base acceleration was 0.29 g where the observed maximum interstory drift was 2.7% for the El Centro 0.3 g (REL030) test. Corresponding values for Taft 0.2 g test (QTA020) were 0.21 g and 1.9%. The maximum story velocity occurring in the third story level was 343 and 239 mm/sec for the REL030 and QTA020 tests, respectively. Normalized story shears were 17.4, 14.1% for the first story and 7.7, 10.1% of the story weight for the second story, respectively. Maximum column axial forces recorded during the EL Centro 0.3 g test were 8.5 kN and 13.3 kN for the first floor exterior and interior columns, respectively. Corresponding values for Taft 0.2 g test were 8.9 kN and 8.7 kN. Total seismic input energy was 3.2 kNm for El Centro 0.3 g and 2.1 kNm for Taft 0.2 g.

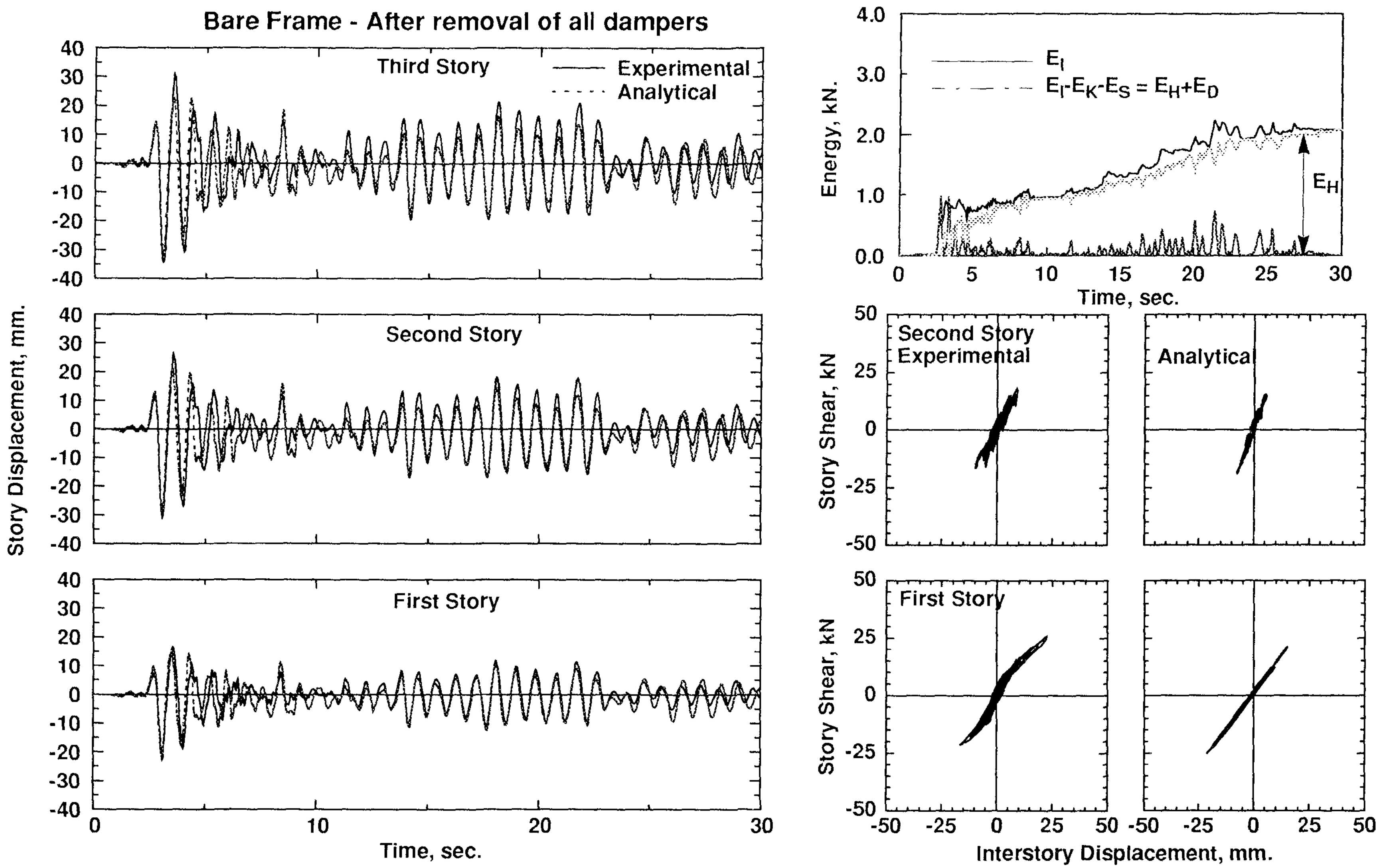

Figure 4.35 Experimental Results - TAFT 0.2g (QTA020)

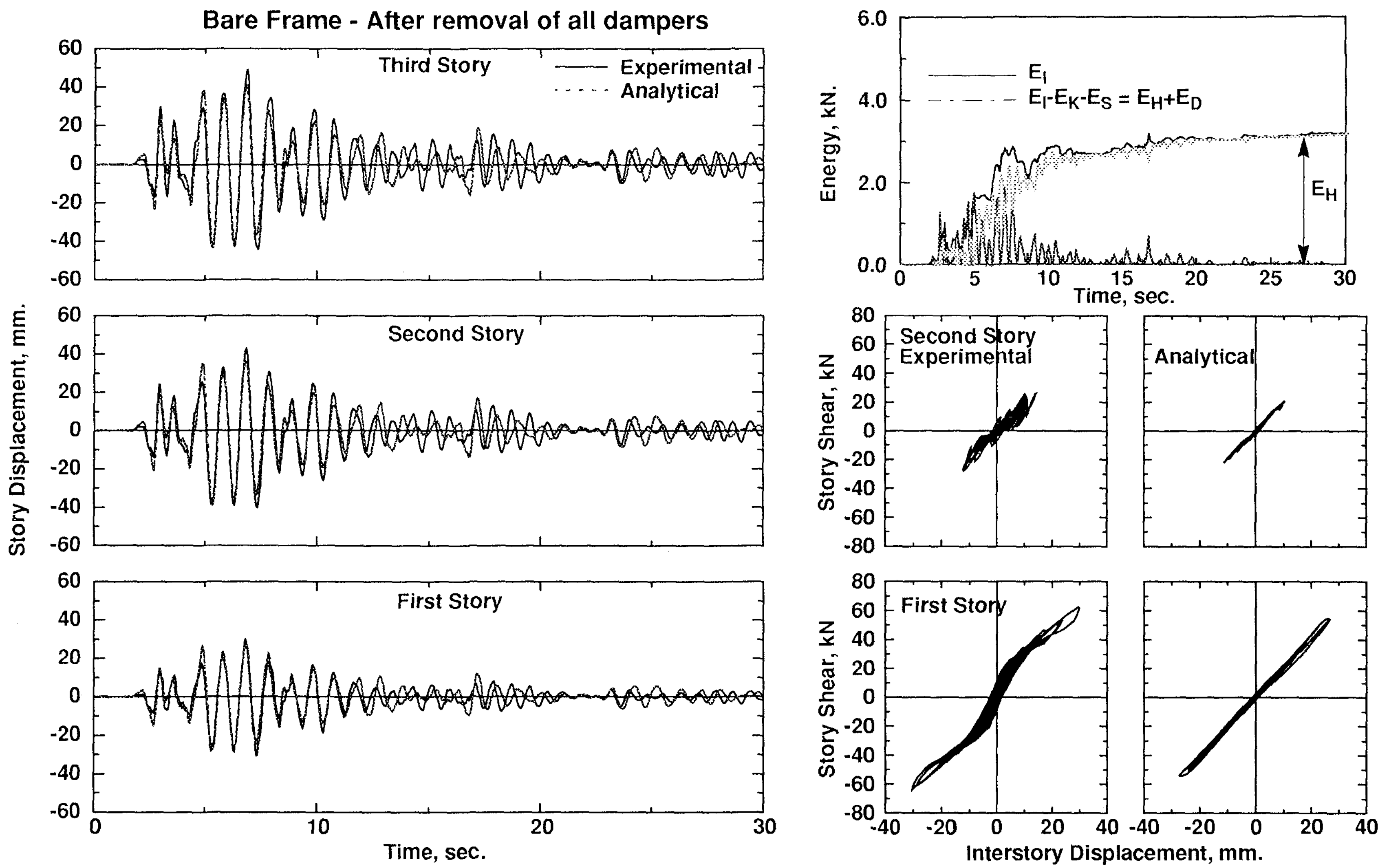

Figure 4.36 Experimental Results - EL CENTRO 0.3g (REL030)

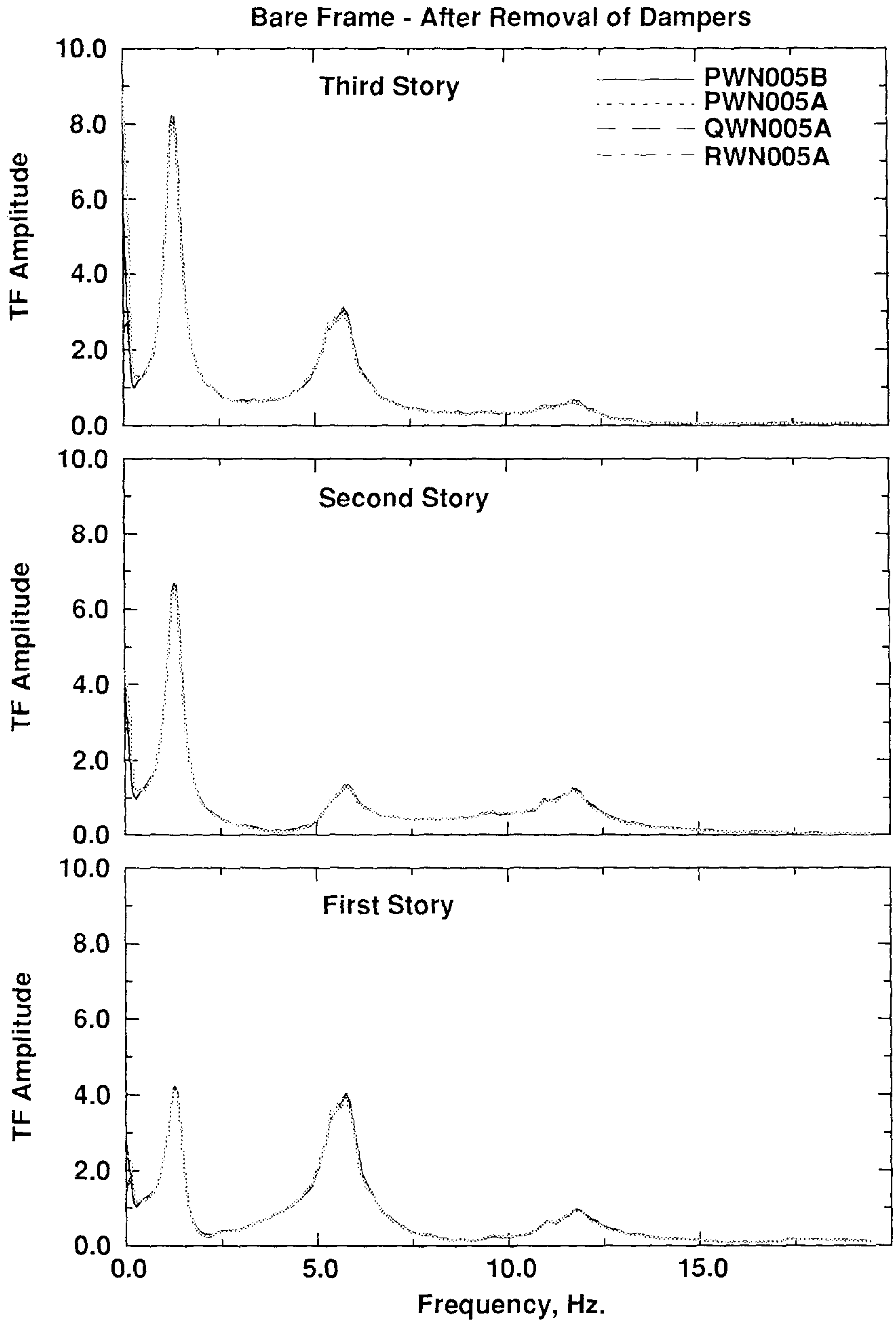

Figure 4.37 Story Transfer Functions
Bare Frame - After Removal of Dampers

SECTION 5

DISCUSSION OF STRUCTURAL RESPONSE AND ANALYTICAL PREDICTIONS

5.1 Introduction

This section is intended to furnish an overall discussion on the structural response observed from shaking table tests which were reported in the previous section. Preliminary effects of the four different damper configurations on the behavior of the test structure are discussed mainly referring to the following type of responses: 1) Story displacement, 2) Story shear, 3) Damper force-displacement relationship, and 4) Energy response.

Performance of the DRAIN-2DX computational model in predicting the structural response under simulated ground motions is also reviewed in comparison with the experimental results. In so doing, Taft and El Centro earthquakes, respectively scaled to 0.2 g and 0.3 g peak ground accelerations, were utilized as the comparative benchmark motions for the reasons mentioned earlier. Story displacement time histories, story shear-interstory displacement response, damper force-deformation relationships and seismic energy time histories were chosen to form the basis for the comparison.

5.2 DRAIN-2DX Computational Model of the Test Structure

Time history analyses were performed for two earthquake motions: El Centro 0.3 g and Taft 0.2 g with different damper configurations. All of the analyses were performed using the shaking table response signals as input for the analysis.

A general observation of the test results given in the previous section shows that analytically obtained story displacement time histories are in very good agreement with those experimentally obtained, especially for the model with the elastomeric spring dampers. However, analytical response for the unretrofitted (undamped) model has a better fit, generally for the first 10 sec. of ground motions, than the rest of the response histories. This can be explained by the fact that the highly damaged-inelastic model structure became more flexible. Crack openings at the column base connections for the lower amplitude motions are small, therefore the structure is stiffer. This type of behavior (rocking behavior) can be accurately modeled with an element whose force deformation relationship possesses the necessary details. However, although it is not impossible to model this in DRAIN-2DX, it was decided that the regular beam-column element with a specified P-M interaction would suffice to capture the overall behavior. This is not an unrealistic assumption, since the dampers reduced the rotation demand at the column ends significantly and kept the load bearing elements mostly within the elastic region.

5.3 Comparison of the Structural Performance with Different Damper Configurations

5.3.1 Structural Dynamic Properties

Dynamic properties of the test structure with and without dampers were determined from the story level transfer functions as explained in Section 4 and shown in Figure 5.1. Table 5.1 summarizes the natural frequencies, mode shapes, stiffness matrices and equivalent viscous damping ratios for the three different damper configurations and for the bare structure. Comparison of the story transfer functions (Figure 5.1) for the damped and undamped structure reveals that the effects of higher modes on the seismic response are reduced to a negligible level by the elastomeric spring dampers.

Natural frequencies of the structure were 1.42, 5.59 and 11.89 Hz for the three modes of the undamped structure and increased to 2.76, 11.18 and 15.97 Hz after the dampers were installed on all stories. This increase reflects the stiffness contribution of the damper braces. The equivalent viscous damping ratios increased approximately three times from 8.9 , 5.4 , 1.9% to 23.4 , 17.7 , 4.3% , respectively. It should be noted here that for small displacement amplitudes, dampers behaved more like bracing elements while still dissipating energy. For large displacement amplitudes energy dissipation characteristics, rather than stiffening, dominated the response. A comparison of two white noise test results

(Table 5.1) for the undamped structure before and after the earthquake ground motion tests indicates that the structure did not suffer any significant damage during these experiments. This implies that the elastomeric spring dampers, while dissipating a major portion of seismic input energy, kept the structural elements within their elastic ranges of behavior as discussed in the following paragraphs.

Table 5.1: Comparison of Structural Dynamic Properties

	Natural Freq. Hz	Mode Shape	Stiffness Matrix kN-m	Story Stiff. kN-m	Damp. Ratio %
No Damper[a]	$\begin{Bmatrix}1.42\\5.59\\11.89\end{Bmatrix}$	$\begin{bmatrix}1.00 & -0.74 & -0.52\\0.86 & 0.28 & 1.00\\0.51 & 1.00 & -0.69\end{bmatrix}$	$\begin{bmatrix}10.4 & -14.1 & 4.8\\-14.1 & 26.0 & -15.6\\4.8 & -15.6 & 18.1\end{bmatrix}$	$\begin{Bmatrix}14.1\\15.6\\2.5\end{Bmatrix}$	$\begin{Bmatrix}8.9\\5.4\\1.9\end{Bmatrix}$
Dampers on All Stories	$\begin{Bmatrix}2.76\\11.18\\15.97\end{Bmatrix}$	$\begin{bmatrix}1.00 & -0.81 & -0.64\\0.92 & 0.50 & 1.00\\0.67 & 1.00 & -0.54\end{bmatrix}$	$\begin{bmatrix}33.6 & -37.3 & 0.4\\-37.3 & 52.7 & -14.4\\0.4 & -14.4 & 34.7\end{bmatrix}$	$\begin{Bmatrix}37.3\\14.4\\20.3\end{Bmatrix}$	$\begin{Bmatrix}23\\18\\4.3\end{Bmatrix}$
Dampers on First 2 Stories	$\begin{Bmatrix}2.71\\7.96\\14.43\end{Bmatrix}$	$\begin{bmatrix}1.00 & -0.83 & -0.32\\0.72 & 0.73 & 1.00\\0.42 & 1.00 & -0.70\end{bmatrix}$	$\begin{bmatrix}11.6 & -17.4 & 2.3\\-17.4 & 46.3 & -21.7\\2.3 & -21.7 & 29.2\end{bmatrix}$	$\begin{Bmatrix}17.4\\21.7\\7.5\end{Bmatrix}$	$\begin{Bmatrix}22\\6.9\\4.6\end{Bmatrix}$
Dampers on First Story Only	$\begin{Bmatrix}2.02\\7.18\\12.30\end{Bmatrix}$	$\begin{bmatrix}1.00 & -0.65 & -0.59\\0.76 & 0.50 & 1.00\\0.32 & 1.00 & -0.87\end{bmatrix}$	$\begin{bmatrix}12.6 & -15.8 & 5.5\\-15.8 & 25.3 & -14.6\\5.5 & -14.6 & 26.7\end{bmatrix}$	$\begin{Bmatrix}15.8\\14.6\\12.1\end{Bmatrix}$	$\begin{Bmatrix}17\\6.1\\3.1\end{Bmatrix}$
No Damper[b]	$\begin{Bmatrix}1.42\\5.86\\11.72\end{Bmatrix}$	$\begin{bmatrix}1.00 & -0.74 & -0.51\\0.86 & 0.31 & 1.00\\0.50 & 1.00 & -0.67\end{bmatrix}$	$\begin{bmatrix}10.3 & -14.1 & 3.9\\-14.1 & 26.0 & -14.7\\3.9 & -14.7 & 17.9\end{bmatrix}$	$\begin{Bmatrix}14.1\\14.7\\3.2\end{Bmatrix}$	$\begin{Bmatrix}7.8\\3.1\\2.4\end{Bmatrix}$

a. Bare frame results before dampers installed.

b. Bare frame results after removal of all dampers.

5.3.2 Response of the Structure

Experimentally obtained story drift time histories for the structure with dampers at all stories and without dampers are compared for the El Centro 0.3 g ground motion and the Taft 0.2 g record in Figures 5.2 and 5.3, respectively. Also plotted on the figures is the analytical response obtained from the enhanced DRAIN-2DX computational model. It should be noted that good agreement has been obtained between analytical and experimental results. Maximum interstory drifts and normalized story shears observed during El Centro 0.3 g and Taft 0.2 g tests for different damper configurations and the undamped structure are summarized in Table 5.2. Significant (50-60%) reduction of interstory drifts can be observed from the table. Story shears were also reduced by some 20-35% compared to the undamped case. Also given in Table 5.2 are the story level accelerations for different damper configurations.

First story displacement time histories of different damper configurations are plotted in Figures 5.4 and 5.5 for El Centro 0.3 g and Taft 0.2 g, respectively. It can be seen from these figures and Table 5.2 that adding dampers to the top story provides little or no response reduction. However, it should be noted here that all the dampers used in this experimental study had similar characteristics. Had the damper properties been chosen for the best performance for specific story levels, response of the structure could be improved. This important issue will be pointed out in the next section.

Figures 5.6 and 5.7 plot the experimental and analytical interstory displacement vs. story shear response of the structure with and without dampers for the El Centro 0.3 g and Taft 0.2 g tests. The nonlinearity evident in the undamped case is indicative of column damage. With a more extreme ground motion, this damage would likely lead to a "soft story" collapse mechanism.

Force-deformation behavior of the dampers for the 0.3g El Centro and 0.2 g Taft tests are plotted in Figure 5.8 and 5.9, respectively. Dampers exhibited hysteretic behavior which was regular, repeatable and accurately predicted from the enhanced DRAIN- 2D computational model. No reduction in strength and/or stiffness was observed upon repeated cycling. Self-centering behavior of the elastomeric spring

Table 5.2: Maximum Responses

Shaking Table Test		Acceleration g.			Interstory Displ. / Story Height[a]			Story Shear / Story Weight[b]		
	Story	1st	2nd	3rd	1st	2nd	3rd	1st	2nd	3rd
Taft 0.2g	No damper	0.313	0.145	0.260	0.019	0.008	0.004	0.144	0.101	0.087
	Dampers on First Story	0.254	0.195	0.264	0.012	0.008	0.005	0.105	0.124	0.089
	Dampers on First 2 Stories	0.200	0.158	0.293	0.009	0.006	0.003	0.090	0.097	0.099
	Dampers on All Stories	0.153	0.168	0.237	0.007	0.006	0.003	0.093	0.090	0.072
El Centro 0.3g	No Damper	0.285	0.186	0.268	0.024	0.011	0.005	0.176	0.129	0.089
	Dampers on First Story	0.192	0.191	0.247	0.013	0.009	0.005	0.108	0.130	0.081
	Dampers on First 2 Stories	0.201	0.232	0.237	0.015	0.008	0.004	0.120	0.096	0.080
	Dampers on All Stories	0.222	0.231	0.281	0.017	0.008	0.003	0.141	0.093	0.097

a. 1.22 m

b. 360 kN

dampers can be observed as well from these figures. One of the drawbacks of some types of damping devices is that they may not be as effective in reducing the initial large peak response as they are in reducing the overall response. However, as can be seen in Figures 5.4 to 5.7, elastomeric spring dampers performed quite well in damping out both the initial peak response and the overall response.

5.3.3 Energy Response

The primary objective of using supplemental damping devices is to dissipate the seismic input energy so as to keep the structural hysteretic energy to a minimum. The seismic input energy can be identified considering the different energy dissipation mechanisms (Uang 1990) as given in Section 4, Equation (4-1).

Experimentally obtained seismic input energy and energy dissipated by the elastomeric spring dampers are plotted in Figure 5.10. As can be seen from the figure, dampers dissipated 50 to 80% of the seismic input energy, leaving only a small amount to be dissipated by the structural elements and by other means. There is some increase in the seismic input energy E_I going from the bare structure case to the fully-damped case due to the additional stiffness provided by the damper braces. However, in each case the increase in the input energy was dissipated by the dampers reducing the hysteretic energy in the structure as well. In general, the amount of energy dissipated by the dampers did not change significantly between the fully-damped and two-story damped cases.

5.3.4 Column Axial Forces

Addition of the damper braces to the structure changes the load transfer pattern in the structure. Hence, more force is induced especially in the columns near the dampers. As can be seen from Tables 4.1 to 4.4, interior column axial forces whereas exterior ones increased about 30 to 50% for the ground motions studied. Therefore, in design of structures employing these types of dampers, care should be taken. A conclusive statement can not be made in the present case, due to the fact that the columns in the test structure were already slightly damaged.

5.4 Final Remarks on Response Comparisons

Maximum response envelopes for the three-story test structure without and with elastomeric spring dampers are presented in Figures 5.11 and 5.12 for the El Centro $0.3g$ and Taft $0.2g$ tests respectively. As can be seen from these figures, overall response of the structure is significantly reduced by the addition of the dampers. It is interesting to note that there is a little or no difference in the performance of the structure with dampers on all stories and dampers only on the first two stories. This observation leads to the conclusion that optimum placement and optimum damper properties should be studied for the most effective response control before implementing the dampers to the structure.

Significant reduction in total and column shear forces imply that the elastomeric spring dampers worked well in reducing the shear demand in the columns. A similar conclusion can be drawn based on the reduction in overturning moments. A different comparison of shear responses which presents profiles of shear coefficients at the three levels of the test structure is also given on Figures 5.11 and 5.12. An inspection of the recorded damper forces for different damper configurations shows that structural response is controlled with slight increase in the damper force in each case, keeping the total story column shear at minimum.

Interstory drift and story total column shears for Hachinohe 0.3g, El Centro 0.3g and 0.4g, and Pacoima 0.4g earthquake ground motions are compared in Figure 5.13 for the structure with and without the presence of the elastomeric spring dampers. Also shown in these figures are the interstory drift limits at which story collapse is expected and story shears when the full plastic mechanism of the frame forms. It must be noted here that results for the bare structure under Hachinohe 0.3g, El Centro 0.4g and Pacoima 0.4g earthquakes are obtained analytically. Figure 5.13 clearly shows that for the bare frame structure (with no dampers) a collapse mechanism generally forms, and collapse (due to high interstory drifts) is expected, when the peak ground acceleration approaches to 0.4g. However, with the presence of the elastomeric spring dampers, the column shears are reduced, and columns thus remain essentially elastic. The interstory drifts are still substantial in the first story, but these are reduced some 30% to 40% when dampers are used.

It is thus evident that, based on interstory displacement limitations, a significantly greater interstory ground shaking can be withstood if dampers are used.

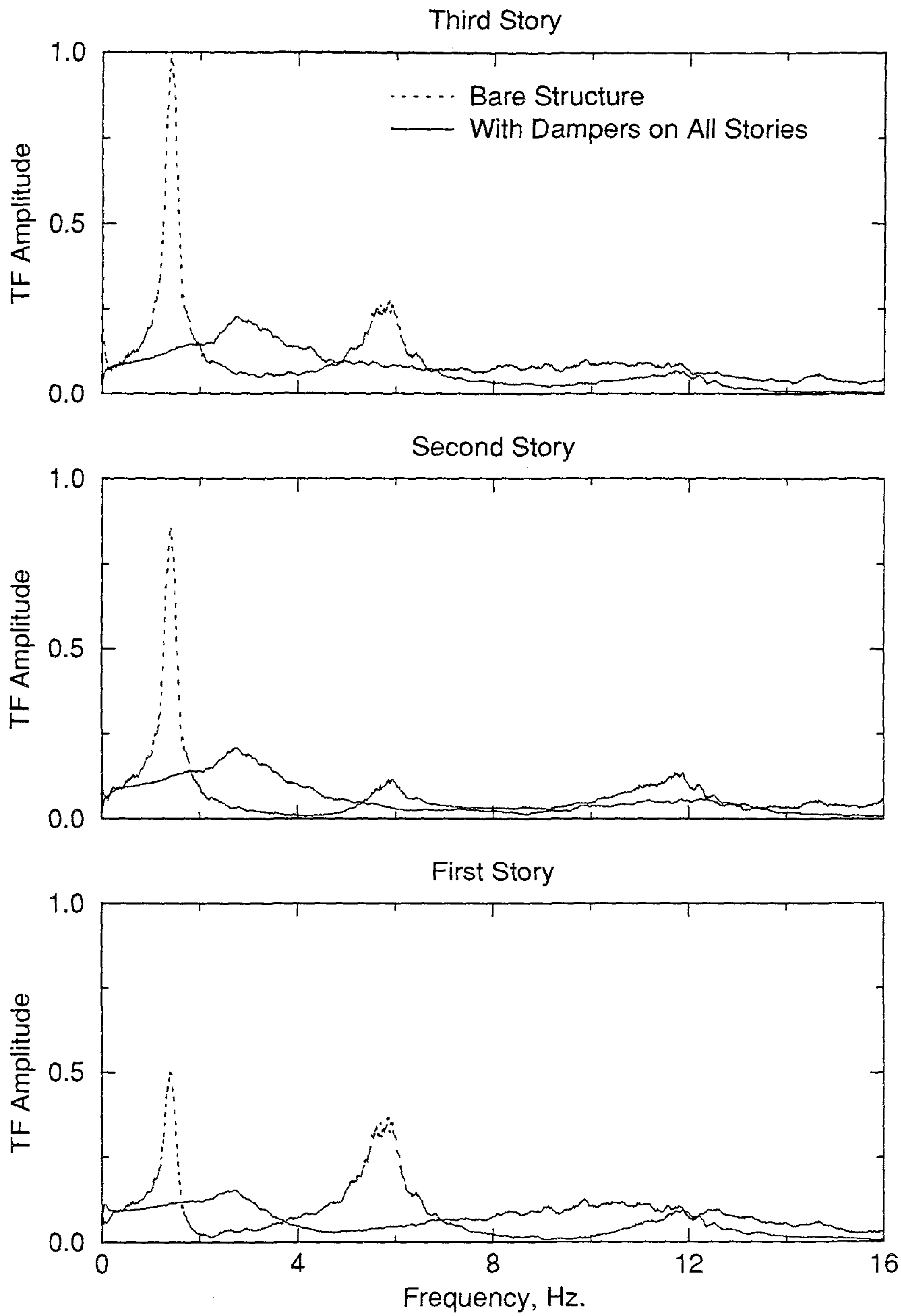

Figure 5.1 Normalized Transfer Functions

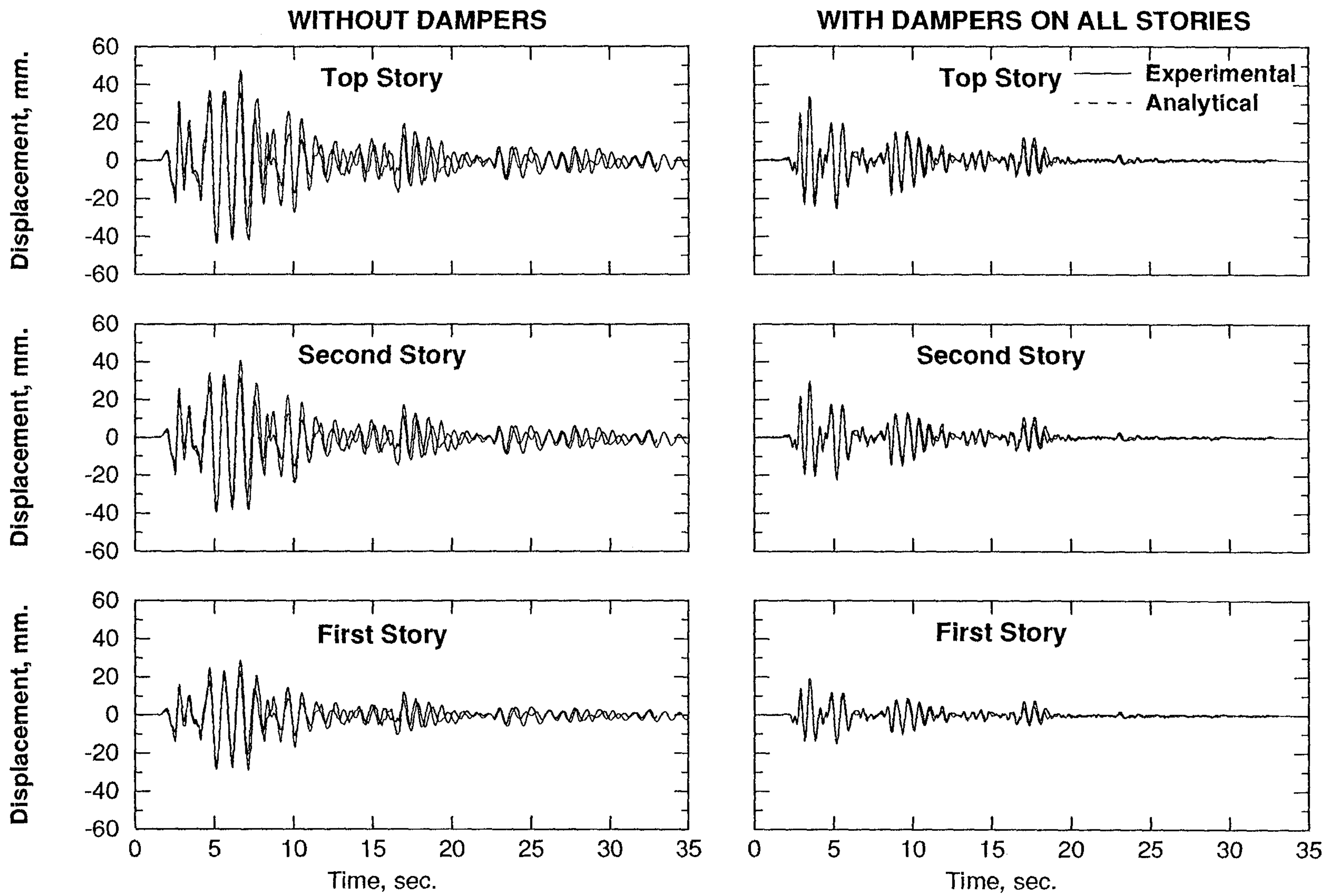

Figure 5.2 Seismic Response of the Structure with and without Dampers - Elcentro 0.3g

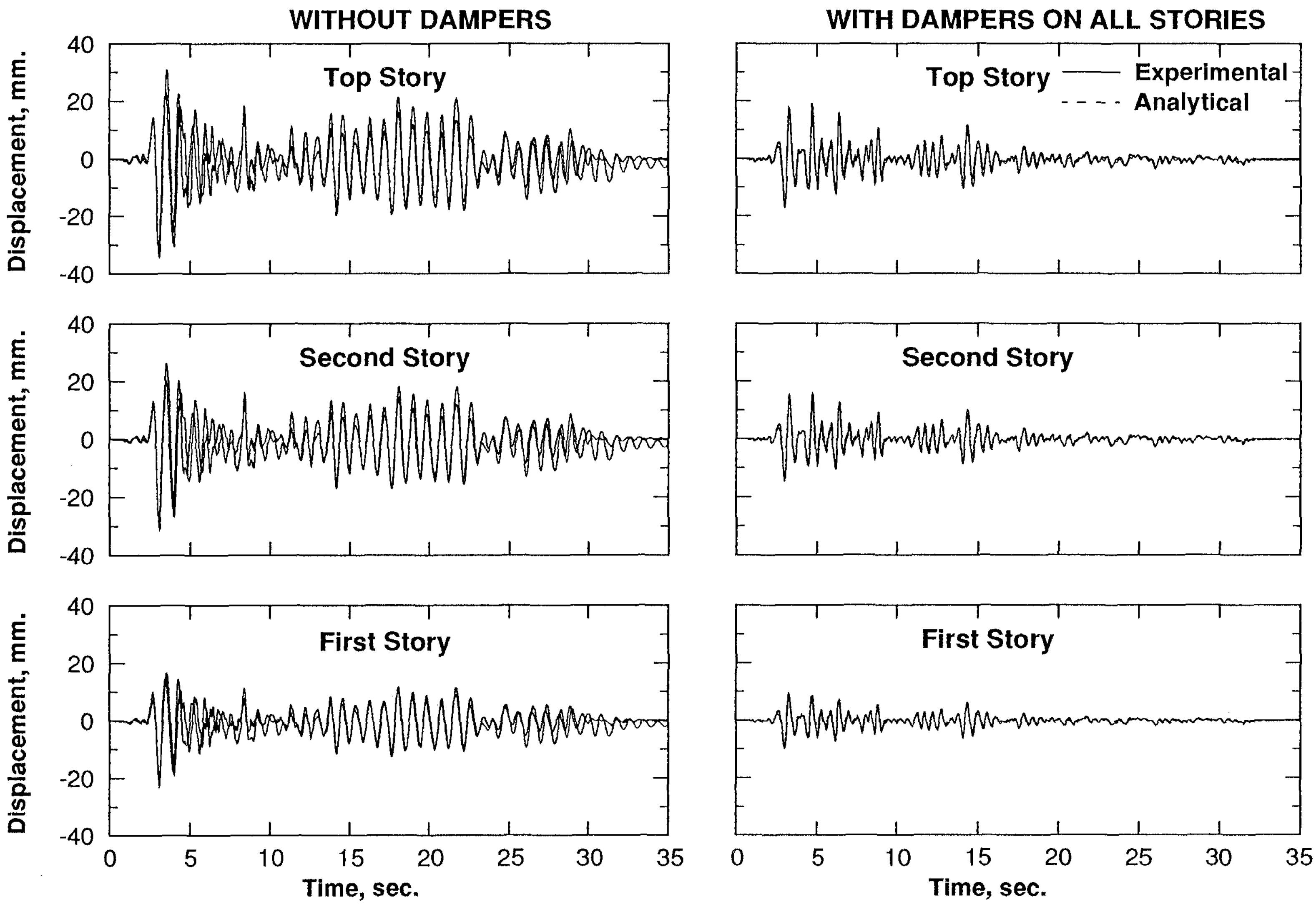

Figure 5.3 Seismic Response of the Structure with and without Dampers - Taft 0.2 g

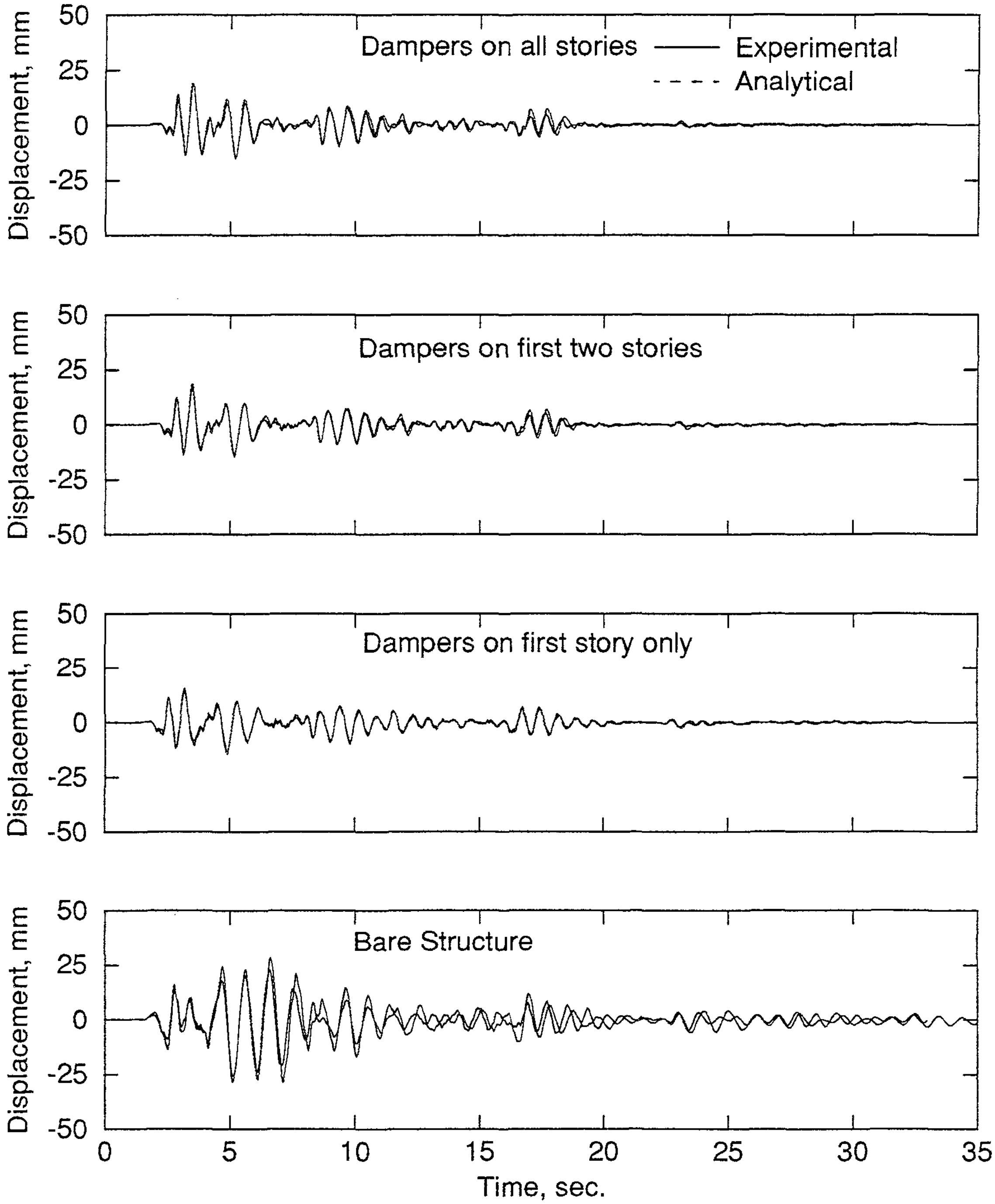

Figure 5.4 Effect of Damper Configuration on the Seismic Response Elcentro 0.3g

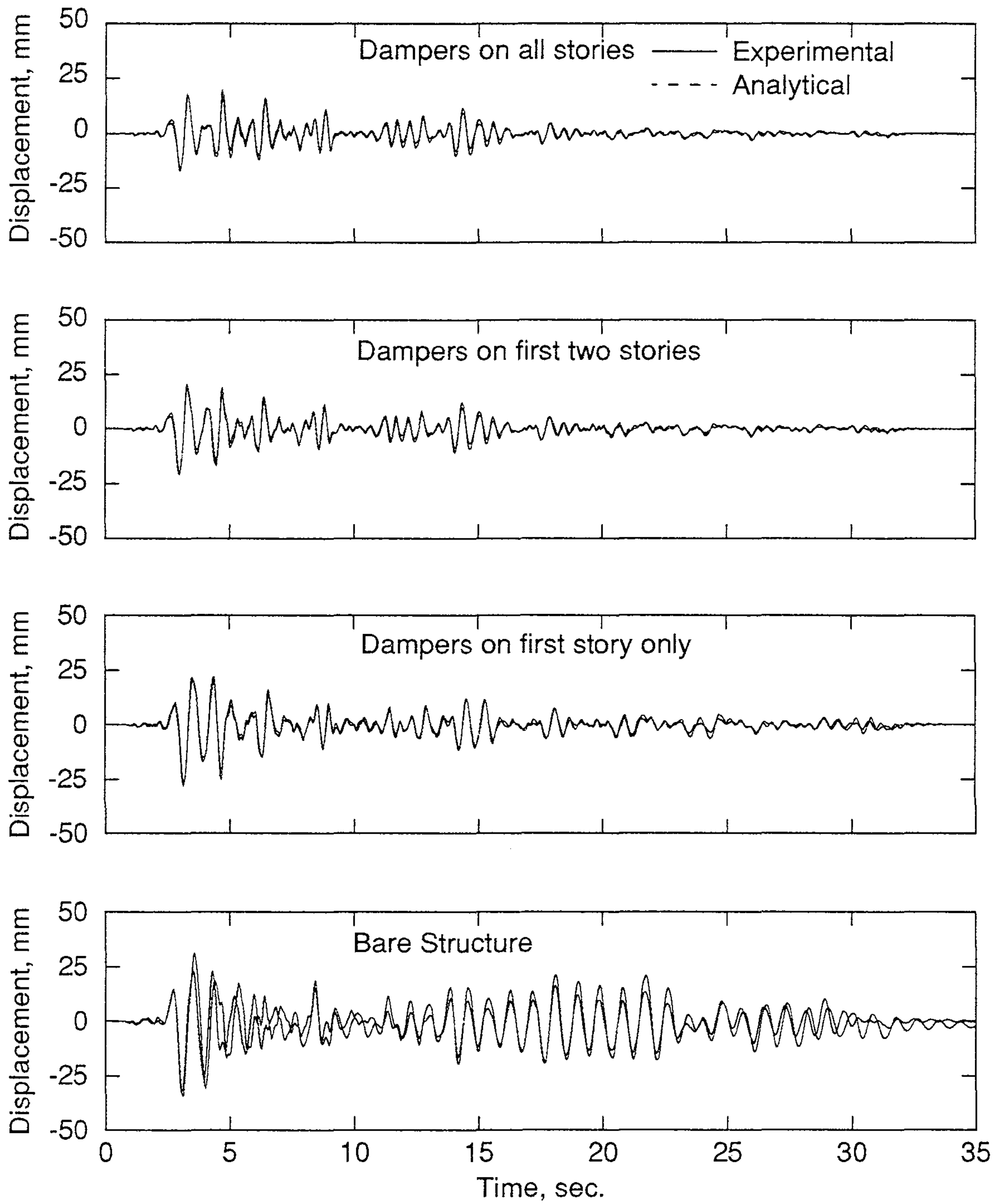

Figure 5.5 Effect of Damper Configuration on the Seismic Response Taft 0.2g

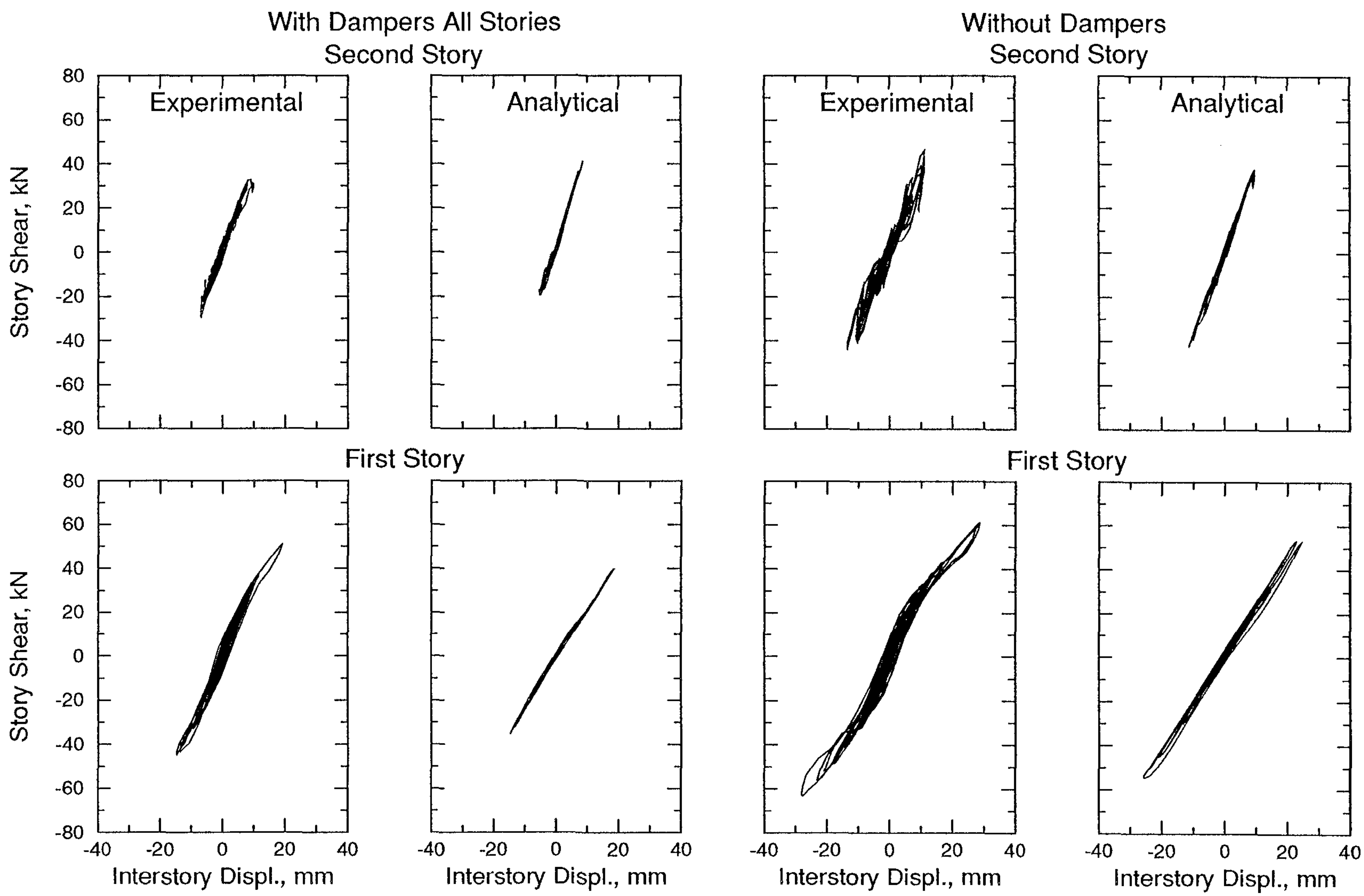

Figure 5.6 Story Shear vs. Inter Story Displacement Comparison - El Centro 0.3g

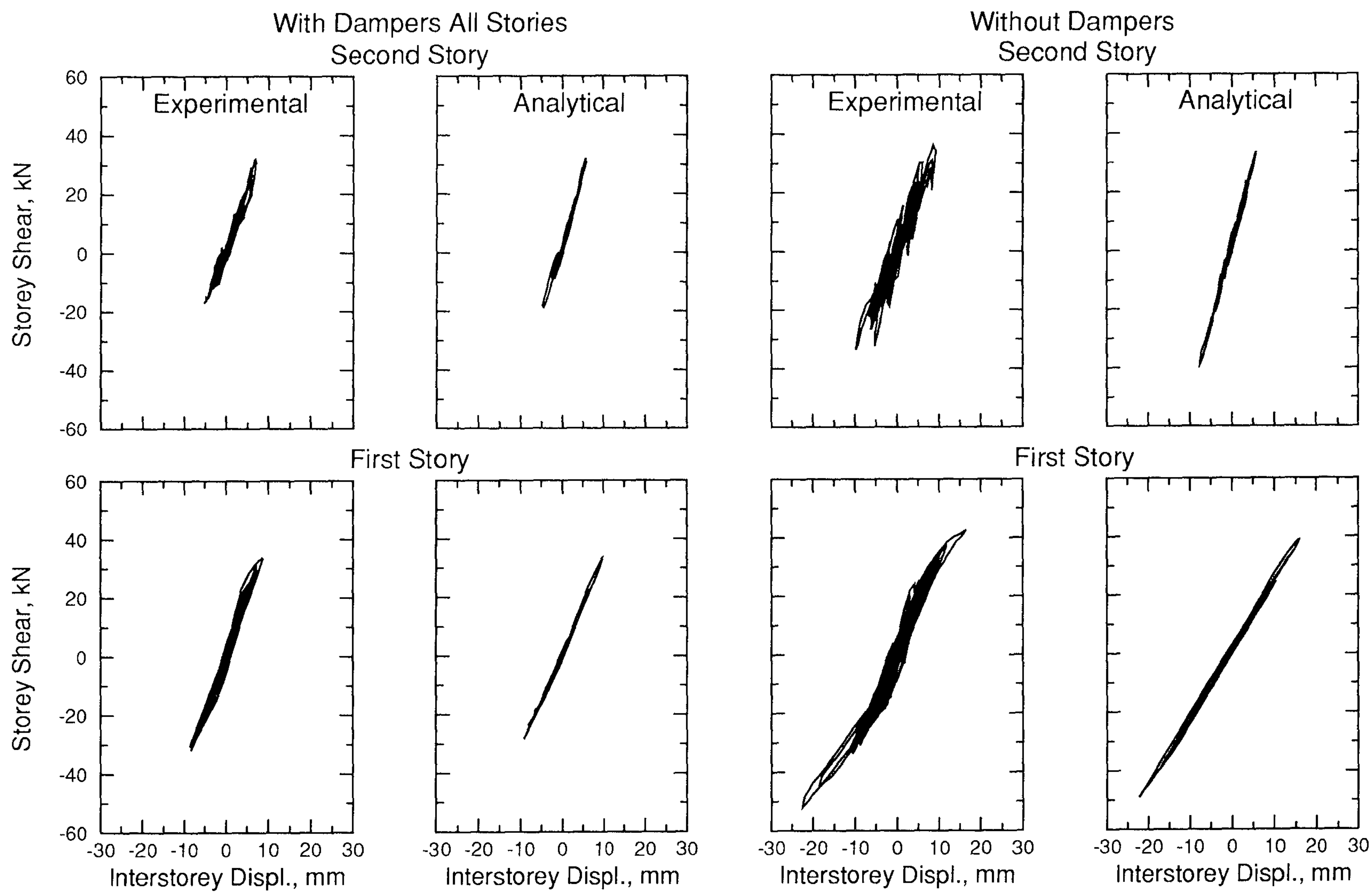

Figure 5.7 Story Shear vs. Inter Story Displacement Comparison - Taft 0.2g

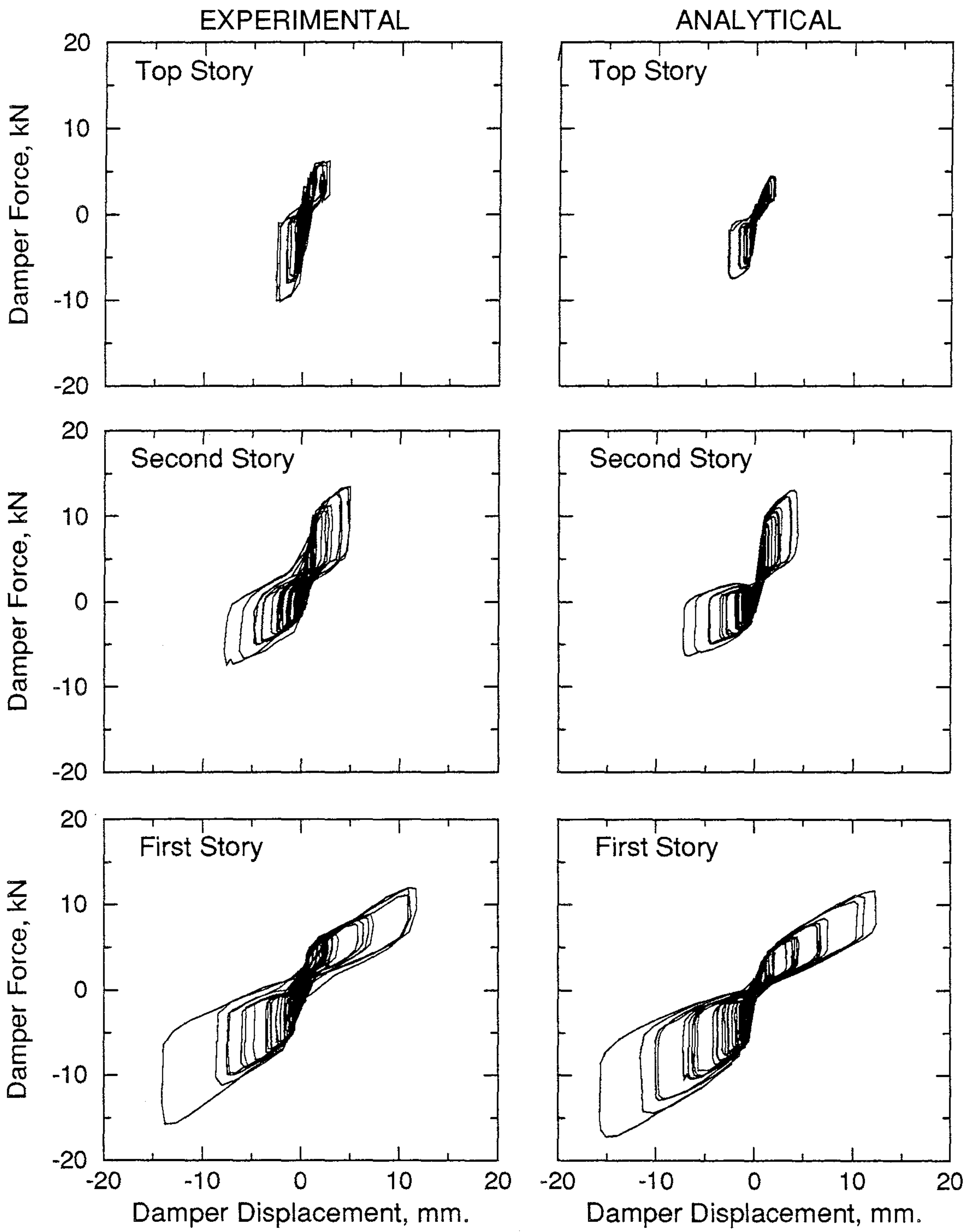

Figure 5.8 Damper Force-Deformation Behavior - El Centro 0.3g

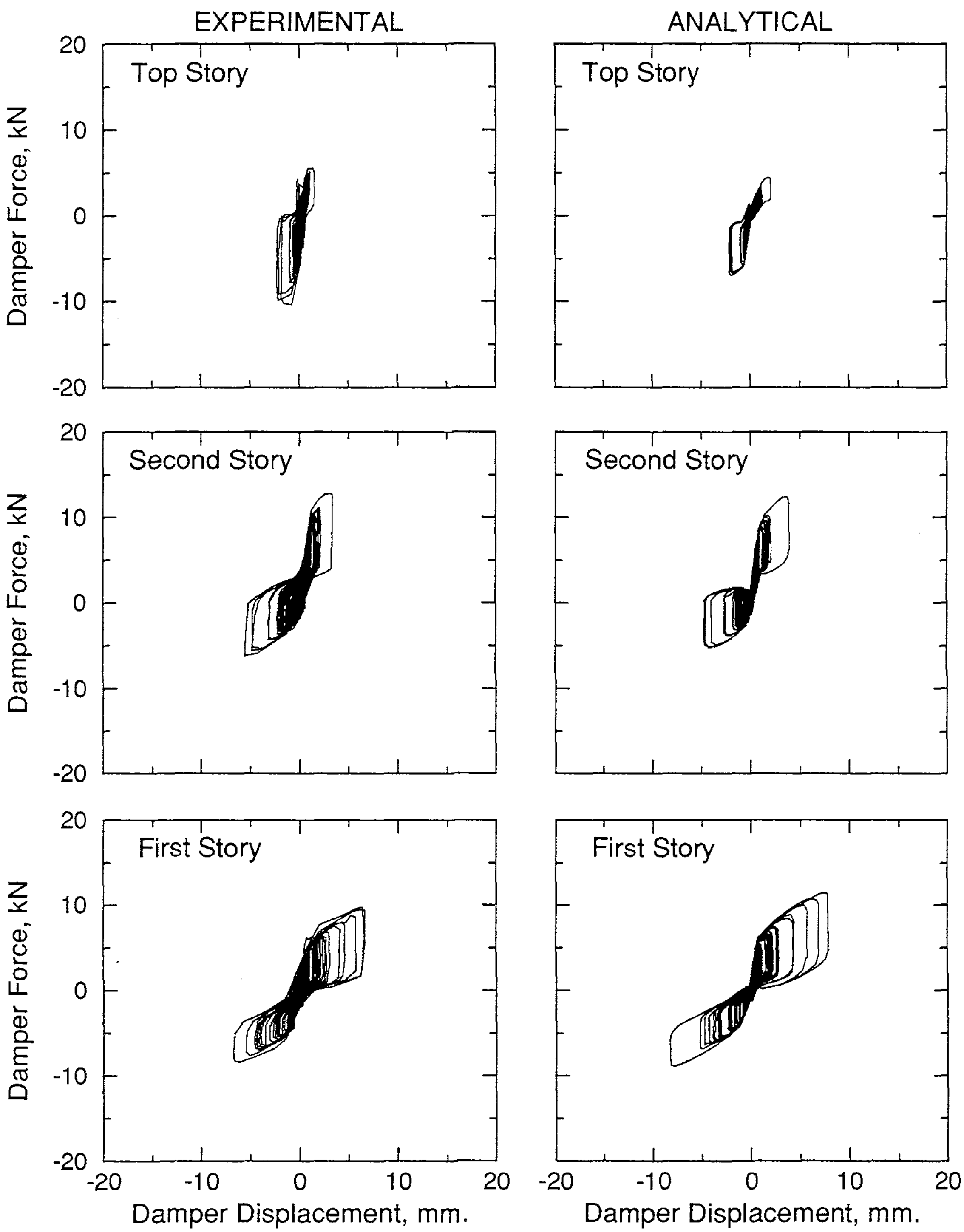

Figure 5.9 Damper Force-Deformation Behavior - Taft 0.2g

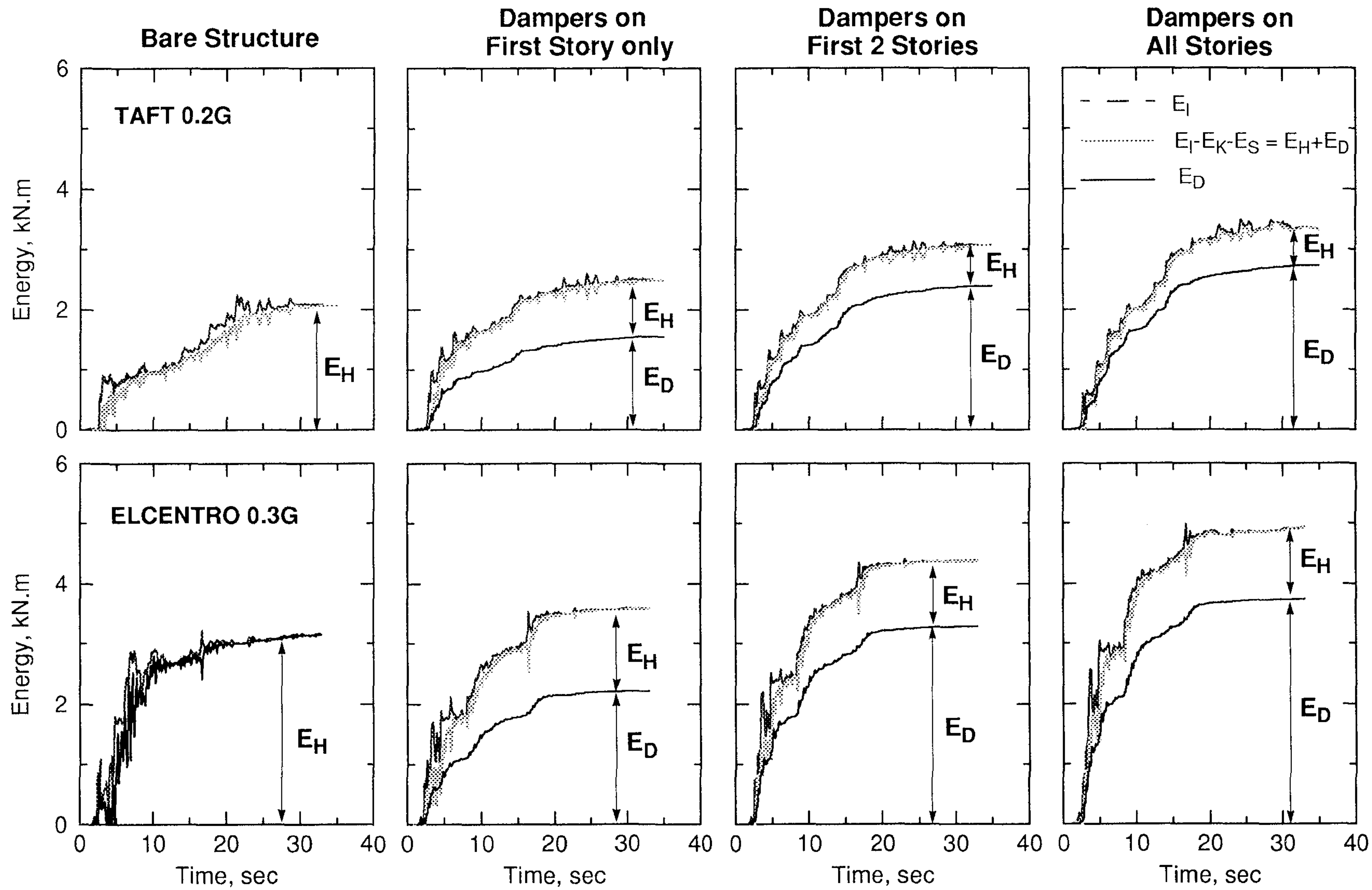

Figure 5.10 Seismic Energy Comparison

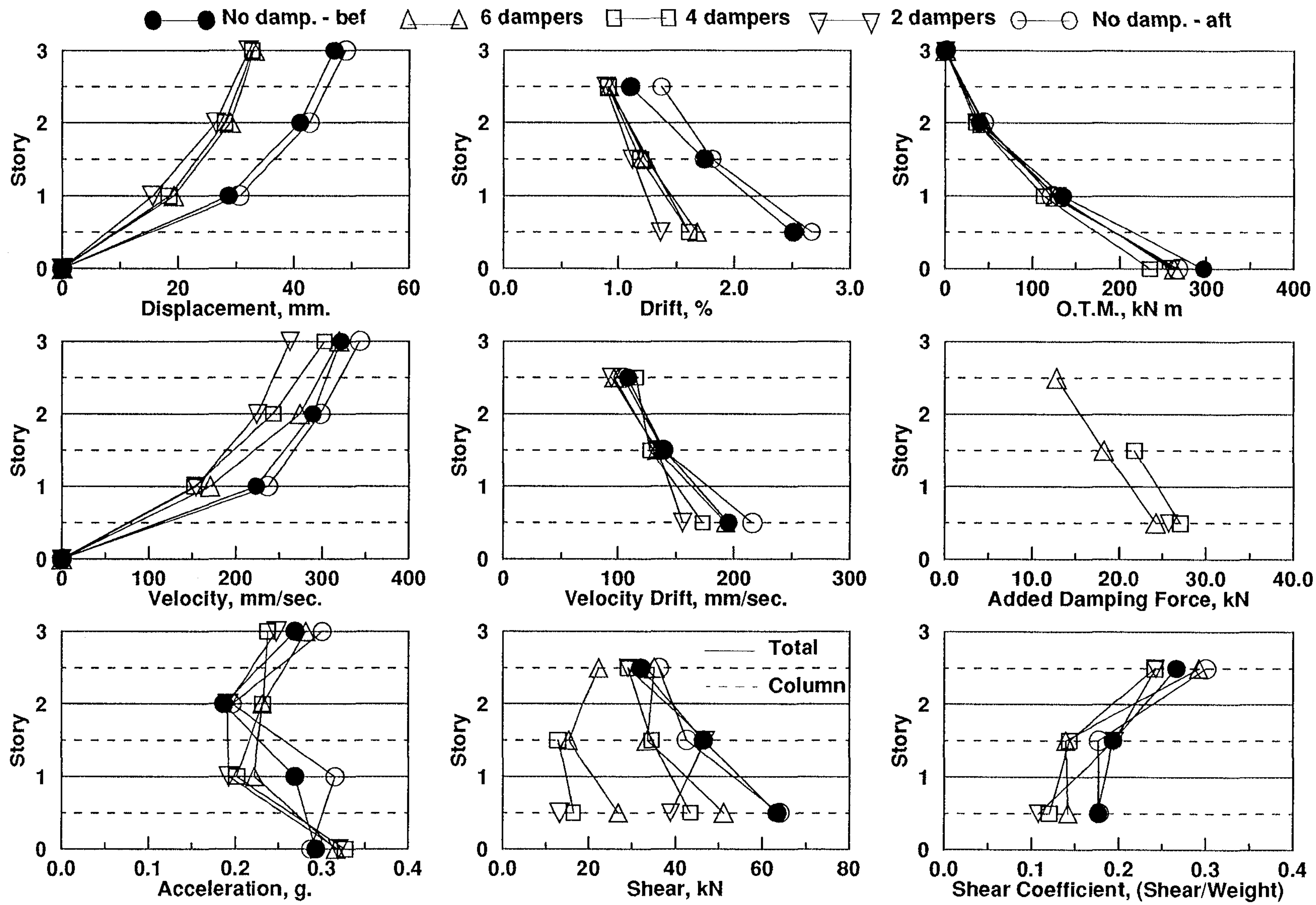

Figure 5.11 Maximum Response Envelopes - El Centro 0.3g

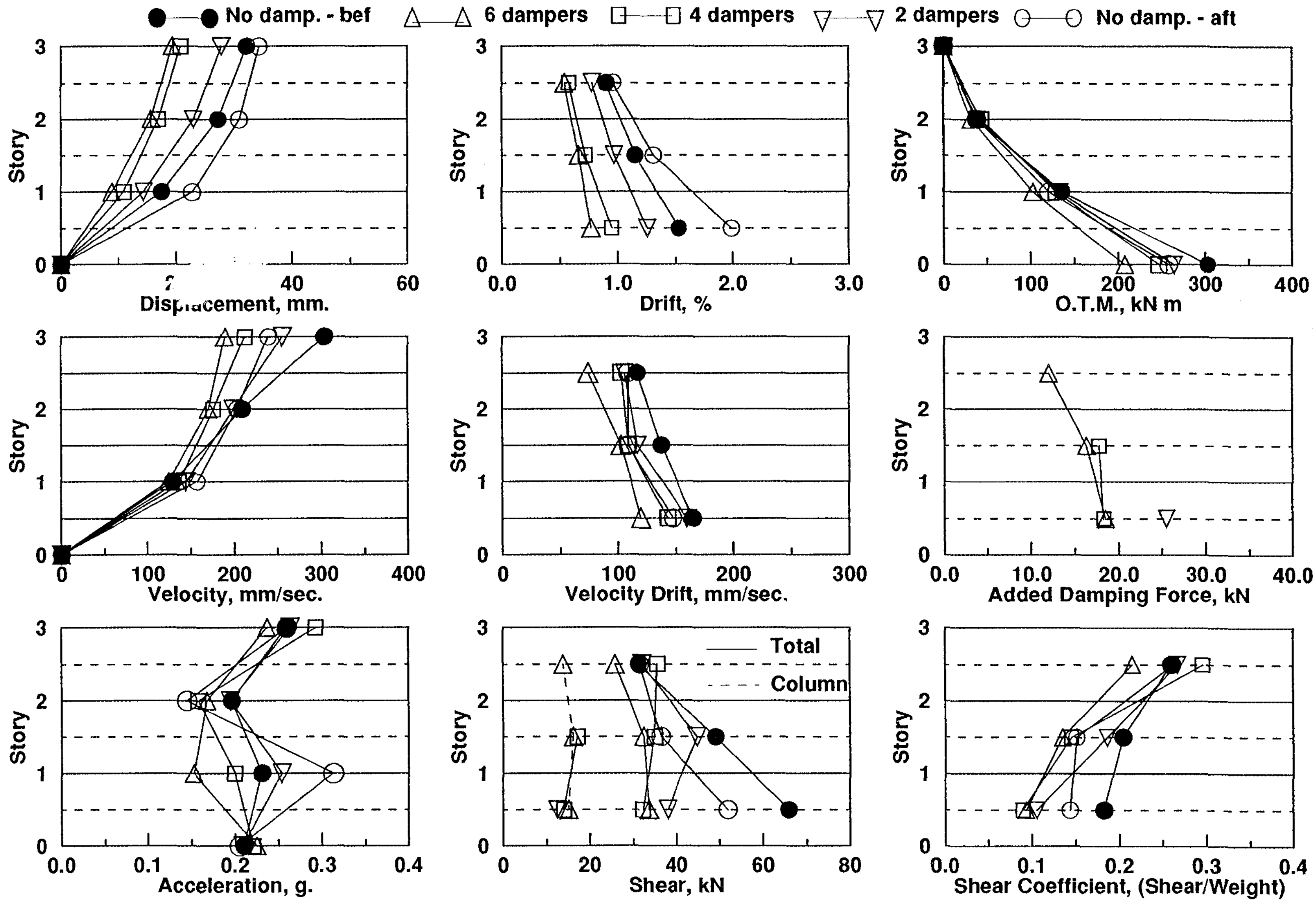

Figure 5.12 Maximum Response Envelopes - Taft 0.2g

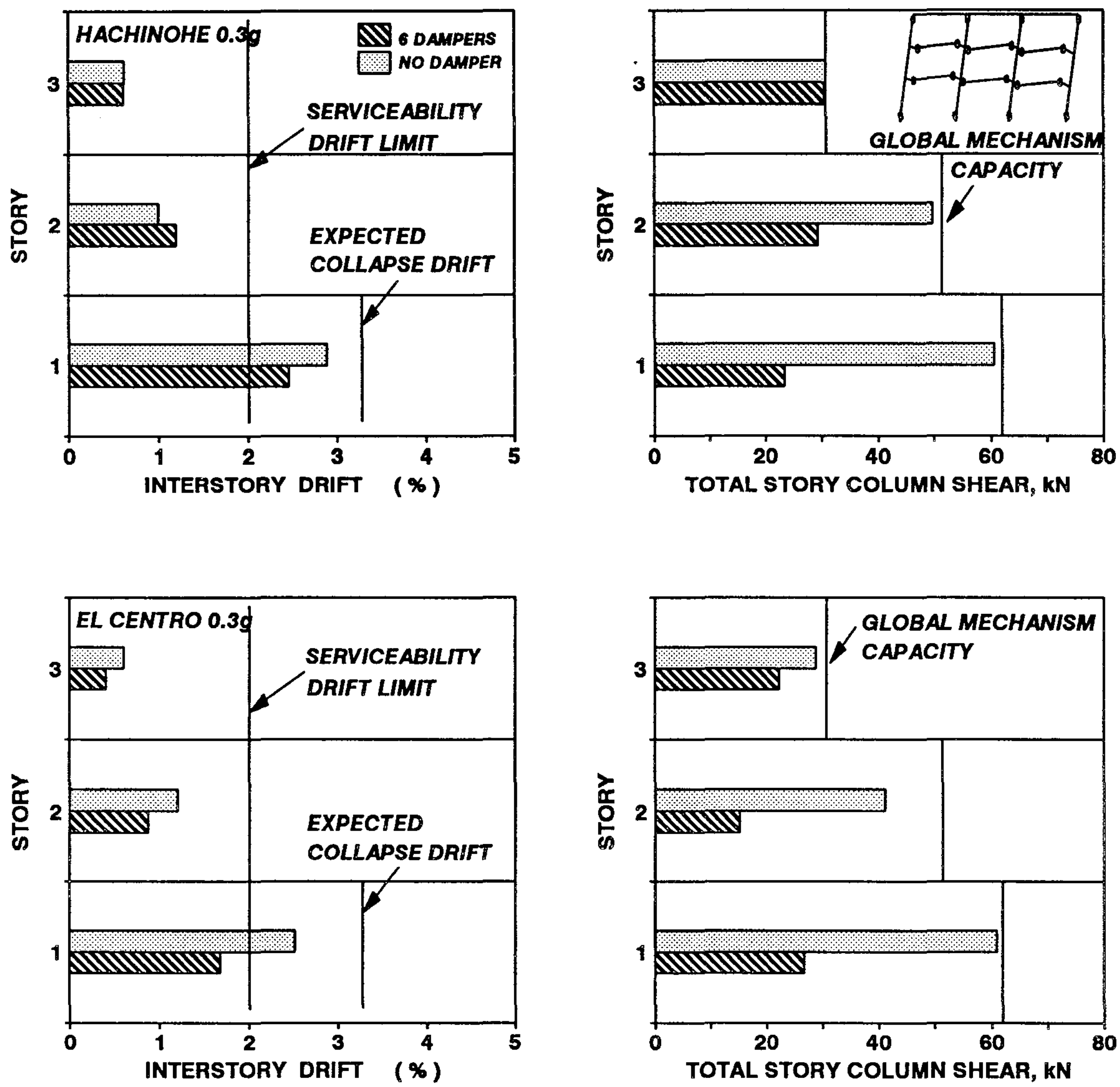

* *Results for bare structure subjected to Hachinohe 0.3g ground motion is analytically obtained.*

Figure 5.13a Benefits of Added Damping under Major Earthquake Ground Motions

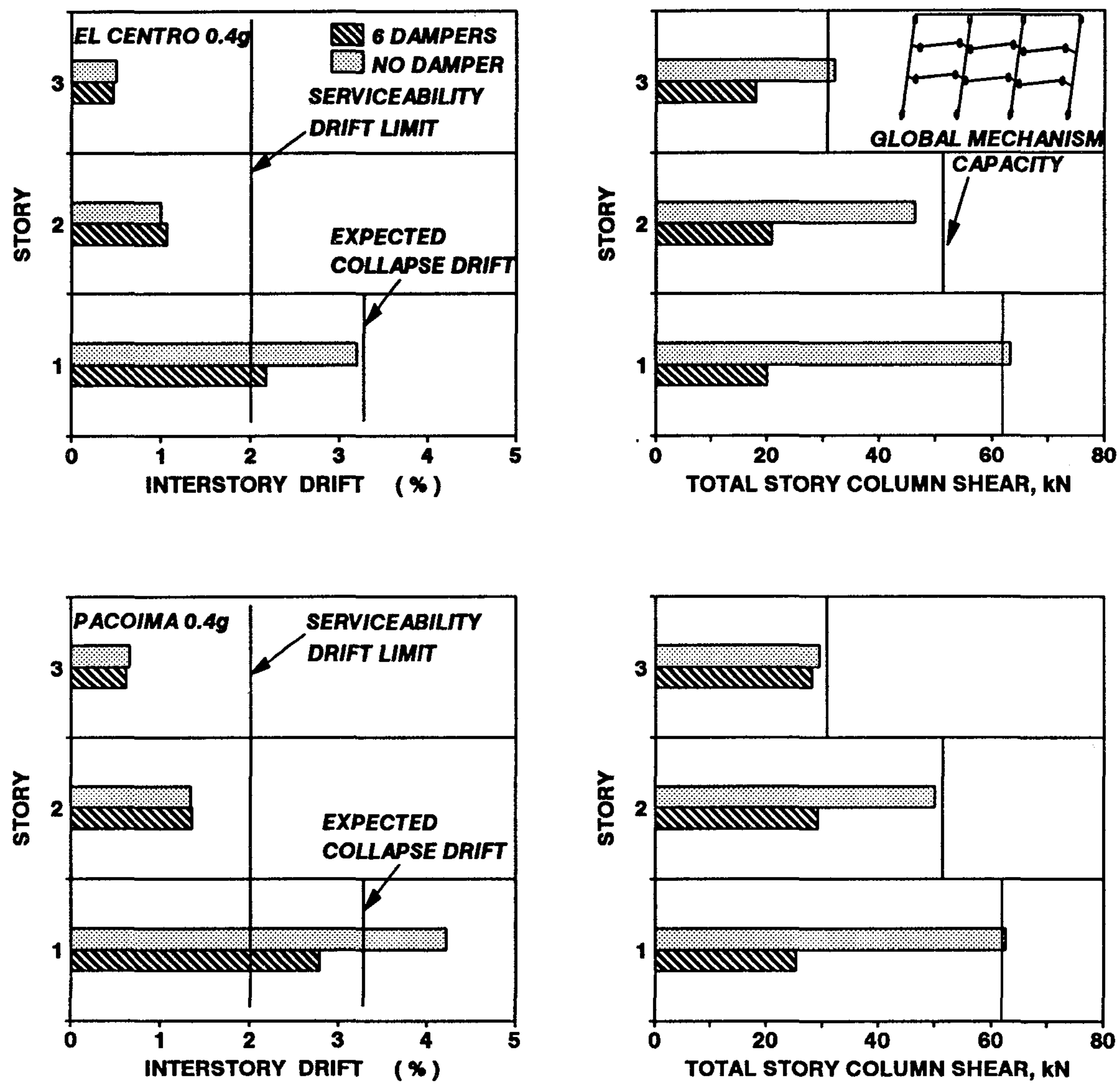

** Results for bare structure subjected to El Centro 0.4g and Pacoima 0.4g ground motions are analytically obtained.*

Figure 5.13b Benefits of Added Damping under Major Earthquake Ground Motions

SECTION 6

SUMMARY AND CONCLUSIONS

Shaking table tests were conducted on a 1/3 scale nonductile reinforced concrete structure both with and without supplemental elastomeric spring damper devices. The self-centering characteristics and frequency dependency of the dampers were investigated experimentally. A simple, yet powerful analytical damper model based on an extended Menegotto-Pinto formulation was developed and incorporated into the non-linear time history analysis computer program DRAIN-2DX (Prakash et al. 1992). This was then used to compare the analytically predicted response with the experimental behavior of the structure both with and without dampers installed. The analytical predictions compared very well with the experimental results. The efficacy of a practical and accurate analytical tool is thought to be encouraging for future analytical-parametric studies as well as for design studies.

In this study, results of four ground motions are reported: Taft N21E, El Centro 1940 S00E, Pacoima Dam S16E, and Hachinohe NS at various PGA levels. The former two at 0.3 g and 0.2 g PGA levels, respectively, formed the basis for comparisons between different damper configurations. The effectiveness of the elastomeric spring dampers was demonstrated both experimentally and analytically. It should here be noted that although these dampers were originally designed for impact velocities which are much higher than those observed in seismic events (100-400 mm/sec), they performed well in reducing the seismic response to a level at which the structural elements were kept in the elastic range. It is believed that the response can be further improved by employing elastomeric spring dampers which are designed to be optimally effective within the expected range of interstory displacements. The self-centering characteristic of the dampers is especially desirable for retrofit of inelastic structures for which permanent deformations are otherwise inevitable.

Based on the experimental and analytical results reported above, the following conclusions are drawn:

1. Elastomeric spring dampers reduced the overall seismic response of the structure while reducing the initial peak response as well.

2. The effectiveness of the elastomeric spring dampers was obvious as they contributed to reducing the response by dissipating 50-80% of the input seismic energy. Meanwhile, 20-40% reduction in story shears was observed along with 50-60% reduction in interstory drifts. However, effects on the column axial forces should be further investigated. This is especially important in retrofit applications where there is a possibility of axial load increase and potential buckling.
3. From the shaking table test results, it is clear that the energy dissipation contribution of the devices more than compensated for the effects of the increased stiffness due to the damper braces. However, it was also observed that the top story dampers did not contribute to the response reduction as much as they did to the stiffness increase of the structure. This raises the question of optimum damper design and placement which should carefully be considered in design of structures with supplemental damping devices. It is believed that had the third story dampers been designed for the expected interstory drifts at that level, response reduction would be further improved.
4. The DRAIN-2DX computational model modified for the incorporation of the damper formulation presented herein provide reliable predictions for behavior of the reinforced concrete frame structure as retrofitted with elastomeric spring dampers.

6.1 Future Research

In light of the experimental results and discussion given in previous sections, the following recommendations are made:

1. Optimum design and configuration of elastomeric spring dampers in application to structures should be analytically investigated.
2. Retrofit design studies of reinforced concrete structures with elastomeric spring dampers should be performed.
3. Further investigations should be carried out for steel structures which comprise various types of frame systems such as moment frames and braced frames. The use of elastomeric spring dampers in semi-rigid steel frames would be attractive, since the dampers can reduce the low-cycle fatigue demand on the connections.

4. Development of simplified design procedures with elastomeric spring dampers for both reinforced concrete and steel structures should be pursued.
5. The suitability of using elastic/inelastic response spectra approach in design of structures with elastomeric spring dampers should be investigated.
6. The effectiveness of elastomeric spring dampers in bridges as well as building structures should be studied both experimentally and analytically, from the point of view of mitigating impulse loadings as well as seismic loading. Due to its self centering and energy dissipation capability, elastomeric spring dampers can be utilized as part of an isolation system in bridges - in conjuntion with rubber or sliding bearings, and for displacement control at girder seats - in conjunction with cable restrainers. This will reduce the displacement demand on such bearings while improving the energy dissipation characteristics.

SECTION 7

REFERENCES

Abbas, H., and Kelly, J.M., (1993), "A Methodology for Design of Viscoelastic Dampers in Earthquake-Resistant Structures," Report No. UCB/EERC-93/09, University of California at Berkeley, November.

Aiken, I.D., Kelly, J.M., and Pall, A.S., (1988), "Seismic Response of a Nine-Story Steel Frame with Friction Damped Cross-Bracing," *Report No. UCB/EERC-88/17, EERC*, University of California at Berkeley, November.

Aiken, I.D., Kelly, J.M., (1990), "Earthquake Simulator Testing and analytical Studies of Two Energy-Absorbing Systems for Multistory Structures," *Report No. UCB/EERC-90/03, EERC*, University of California at Berkeley, October.

Aiken, I.D., Nims, D.K., Kelly, J.M., (1992), "Comparative Study of Four Passive Energy Dissipation Systems," *Bulletin of New Zealand National Society for Earthquake Engineering, 25(3)*, September.

Aiken, I.D., Nims, D.K., Whittaker, A.S., Kelly, J.M., (1993), "Testing of Passive Energy Dissipation Systems," *Earthquake Spectra*, Vol. 9, No. 3, pp. 336-370, August.

Bergman, D.M., and Goel, S.C., (1987), "Evaluation of Cyclic Testing of Steel Plate Devices for Added Damping and Stiffness," *Report No. UMCE 87-10*, Civil Engineering Department, University of Michigan, November.

Bracci, J.M., Reinhorn, A.M., Mander, J.B., (1992a), "Seismic Resistance of Reinforced Concrete Frame Structures Designed only for Gravity Loads: Part I - Design and Properties of One-Third Scale Model Structure," *Technical Report NCEER 92-0027*, NCEER, State University of New York at Buffalo.

Bracci, J.M., Reinhorn, A.M., Mander, J.B., (1992b), "Seismic Resistance of Reinforced Concrete Frame Structures Designed only for Gravity Loads: Part II - Experimental Performance and Analytical Study of Structural Model," *Technical Report NCEER 92-0029*, NCEER, State University of New York at Buffalo.

Bracci, J.M., Reinhorn, A.M., Mander, J.B., (1992c), "Seismic Resistance of Reinforced

Concrete Frame Structures Designed only for Gravity Loads: Part III - Experimental Performance and Analytical Study of Retrofitted Model Structure," *Technical Report NCEER 92-0031*, NCEER, State University of New York at Buffalo.

Clough, R.W., Penzien, J., (1993), "Dynamics of Structures," McGraw-Hill, Inc., 2nd Edition, New York, USA.

Constantinou, M.C., Symans, M.D., Tsopelas, P., and Taylor, D.P., (1993), "Fluid Viscous Dampers in Application of Seismic Energy Dissipation and Seismic Isolation," *Proceeding of Seminar on Seismic Isolation, Passive Energy Dissipation, and Active Control, ATC 17-1*, Vol.2, pp. 581-592.

Filiatrault, A., Cherry, S., (1987), "Performance Evaluation of Friction Damped Braced Steel Frames Under Simulated Earthquake Loads," *Earthquake Spectra, 3(1)*, EERI.

Filiatrault, A., Cherry, S., (1990), "A Simplified Design Procedure for Friction Damped Structures," *Proceeding of 4USNCEE*, Palm Springs, California, May.

Fitzgerald, T.F., Anagnos, T., Goodson, M., and Zsutty, T., (1989), "Slotted Bolted Connections in Aseismic Design for Concentrically Braced Connections," *Earthquake Spectra, 5(2)*, EERI, May, pp. 383-391.

Grigorian, C.E., Popov, E.P., (1994), "Energy Dissipation with Slotted Bolted Connections," *Report No. UCB/EERC-94/02*, University of California at Berkeley, February.

Grigorian, C.E., Yang, T.S., and Popov, E.P., (1992), "Slotted Bolted Connection Energy Dissipator," *Report No. UCB/EERC-92/10, EERC*, University of California at Berkeley, July.

Keel, C.J., and Mahmoodi, P., (1986), "Designing of Viscoelastic Dampers for the Colombia Center Building," *Building Motion in Wind (Eds. N. Kyumov and T. Tschanz), ASCE*, New York, pp. 66-82.

Kelly, J.M., Skinner, R.I., and Heinne, A.J., (1972), "Mechanism of Energy Absorption in Special Devices for Use in Earthquake Resistant Structures," *Bulletin of New Zealand National Society for Earthquake Engineering, 5(3)*, September.

Lin, R.C., Liang, Z., Soong, T.T., and Zhang, R.H., (1988), "An experimental Study of Seismic Structural Response with Added Viscoelatic Dampers," *Report NCEER-88-0018*, NCEER, State University of New York at Buffalo.

Lobo, R.F., Bracci, J.M., Shen, K.L., Reinhorn, A.M., and Soong, T.T., (1993), "Inelastic

Response of Reinforced Concrete Structures with Viscoelastic Braces," *Report NCEER-93-0006*, NCEER, State University of New York at Buffalo.

Mahmoodi, P., (1969), "Structural Dampers," *Journal of the Structural Division*, 95(ST8), ASCE, New York.

Mahmoodi, P., Robertson, L.E., Yontar, M., Moy, C., and Feld, L., (1987), "Performance of Viscoelastic Dampers in World Trade Center Towers," *Proceedings of 5th ASCE Structural Congress*, Orlando, April.

Menegotto, M., and Pinto, P.E., (1973), "Method of Analysis for Cyclically Loaded Reinforced Concrete Plane Frames Including Changes in Geometry and Non-elastic Behavior of Elements Under Combined Normal Forces and Bending", *IABSE Symposium on the Resistance and Ultimate Deformability of Structures Acted on by Well-Defined Repeated Loads*, Lisbon.

Nims, D.K., Inaudi, J.A., Richter, P.J., and Kelly, J.M., (1993), "Application of the Energy Dissipating Restraints to Buildings," *Proceedings of Seminar on Seismic Isolation, Passive Energy Dissipation, and Active Control, ATC 17-1*, Vol.2, pp. 627-638.

Pall, A.S., Verganelakis, V., and Marsh, C., (1987), "Friction Dampers for Seismic Control of Concordia University Library Building," *Proceeding of 5th Canadian Conference on Earthquake Engineering*, Ottawa, Canada, pp. 191-200.

Pall, A.S., Ghorayedo, F., and Pall, R., (1991), "Friction Dampers for Rehabilitation of Ecole Ployvalente at Sorel, Quebec," *Proceedings of 6th Canadian Conference on Earthquake Engineering*, Toronto, Canada, pp. 389-396.

Prakash, V., Powell, G.H., Filippou, F.C., (1992), "Drain-2DX: Base Program User Guide," *Report No. UCB/SEMM-92/29*, University of California at Berkeley, December.

Reinhorn, A.M., Li, C., Constantinou, M.C., (1995), "Experimental and Analytical Investigation of Seismic Retrofit with Supplemental Damping, PART I: Fluid Viscous Damping Devices," *Technical Report NCEER-95-0001*, National Center for Earthquake Engineering Research, SUNY at Buffalo, January.

Richter, P.J., Nims, D.K., Kelly, J.M., (1990), "The EDR - Energy Dissipating Restraint, A New Device for Mitigation of Seismic Effects," *Proceedings of SEAOC 59th Annual Convention*, Lake Tahoe, September.

Skinner, R.I., Robinson, W.H., McVerry, G.H., (1993), *Introduction to Seismic Isolation*, Wiley Inc.

Skinner, R.I., Tyler, R.G., Heine, A.J., and Robinson, W.J., (1980), "Hysteretic Dampers for the Protection of Structures From Earthquakes," *Bulletin of New Zealand National Society of Earthquake Engineering, 13(1)*, March.

Stiemer, S.F., Godden, W.G., and Kelly, J.M., (1981), "Experimental Behavior of a Spatial Piping System with Steel Energy Absorbing Subjected to a Simulated Differential Seismic Input," *Report No. UCB/EERC-81/09*, EERC, University of California at Berkeley, July.

Tsopelas, P., and Constantinou M.C., (1994), "NCEER-Taisei Corporation Research Program on Sliding Seismic Isolation Systems for Bridges: Experimental and Analytical Study of a System Consisting of Sliding Bearings and Fluid Restoring Force/Damping Devices", *Technical Report NCEER-94-0014*, National Center for Earthquake Engineering Research, SUNY at Buffalo.

Tyler, R.G., (1985), "Further Notes on a Steel Energy Absorbing Element for Braced Frameworks," *Bulletin of New Zealand National Society for Earthquake Engineering, 18(3)*, September.

Tyler, R.G., (1978), "Tapered Steel Energy Dissipators for Earthquake Resistant Structures," *Bulletin of New Zealand National Society for Earthquake Engineering, 18(2)*, December.

Uang, C.M., Bertero, V.V., (1990), "Evaluation of Seismic Energy in Structures," *Earthquake Engineering and Structural Dynamics*, Vol. 19, pp.77-90.

Whittaker, A.S., Bertero, V.V., Thompson, C.L., and Alonso, L.J., (1991), "Seismic Testing of Steel Plate Energy Dissipation Devices," *Earthquake Spectra, 7(4)*, EERI, November, pp. 563-604.

Witting, P.R., and Cozzarelli, F.A., (1992), "Shape Memory Structural Dampers: Material Properties, Design and Seismic Testing," *Report No. NCEER-92-0013*, NCEER, State University of New York at Buffalo.

Zhang R.H., and Soong T.T., (1992), “Seismic Design of Viscoelastic Dampers for Structural Applications,” *Journal of Structural Engineering, ASCE*, Vol. 118, No. 5, pp. 1375-1391.

NATIONAL CENTER FOR EARTHQUAKE ENGINEERING RESEARCH
LIST OF TECHNICAL REPORTS

The National Center for Earthquake Engineering Research (NCEER) publishes technical reports on a variety of subjects related to earthquake engineering written by authors funded through NCEER. These reports are available from both NCEER's Publications Department and the National Technical Information Service (NTIS). Requests for reports should be directed to the Publications Department, National Center for Earthquake Engineering Research, State University of New York at Buffalo, Red Jacket Quadrangle, Buffalo, New York 14261. Reports can also be requested through NTIS, 5285 Port Royal Road, Springfield, Virginia 22161. NTIS accession numbers are shown in parenthesis, if available.

NCEER-87-0001 "First-Year Program in Research, Education and Technology Transfer," 3/5/87, (PB88-134275).

NCEER-87-0002 "Experimental Evaluation of Instantaneous Optimal Algorithms for Structural Control," by R.C. Lin, T.T. Soong and A.M. Reinhorn, 4/20/87, (PB88-134341).

NCEER-87-0003 "Experimentation Using the Earthquake Simulation Facilities at University at Buffalo," by A.M. Reinhorn and R.L. Ketter, to be published.

NCEER-87-0004 "The System Characteristics and Performance of a Shaking Table," by J.S. Hwang, K.C. Chang and G.C. Lee, 6/1/87, (PB88-134259). This report is available only through NTIS (see address given above).

NCEER-87-0005 "A Finite Element Formulation for Nonlinear Viscoplastic Material Using a Q Model," by O. Gyebi and G. Dasgupta, 11/2/87, (PB88-213764).

NCEER-87-0006 "Symbolic Manipulation Program (SMP) - Algebraic Codes for Two and Three Dimensional Finite Element Formulations," by X. Lee and G. Dasgupta, 11/9/87, (PB88-218522).

NCEER-87-0007 "Instantaneous Optimal Control Laws for Tall Buildings Under Seismic Excitations," by J.N. Yang, A. Akbarpour and P. Ghaemmaghami, 6/10/87, (PB88-134333). This report is only available through NTIS (see address given above).

NCEER-87-0008 "IDARC: Inelastic Damage Analysis of Reinforced Concrete Frame - Shear-Wall Structures," by Y.J. Park, A.M. Reinhorn and S.K. Kunnath, 7/20/87, (PB88-134325).

NCEER-87-0009 "Liquefaction Potential for New York State: A Preliminary Report on Sites in Manhattan and Buffalo," by M. Budhu, V. Vijayakumar, R.F. Giese and L. Baumgras, 8/31/87, (PB88-163704). This report is available only through NTIS (see address given above).

NCEER-87-0010 "Vertical and Torsional Vibration of Foundations in Inhomogeneous Media," by A.S. Veletsos and K.W. Dotson, 6/1/87, (PB88-134291).

NCEER-87-0011 "Seismic Probabilistic Risk Assessment and Seismic Margins Studies for Nuclear Power Plants," by Howard H.M. Hwang, 6/15/87, (PB88-134267).

NCEER-87-0012 "Parametric Studies of Frequency Response of Secondary Systems Under Ground-Acceleration Excitations," by Y. Yong and Y.K. Lin, 6/10/87, (PB88-134309).

NCEER-87-0013 "Frequency Response of Secondary Systems Under Seismic Excitation," by J.A. HoLung, J. Cai and Y.K. Lin, 7/31/87, (PB88-134317).

NCEER-87-0014 "Modelling Earthquake Ground Motions in Seismically Active Regions Using Parametric Time Series Methods," by G.W. Ellis and A.S. Cakmak, 8/25/87, (PB88-134283).

NCEER-87-0015 "Detection and Assessment of Seismic Structural Damage," by E. DiPasquale and A.S. Cakmak, 8/25/87, (PB88-163712).

NCEER-87-0016 "Pipeline Experiment at Parkfield, California," by J. Isenberg and E. Richardson, 9/15/87, (PB88-163720). This report is available only through NTIS (see address given above).

NCEER-87-0017 "Digital Simulation of Seismic Ground Motion," by M. Shinozuka, G. Deodatis and T. Harada, 8/31/87, (PB88-155197). This report is available only through NTIS (see address given above).

NCEER-87-0018 "Practical Considerations for Structural Control: System Uncertainty, System Time Delay and Truncation of Small Control Forces," J.N. Yang and A. Akbarpour, 8/10/87, (PB88-163738).

NCEER-87-0019 "Modal Analysis of Nonclassically Damped Structural Systems Using Canonical Transformation," by J.N. Yang, S. Sarkani and F.X. Long, 9/27/87, (PB88-187851).

NCEER-87-0020 "A Nonstationary Solution in Random Vibration Theory," by J.R. Red-Horse and P.D. Spanos, 11/3/87, (PB88-163746).

NCEER-87-0021 "Horizontal Impedances for Radially Inhomogeneous Viscoelastic Soil Layers," by A.S. Veletsos and K.W. Dotson, 10/15/87, (PB88-150859).

NCEER-87-0022 "Seismic Damage Assessment of Reinforced Concrete Members," by Y.S. Chung, C. Meyer and M. Shinozuka, 10/9/87, (PB88-150867). This report is available only through NTIS (see address given above).

NCEER-87-0023 "Active Structural Control in Civil Engineering," by T.T. Soong, 11/11/87, (PB88-187778).

NCEER-87-0024 "Vertical and Torsional Impedances for Radially Inhomogeneous Viscoelastic Soil Layers," by K.W. Dotson and A.S. Veletsos, 12/87, (PB88-187786).

NCEER-87-0025 "Proceedings from the Symposium on Seismic Hazards, Ground Motions, Soil-Liquefaction and Engineering Practice in Eastern North America," October 20-22, 1987, edited by K.H. Jacob, 12/87, (PB88-188115).

NCEER-87-0026 "Report on the Whittier-Narrows, California, Earthquake of October 1, 1987," by J. Pantelic and A. Reinhorn, 11/87, (PB88-187752). This report is available only through NTIS (see address given above).

NCEER-87-0027 "Design of a Modular Program for Transient Nonlinear Analysis of Large 3-D Building Structures," by S. Srivastav and J.F. Abel, 12/30/87, (PB88-187950).

NCEER-87-0028 "Second-Year Program in Research, Education and Technology Transfer," 3/8/88, (PB88-219480).

NCEER-88-0001 "Workshop on Seismic Computer Analysis and Design of Buildings With Interactive Graphics," by W. McGuire, J.F. Abel and C.H. Conley, 1/18/88, (PB88-187760).

NCEER-88-0002 "Optimal Control of Nonlinear Flexible Structures," by J.N. Yang, F.X. Long and D. Wong, 1/22/88, (PB88-213772).

NCEER-88-0003 "Substructuring Techniques in the Time Domain for Primary-Secondary Structural Systems," by G.D. Manolis and G. Juhn, 2/10/88, (PB88-213780).

NCEER-88-0004 "Iterative Seismic Analysis of Primary-Secondary Systems," by A. Singhal, L.D. Lutes and P.D. Spanos, 2/23/88, (PB88-213798).

NCEER-88-0005 "Stochastic Finite Element Expansion for Random Media," by P.D. Spanos and R. Ghanem, 3/14/88, (PB88-213806).

NCEER-88-0006 "Combining Structural Optimization and Structural Control," by F.Y. Cheng and C.P. Pantelides, 1/10/88, (PB88-213814).

NCEER-88-0007 "Seismic Performance Assessment of Code-Designed Structures," by H.H-M. Hwang, J-W. Jaw and H-J. Shau, 3/20/88, (PB88-219423).

NCEER-88-0008 "Reliability Analysis of Code-Designed Structures Under Natural Hazards," by H.H-M. Hwang, H. Ushiba and M. Shinozuka, 2/29/88, (PB88-229471).

NCEER-88-0009 "Seismic Fragility Analysis of Shear Wall Structures," by J-W Jaw and H.H-M. Hwang, 4/30/88, (PB89-102867).

NCEER-88-0010 "Base Isolation of a Multi-Story Building Under a Harmonic Ground Motion - A Comparison of Performances of Various Systems," by F-G Fan, G. Ahmadi and I.G. Tadjbakhsh, 5/18/88, (PB89-122238).

NCEER-88-0011 "Seismic Floor Response Spectra for a Combined System by Green's Functions," by F.M. Lavelle, L.A. Bergman and P.D. Spanos, 5/1/88, (PB89-102875).

NCEER-88-0012 "A New Solution Technique for Randomly Excited Hysteretic Structures," by G.Q. Cai and Y.K. Lin, 5/16/88, (PB89-102883).

NCEER-88-0013 "A Study of Radiation Damping and Soil-Structure Interaction Effects in the Centrifuge," by K. Weissman, supervised by J.H. Prevost, 5/24/88, (PB89-144703).

NCEER-88-0014 "Parameter Identification and Implementation of a Kinematic Plasticity Model for Frictional Soils," by J.H. Prevost and D.V. Griffiths, to be published.

NCEER-88-0015 "Two- and Three- Dimensional Dynamic Finite Element Analyses of the Long Valley Dam," by D.V. Griffiths and J.H. Prevost, 6/17/88, (PB89-144711).

NCEER-88-0016 "Damage Assessment of Reinforced Concrete Structures in Eastern United States," by A.M. Reinhorn, M.J. Seidel, S.K. Kunnath and Y.J. Park, 6/15/88, (PB89-122220).

NCEER-88-0017 "Dynamic Compliance of Vertically Loaded Strip Foundations in Multilayered Viscoelastic Soils," by S. Ahmad and A.S.M. Israil, 6/17/88, (PB89-102891).

NCEER-88-0018 "An Experimental Study of Seismic Structural Response With Added Viscoelastic Dampers," by R.C. Lin, Z. Liang, T.T. Soong and R.H. Zhang, 6/30/88, (PB89-122212). This report is available only through NTIS (see address given above).

NCEER-88-0019 "Experimental Investigation of Primary - Secondary System Interaction," by G.D. Manolis, G. Juhn and A.M. Reinhorn, 5/27/88, (PB89-122204).

NCEER-88-0020 "A Response Spectrum Approach For Analysis of Nonclassically Damped Structures," by J.N. Yang, S. Sarkani and F.X. Long, 4/22/88, (PB89-102909).

NCEER-88-0021 "Seismic Interaction of Structures and Soils: Stochastic Approach," by A.S. Veletsos and A.M. Prasad, 7/21/88, (PB89-122196).

NCEER-88-0022 "Identification of the Serviceability Limit State and Detection of Seismic Structural Damage," by E. DiPasquale and A.S. Cakmak, 6/15/88, (PB89-122188). This report is available only through NTIS (see address given above).

NCEER-88-0023 "Multi-Hazard Risk Analysis: Case of a Simple Offshore Structure," by B.K. Bhartia and E.H. Vanmarcke, 7/21/88, (PB89-145213).

NCEER-88-0024 "Automated Seismic Design of Reinforced Concrete Buildings," by Y.S. Chung, C. Meyer and M. Shinozuka, 7/5/88, (PB89-122170). This report is available only through NTIS (see address given above).

NCEER-88-0025 "Experimental Study of Active Control of MDOF Structures Under Seismic Excitations," by L.L. Chung, R.C. Lin, T.T. Soong and A.M. Reinhorn, 7/10/88, (PB89-122600).

NCEER-88-0026 "Earthquake Simulation Tests of a Low-Rise Metal Structure," by J.S. Hwang, K.C. Chang, G.C. Lee and R.L. Ketter, 8/1/88, (PB89-102917).

NCEER-88-0027 "Systems Study of Urban Response and Reconstruction Due to Catastrophic Earthquakes," by F. Kozin and H.K. Zhou, 9/22/88, (PB90-162348).

NCEER-88-0028 "Seismic Fragility Analysis of Plane Frame Structures," by H.H-M. Hwang and Y.K. Low, 7/31/88, (PB89-131445).

NCEER-88-0029 "Response Analysis of Stochastic Structures," by A. Kardara, C. Bucher and M. Shinozuka, 9/22/88, (PB89-174429).

NCEER-88-0030 "Nonnormal Accelerations Due to Yielding in a Primary Structure," by D.C.K. Chen and L.D. Lutes, 9/19/88, (PB89-131437).

NCEER-88-0031 "Design Approaches for Soil-Structure Interaction," by A.S. Veletsos, A.M. Prasad and Y. Tang, 12/30/88, (PB89-174437). This report is available only through NTIS (see address given above).

NCEER-88-0032 "A Re-evaluation of Design Spectra for Seismic Damage Control," by C.J. Turkstra and A.G. Tallin, 11/7/88, (PB89-145221).

NCEER-88-0033 "The Behavior and Design of Noncontact Lap Splices Subjected to Repeated Inelastic Tensile Loading," by V.E. Sagan, P. Gergely and R.N. White, 12/8/88, (PB89-163737).

NCEER-88-0034 "Seismic Response of Pile Foundations," by S.M. Mamoon, P.K. Banerjee and S. Ahmad, 11/1/88, (PB89-145239).

NCEER-88-0035 "Modeling of R/C Building Structures With Flexible Floor Diaphragms (IDARC2)," by A.M. Reinhorn, S.K. Kunnath and N. Panahshahi, 9/7/88, (PB89-207153).

NCEER-88-0036 "Solution of the Dam-Reservoir Interaction Problem Using a Combination of FEM, BEM with Particular Integrals, Modal Analysis, and Substructuring," by C-S. Tsai, G.C. Lee and R.L. Ketter, 12/31/88, (PB89-207146).

NCEER-88-0037 "Optimal Placement of Actuators for Structural Control," by F.Y. Cheng and C.P. Pantelides, 8/15/88, (PB89-162846).

NCEER-88-0038 "Teflon Bearings in Aseismic Base Isolation: Experimental Studies and Mathematical Modeling," by A. Mokha, M.C. Constantinou and A.M. Reinhorn, 12/5/88, (PB89-218457). This report is available only through NTIS (see address given above).

NCEER-88-0039 "Seismic Behavior of Flat Slab High-Rise Buildings in the New York City Area," by P. Weidlinger and M. Ettouney, 10/15/88, (PB90-145681).

NCEER-88-0040 "Evaluation of the Earthquake Resistance of Existing Buildings in New York City," by P. Weidlinger and M. Ettouney, 10/15/88, to be published.

NCEER-88-0041 "Small-Scale Modeling Techniques for Reinforced Concrete Structures Subjected to Seismic Loads," by W. Kim, A. El-Attar and R.N. White, 11/22/88, (PB89-189625).

NCEER-88-0042 "Modeling Strong Ground Motion from Multiple Event Earthquakes," by G.W. Ellis and A.S. Cakmak, 10/15/88, (PB89-174445).

NCEER-88-0043 "Nonstationary Models of Seismic Ground Acceleration," by M. Grigoriu, S.E. Ruiz and E. Rosenblueth, 7/15/88, (PB89-189617).

NCEER-88-0044 "SARCF User's Guide: Seismic Analysis of Reinforced Concrete Frames," by Y.S. Chung, C. Meyer and M. Shinozuka, 11/9/88, (PB89-174452).

NCEER-88-0045 "First Expert Panel Meeting on Disaster Research and Planning," edited by J. Pantelic and J. Stoyle, 9/15/88, (PB89-174460).

NCEER-88-0046 "Preliminary Studies of the Effect of Degrading Infill Walls on the Nonlinear Seismic Response of Steel Frames," by C.Z. Chrysostomou, P. Gergely and J.F. Abel, 12/19/88, (PB89-208383).

NCEER-88-0047 "Reinforced Concrete Frame Component Testing Facility - Design, Construction, Instrumentation and Operation," by S.P. Pessiki, C. Conley, T. Bond, P. Gergely and R.N. White, 12/16/88, (PB89-174478).

NCEER-89-0001 "Effects of Protective Cushion and Soil Compliancy on the Response of Equipment Within a Seismically Excited Building," by J.A. HoLung, 2/16/89, (PB89-207179).

NCEER-89-0002 "Statistical Evaluation of Response Modification Factors for Reinforced Concrete Structures," by H.H-M. Hwang and J-W. Jaw, 2/17/89, (PB89-207187).

NCEER-89-0003 "Hysteretic Columns Under Random Excitation," by G-Q. Cai and Y.K. Lin, 1/9/89, (PB89-196513).

NCEER-89-0004 "Experimental Study of `Elephant Foot Bulge' Instability of Thin-Walled Metal Tanks," by Z-H. Jia and R.L. Ketter, 2/22/89, (PB89-207195).

NCEER-89-0005 "Experiment on Performance of Buried Pipelines Across San Andreas Fault," by J. Isenberg, E. Richardson and T.D. O'Rourke, 3/10/89, (PB89-218440). This report is available only through NTIS (see address given above).

NCEER-89-0006 "A Knowledge-Based Approach to Structural Design of Earthquake-Resistant Buildings," by M. Subramani, P. Gergely, C.H. Conley, J.F. Abel and A.H. Zaghw, 1/15/89, (PB89-218465).

NCEER-89-0007 "Liquefaction Hazards and Their Effects on Buried Pipelines," by T.D. O'Rourke and P.A. Lane, 2/1/89, (PB89-218481).

NCEER-89-0008 "Fundamentals of System Identification in Structural Dynamics," by H. Imai, C-B. Yun, O. Maruyama and M. Shinozuka, 1/26/89, (PB89-207211).

NCEER-89-0009 "Effects of the 1985 Michoacan Earthquake on Water Systems and Other Buried Lifelines in Mexico," by A.G. Ayala and M.J. O'Rourke, 3/8/89, (PB89-207229).

NCEER-89-R010 "NCEER Bibliography of Earthquake Education Materials," by K.E.K. Ross, Second Revision, 9/1/89, (PB90-125352).

NCEER-89-0011 "Inelastic Three-Dimensional Response Analysis of Reinforced Concrete Building Structures (IDARC-3D), Part I - Modeling," by S.K. Kunnath and A.M. Reinhorn, 4/17/89, (PB90-114612).

NCEER-89-0012 "Recommended Modifications to ATC-14," by C.D. Poland and J.O. Malley, 4/12/89, (PB90-108648).

NCEER-89-0013 "Repair and Strengthening of Beam-to-Column Connections Subjected to Earthquake Loading," by M. Corazao and A.J. Durrani, 2/28/89, (PB90-109885).

NCEER-89-0014 "Program EXKAL2 for Identification of Structural Dynamic Systems," by O. Maruyama, C-B. Yun, M. Hoshiya and M. Shinozuka, 5/19/89, (PB90-109877).

NCEER-89-0015 "Response of Frames With Bolted Semi-Rigid Connections, Part I - Experimental Study and Analytical Predictions," by P.J. DiCorso, A.M. Reinhorn, J.R. Dickerson, J.B. Radziminski and W.L. Harper, 6/1/89, to be published.

NCEER-89-0016 "ARMA Monte Carlo Simulation in Probabilistic Structural Analysis," by P.D. Spanos and M.P. Mignolet, 7/10/89, (PB90-109893).

NCEER-89-P017 "Preliminary Proceedings from the Conference on Disaster Preparedness - The Place of Earthquake Education in Our Schools," Edited by K.E.K. Ross, 6/23/89, (PB90-108606).

NCEER-89-0017 "Proceedings from the Conference on Disaster Preparedness - The Place of Earthquake Education in Our Schools," Edited by K.E.K. Ross, 12/31/89, (PB90-207895). This report is available only through NTIS (see address given above).

NCEER-89-0018 "Multidimensional Models of Hysteretic Material Behavior for Vibration Analysis of Shape Memory Energy Absorbing Devices, by E.J. Graesser and F.A. Cozzarelli, 6/7/89, (PB90-164146).

NCEER-89-0019 "Nonlinear Dynamic Analysis of Three-Dimensional Base Isolated Structures (3D-BASIS)," by S. Nagarajaiah, A.M. Reinhorn and M.C. Constantinou, 8/3/89, (PB90-161936). This report is available only through NTIS (see address given above).

NCEER-89-0020 "Structural Control Considering Time-Rate of Control Forces and Control Rate Constraints," by F.Y. Cheng and C.P. Pantelides, 8/3/89, (PB90-120445).

NCEER-89-0021 "Subsurface Conditions of Memphis and Shelby County," by K.W. Ng, T-S. Chang and H-H.M. Hwang, 7/26/89, (PB90-120437).

NCEER-89-0022 "Seismic Wave Propagation Effects on Straight Jointed Buried Pipelines," by K. Elhmadi and M.J. O'Rourke, 8/24/89, (PB90-162322).

NCEER-89-0023 "Workshop on Serviceability Analysis of Water Delivery Systems," edited by M. Grigoriu, 3/6/89, (PB90-127424).

NCEER-89-0024 "Shaking Table Study of a 1/5 Scale Steel Frame Composed of Tapered Members," by K.C. Chang, J.S. Hwang and G.C. Lee, 9/18/89, (PB90-160169).

NCEER-89-0025 "DYNA1D: A Computer Program for Nonlinear Seismic Site Response Analysis - Technical Documentation," by Jean H. Prevost, 9/14/89, (PB90-161944). This report is available only through NTIS (see address given above).

NCEER-89-0026 "1:4 Scale Model Studies of Active Tendon Systems and Active Mass Dampers for Aseismic Protection," by A.M. Reinhorn, T.T. Soong, R.C. Lin, Y.P. Yang, Y. Fukao, H. Abe and M. Nakai, 9/15/89, (PB90-173246).

NCEER-89-0027 "Scattering of Waves by Inclusions in a Nonhomogeneous Elastic Half Space Solved by Boundary Element Methods," by P.K. Hadley, A. Askar and A.S. Cakmak, 6/15/89, (PB90-145699).

NCEER-89-0028 "Statistical Evaluation of Deflection Amplification Factors for Reinforced Concrete Structures," by H.H.M. Hwang, J-W. Jaw and A.L. Ch'ng, 8/31/89, (PB90-164633).

NCEER-89-0029 "Bedrock Accelerations in Memphis Area Due to Large New Madrid Earthquakes," by H.H.M. Hwang, C.H.S. Chen and G. Yu, 11/7/89, (PB90-162330).

NCEER-89-0030 "Seismic Behavior and Response Sensitivity of Secondary Structural Systems," by Y.Q. Chen and T.T. Soong, 10/23/89, (PB90-164658).

NCEER-89-0031 "Random Vibration and Reliability Analysis of Primary-Secondary Structural Systems," by Y. Ibrahim, M. Grigoriu and T.T. Soong, 11/10/89, (PB90-161951).

NCEER-89-0032 "Proceedings from the Second U.S. - Japan Workshop on Liquefaction, Large Ground Deformation and Their Effects on Lifelines, September 26-29, 1989," Edited by T.D. O'Rourke and M. Hamada, 12/1/89, (PB90-209388).

NCEER-89-0033 "Deterministic Model for Seismic Damage Evaluation of Reinforced Concrete Structures," by J.M. Bracci, A.M. Reinhorn, J.B. Mander and S.K. Kunnath, 9/27/89.

NCEER-89-0034 "On the Relation Between Local and Global Damage Indices," by E. DiPasquale and A.S. Cakmak, 8/15/89, (PB90-173865).

NCEER-89-0035 "Cyclic Undrained Behavior of Nonplastic and Low Plasticity Silts," by A.J. Walker and H.E. Stewart, 7/26/89, (PB90-183518).

NCEER-89-0036 "Liquefaction Potential of Surficial Deposits in the City of Buffalo, New York," by M. Budhu, R. Giese and L. Baumgrass, 1/17/89, (PB90-208455).

NCEER-89-0037 "A Deterministic Assessment of Effects of Ground Motion Incoherence," by A.S. Veletsos and Y. Tang, 7/15/89, (PB90-164294).

NCEER-89-0038 "Workshop on Ground Motion Parameters for Seismic Hazard Mapping," July 17-18, 1989, edited by R.V. Whitman, 12/1/89, (PB90-173923).

NCEER-89-0039 "Seismic Effects on Elevated Transit Lines of the New York City Transit Authority," by C.J. Costantino, C.A. Miller and E. Heymsfield, 12/26/89, (PB90-207887).

NCEER-89-0040 "Centrifugal Modeling of Dynamic Soil-Structure Interaction," by K. Weissman, Supervised by J.H. Prevost, 5/10/89, (PB90-207879).

NCEER-89-0041 "Linearized Identification of Buildings With Cores for Seismic Vulnerability Assessment," by I-K. Ho and A.E. Aktan, 11/1/89, (PB90-251943).

NCEER-90-0001 "Geotechnical and Lifeline Aspects of the October 17, 1989 Loma Prieta Earthquake in San Francisco," by T.D. O'Rourke, H.E. Stewart, F.T. Blackburn and T.S. Dickerman, 1/90, (PB90-208596).

NCEER-90-0002 "Nonnormal Secondary Response Due to Yielding in a Primary Structure," by D.C.K. Chen and L.D. Lutes, 2/28/90, (PB90-251976).

NCEER-90-0003 "Earthquake Education Materials for Grades K-12," by K.E.K. Ross, 4/16/90, (PB91-251984).

NCEER-90-0004 "Catalog of Strong Motion Stations in Eastern North America," by R.W. Busby, 4/3/90, (PB90-251984).

NCEER-90-0005 "NCEER Strong-Motion Data Base: A User Manual for the GeoBase Release (Version 1.0 for the Sun3)," by P. Friberg and K. Jacob, 3/31/90 (PB90-258062).

NCEER-90-0006 "Seismic Hazard Along a Crude Oil Pipeline in the Event of an 1811-1812 Type New Madrid Earthquake," by H.H.M. Hwang and C-H.S. Chen, 4/16/90(PB90-258054).

NCEER-90-0007 "Site-Specific Response Spectra for Memphis Sheahan Pumping Station," by H.H.M. Hwang and C.S. Lee, 5/15/90, (PB91-108811).

NC 90-0008 "Pilot Study on Seismic Vulnerability of Crude Oil Transmission Systems," by T. Ariman, R. Dobry, M. Grigoriu, F. Kozin, M. O'Rourke, T. O'Rourke and M. Shinozuka, 5/25/90, (PB91-108837).

NCEER-90-0009 "A Program to Generate Site Dependent Time Histories: EQGEN," by G.W. Ellis, M. Srinivasan and A.S. Cakmak, 1/30/90, (PB91-108829).

NCEER-90-0010 "Active Isolation for Seismic Protection of Operating Rooms," by M.E. Talbott, Supervised by M. Shinozuka, 6/8/9, (PB91-110205).

NCEER-90-0011 "Program LINEARID for Identification of Linear Structural Dynamic Systems," by C-B. Yun and M. Shinozuka, 6/25/90, (PB91-110312).

NCEER-90-0012 "Two-Dimensional Two-Phase Elasto-Plastic Seismic Response of Earth Dams," by A.N. Yiagos, Supervised by J.H. Prevost, 6/20/90, (PB91-110197).

NCEER-90-0013 "Secondary Systems in Base-Isolated Structures: Experimental Investigation, Stochastic Response and Stochastic Sensitivity," by G.D. Manolis, G. Juhn, M.C. Constantinou and A.M. Reinhorn, 7/1/90, (PB91-110320).

NCEER-90-0014 "Seismic Behavior of Lightly-Reinforced Concrete Column and Beam-Column Joint Details," by S.P. Pessiki, C.H. Conley, P. Gergely and R.N. White, 8/22/90, (PB91-108795).

NCEER-90-0015 "Two Hybrid Control Systems for Building Structures Under Strong Earthquakes," by J.N. Yang and A. Danielians, 6/29/90, (PB91-125393).

NCEER-90-0016 "Instantaneous Optimal Control with Acceleration and Velocity Feedback," by J.N. Yang and Z. Li, 6/29/90, (PB91-125401).

NCEER-90-0017 "Reconnaissance Report on the Northern Iran Earthquake of June 21, 1990," by M. Mehrain, 10/4/90, (PB91-125377).

NCEER-90-0018 "Evaluation of Liquefaction Potential in Memphis and Shelby County," by T.S. Chang, P.S. Tang, C.S. Lee and H. Hwang, 8/10/90, (PB91-125427).

NCEER-90-0019 "Experimental and Analytical Study of a Combined Sliding Disc Bearing and Helical Steel Spring Isolation System," by M.C. Constantinou, A.S. Mokha and A.M. Reinhorn, 10/4/90, (PB91-125385).

NCEER-90-0020 "Experimental Study and Analytical Prediction of Earthquake Response of a Sliding Isolation System with a Spherical Surface," by A.S. Mokha, M.C. Constantinou and A.M. Reinhorn, 10/11/90, (PB91-125419).

NCEER-90-0021 "Dynamic Interaction Factors for Floating Pile Groups," by G. Gazetas, K. Fan, A. Kaynia and E. Kausel, 9/10/90, (PB91-170381).

NCEER-90-0022 "Evaluation of Seismic Damage Indices for Reinforced Concrete Structures," by S. Rodriguez-Gomez and A.S. Cakmak, 9/30/90, PB91-171322).

NCEER-90-0023 "Study of Site Response at a Selected Memphis Site," by H. Desai, S. Ahmad, E.S. Gazetas and M.R. Oh, 10/11/90, (PB91-196857).

NCEER-90-0024 "A User's Guide to Strongmo: Version 1.0 of NCEER's Strong-Motion Data Access Tool for PCs and Terminals," by P.A. Friberg and C.A.T. Susch, 11/15/90, (PB91-171272).

NCEER-90-0025 "A Three-Dimensional Analytical Study of Spatial Variability of Seismic Ground Motions," by L-L. Hong and A.H.-S. Ang, 10/30/90, (PB91-170399).

NCEER-90-0026 "MUMOID User's Guide - A Program for the Identification of Modal Parameters," by S. Rodriguez-Gomez and E. DiPasquale, 9/30/90, (PB91-171298).

NCEER-90-0027 "SARCF-II User's Guide - Seismic Analysis of Reinforced Concrete Frames," by S. Rodriguez-Gomez, Y.S. Chung and C. Meyer, 9/30/90, (PB91-171280).

NCEER-90-0028 "Viscous Dampers: Testing, Modeling and Application in Vibration and Seismic Isolation," by N. Makris and M.C. Constantinou, 12/20/90 (PB91-190561).

NCEER-90-0029 "Soil Effects on Earthquake Ground Motions in the Memphis Area," by H. Hwang, C.S. Lee, K.W. Ng and T.S. Chang, 8/2/90, (PB91-190751).

NCEER-91-0001 "Proceedings from the Third Japan-U.S. Workshop on Earthquake Resistant Design of Lifeline Facilities and Countermeasures for Soil Liquefaction, December 17-19, 1990," edited by T.D. O'Rourke and M. Hamada, 2/1/91, (PB91-179259).

NCEER-91-0002 "Physical Space Solutions of Non-Proportionally Damped Systems," by M. Tong, Z. Liang and G.C. Lee, 1/15/91, (PB91-179242).

NCEER-91-0003 "Seismic Response of Single Piles and Pile Groups," by K. Fan and G. Gazetas, 1/10/91, (PB92-174994).

NCEER-91-0004 "Damping of Structures: Part 1 - Theory of Complex Damping," by Z. Liang and G. Lee, 10/10/91, (PB92-197235).

NCEER-91-0005 "3D-BASIS - Nonlinear Dynamic Analysis of Three Dimensional Base Isolated Structures: Part II," by S. Nagarajaiah, A.M. Reinhorn and M.C. Constantinou, 2/28/91, (PB91-190553).

NCEER-91-0006 "A Multidimensional Hysteretic Model for Plasticity Deforming Metals in Energy Absorbing Devices," by E.J. Graesser and F.A. Cozzarelli, 4/9/91, (PB92-108364).

NCEER-91-0007 "A Framework for Customizable Knowledge-Based Expert Systems with an Application to a KBES for Evaluating the Seismic Resistance of Existing Buildings," by E.G. Ibarra-Anaya and S.J. Fenves, 4/9/91, (PB91-210930).

NCEER-91-0008 "Nonlinear Analysis of Steel Frames with Semi-Rigid Connections Using the Capacity Spectrum Method," by G.G. Deierlein, S-H. Hsieh, Y-J. Shen and J.F. Abel, 7/2/91, (PB92-113828).

NCEER-91-0009 "Earthquake Education Materials for Grades K-12," by K.E.K. Ross, 4/30/91, (PB91-212142).

NCEER-91-0010 "Phase Wave Velocities and Displacement Phase Differences in a Harmonically Oscillating Pile," by N. Makris and G. Gazetas, 7/8/91, (PB92-108356).

NCEER-91-0011 "Dynamic Characteristics of a Full-Size Five-Story Steel Structure and a 2/5 Scale Model," by K.C. Chang, G.C. Yao, G.C. Lee, D.S. Hao and Y.C. Yeh," 7/2/91, (PB93-116648).

NCEER-91-0012 "Seismic Response of a 2/5 Scale Steel Structure with Added Viscoelastic Dampers," by K.C. Chang, T.T. Soong, S-T. Oh and M.L. Lai, 5/17/91, (PB92-110816).

NCEER-91-0013 "Earthquake Response of Retaining Walls; Full-Scale Testing and Computational Modeling," by S. Alampalli and A-W.M. Elgamal, 6/20/91, to be published.

NCEER-91-0014 "3D-BASIS-M: Nonlinear Dynamic Analysis of Multiple Building Base Isolated Structures," by P.C. Tsopelas, S. Nagarajaiah, M.C. Constantinou and A.M. Reinhorn, 5/28/91, (PB92-113885).

NCEER-91-0015 "Evaluation of SEAOC Design Requirements for Sliding Isolated Structures," by D. Theodossiou and M.C. Constantinou, 6/10/91, (PB92-114602).

NCEER-91-0016 "Closed-Loop Modal Testing of a 27-Story Reinforced Concrete Flat Plate-Core Building," by H.R. Somaprasad, T. Toksoy, H. Yoshiyuki and A.E. Aktan, 7/15/91, (PB92-129980).

NCEER-91-0017 "Shake Table Test of a 1/6 Scale Two-Story Lightly Reinforced Concrete Building," by A.G. El-Attar, R.N. White and P. Gergely, 2/28/91, (PB92-222447).

NCEER-91-0018 "Shake Table Test of a 1/8 Scale Three-Story Lightly Reinforced Concrete Building," by A.G. El-Attar, R.N. White and P. Gergely, 2/28/91, (PB93-116630).

NCEER-91-0019 "Transfer Functions for Rigid Rectangular Foundations," by A.S. Veletsos, A.M. Prasad and W.H. Wu, 7/31/91.

NCEER-91-0020 "Hybrid Control of Seismic-Excited Nonlinear and Inelastic Structural Systems," by J.N. Yang, Z. Li and A. Danielians, 8/1/91, (PB92-143171).

NCEER-91-0021 "The NCEER-91 Earthquake Catalog: Improved Intensity-Based Magnitudes and Recurrence Relations for U.S. Earthquakes East of New Madrid," by L. Seeber and J.G. Armbruster, 8/28/91, (PB92-176742).

NCEER-91-0022 "Proceedings from the Implementation of Earthquake Planning and Education in Schools: The Need for Change - The Roles of the Changemakers," by K.E.K. Ross and F. Winslow, 7/23/91, (PB92-129998).

NCEER-91-0023 "A Study of Reliability-Based Criteria for Seismic Design of Reinforced Concrete Frame Buildings," by H.H.M. Hwang and H-M. Hsu, 8/10/91, (PB92-140235).

NCEER-91-0024 "Experimental Verification of a Number of Structural System Identification Algorithms," by R.G. Ghanem, H. Gavin and M. Shinozuka, 9/18/91, (PB92-176577).

NCEER-91-0025 "Probabilistic Evaluation of Liquefaction Potential," by H.H.M. Hwang and C.S. Lee," 11/25/91, (PB92-143429).

NCEER-91-0026 "Instantaneous Optimal Control for Linear, Nonlinear and Hysteretic Structures - Stable Controllers," by J.N. Yang and Z. Li, 11/15/91, (PB92-163807).

NCEER-91-0027 "Experimental and Theoretical Study of a Sliding Isolation System for Bridges," by M.C. Constantinou, A. Kartoum, A.M. Reinhorn and P. Bradford, 11/15/91, (PB92-176973).

NCEER-92-0001 "Case Studies of Liquefaction and Lifeline Performance During Past Earthquakes, Volume 1: Japanese Case Studies," Edited by M. Hamada and T. O'Rourke, 2/17/92, (PB92-197243).

NCEER-92-0002 "Case Studies of Liquefaction and Lifeline Performance During Past Earthquakes, Volume 2: United States Case Studies," Edited by T. O'Rourke and M. Hamada, 2/17/92, (PB92-197250).

NCEER-92-0003 "Issues in Earthquake Education," Edited by K. Ross, 2/3/92, (PB92-222389).

NCEER-92-0004 "Proceedings from the First U.S. - Japan Workshop on Earthquake Protective Systems for Bridges," Edited by I.G. Buckle, 2/4/92, (PB94-142239, A99, MF-A06).

NCEER-92-0005 "Seismic Ground Motion from a Haskell-Type Source in a Multiple-Layered Half-Space," A.P. Theoharis, G. Deodatis and M. Shinozuka, 1/2/92, to be published.

NCEER-92-0006 "Proceedings from the Site Effects Workshop," Edited by R. Whitman, 2/29/92, (PB92-197201).

NCEER-92-0007 "Engineering Evaluation of Permanent Ground Deformations Due to Seismically-Induced Liquefaction," by M.H. Baziar, R. Dobry and A-W.M. Elgamal, 3/24/92, (PB92-222421).

NCEER-92-0008 "A Procedure for the Seismic Evaluation of Buildings in the Central and Eastern United States," by C.D. Poland and J.O. Malley, 4/2/92, (PB92-222439).

NCEER-92-0009 "Experimental and Analytical Study of a Hybrid Isolation System Using Friction Controllable Sliding Bearings," by M.Q. Feng, S. Fujii and M. Shinozuka, 5/15/92, (PB93-150282).

NCEER-92-0010 "Seismic Resistance of Slab-Column Connections in Existing Non-Ductile Flat-Plate Buildings," by A.J. Durrani and Y. Du, 5/18/92.

NCEER-92-0011 "The Hysteretic and Dynamic Behavior of Brick Masonry Walls Upgraded by Ferrocement Coatings Under Cyclic Loading and Strong Simulated Ground Motion," by H. Lee and S.P. Prawel, 5/11/92, to be published.

NCEER-92-0012 "Study of Wire Rope Systems for Seismic Protection of Equipment in Buildings," by G.F. Demetriades, M.C. Constantinou and A.M. Reinhorn, 5/20/92.

NCEER-92-0013 "Shape Memory Structural Dampers: Material Properties, Design and Seismic Testing," by P.R. Witting and F.A. Cozzarelli, 5/26/92.

NCEER-92-0014 "Longitudinal Permanent Ground Deformation Effects on Buried Continuous Pipelines," by M.J. O'Rourke, and C. Nordberg, 6/15/92.

NCEER-92-0015 "A Simulation Method for Stationary Gaussian Random Functions Based on the Sampling Theorem," by M. Grigoriu and S. Balopoulou, 6/11/92, (PB93-127496).

NCEER-92-0016 "Gravity-Load-Designed Reinforced Concrete Buildings: Seismic Evaluation of Existing Construction and Detailing Strategies for Improved Seismic Resistance," by G.W. Hoffmann, S.K. Kunnath, A.M. Reinhorn and J.B. Mander, 7/15/92, (PB94-142007, A08, MF-A02).

NCEER-92-0017 "Observations on Water System and Pipeline Performance in the Limón Area of Costa Rica Due to the April 22, 1991 Earthquake," by M. O'Rourke and D. Ballantyne, 6/30/92, (PB93-126811).

NCEER-92-0018 "Fourth Edition of Earthquake Education Materials for Grades K-12," Edited by K.E.K. Ross, 8/10/92.

NCEER-92-0019 "Proceedings from the Fourth Japan-U.S. Workshop on Earthquake Resistant Design of Lifeline Facilities and Countermeasures for Soil Liquefaction," Edited by M. Hamada and T.D. O'Rourke, 8/12/92, (PB93-163939).

NCEER-92-0020 "Active Bracing System: A Full Scale Implementation of Active Control," by A.M. Reinhorn, T.T. Soong, R.C. Lin, M.A. Riley, Y.P. Wang, S. Aizawa and M. Higashino, 8/14/92, (PB93-127512).

NCEER-92-0021 "Empirical Analysis of Horizontal Ground Displacement Generated by Liquefaction-Induced Lateral Spreads," by S.F. Bartlett and T.L. Youd, 8/17/92, (PB93-188241).

NCEER-92-0022 "IDARC Version 3.0: Inelastic Damage Analysis of Reinforced Concrete Structures," by S.K. Kunnath, A.M. Reinhorn and R.F. Lobo, 8/31/92, (PB93-227502, A07, MF-A02).

NCEER-92-0023 "A Semi-Empirical Analysis of Strong-Motion Peaks in Terms of Seismic Source, Propagation Path and Local Site Conditions, by M. Kamiyama, M.J. O'Rourke and R. Flores-Berrones, 9/9/92, (PB93-150266).

NCEER-92-0024 "Seismic Behavior of Reinforced Concrete Frame Structures with Nonductile Details, Part I: Summary of Experimental Findings of Full Scale Beam-Column Joint Tests," by A. Beres, R.N. White and P. Gergely, 9/30/92, (PB93-227783, A05, MF-A01).

NCEER-92-0025 "Experimental Results of Repaired and Retrofitted Beam-Column Joint Tests in Lightly Reinforced Concrete Frame Buildings," by A. Beres, S. El-Borgi, R.N. White and P. Gergely, 10/29/92, (PB93-227791, A05, MF-A01).

NCEER-92-0026 "A Generalization of Optimal Control Theory: Linear and Nonlinear Structures," by J.N. Yang, Z. Li and S. Vongchavalitkul, 11/2/92, (PB93-188621).

NCEER-92-0027 "Seismic Resistance of Reinforced Concrete Frame Structures Designed Only for Gravity Loads: Part I - Design and Properties of a One-Third Scale Model Structure," by J.M. Bracci, A.M. Reinhorn and J.B. Mander, 12/1/92, (PB94-104502, A08, MF-A02).

NCEER-92-0028 "Seismic Resistance of Reinforced Concrete Frame Structures Designed Only for Gravity Loads: Part II - Experimental Performance of Subassemblages," by L.E. Aycardi, J.B. Mander and A.M. Reinhorn, 12/1/92, (PB94-104510, A08, MF-A02).

NCEER-92-0029 "Seismic Resistance of Reinforced Concrete Frame Structures Designed Only for Gravity Loads: Part III - Experimental Performance and Analytical Study of a Structural Model," by J.M. Bracci, A.M. Reinhorn and J.B. Mander, 12/1/92, (PB93-227528, A09, MF-A01).

NCEER-92-0030 "Evaluation of Seismic Retrofit of Reinforced Concrete Frame Structures: Part I - Experimental Performance of Retrofitted Subassemblages," by D. Choudhuri, J.B. Mander and A.M. Reinhorn, 12/8/92, (PB93-198307, A07, MF-A02).

NCEER-92-0031 "Evaluation of Seismic Retrofit of Reinforced Concrete Frame Structures: Part II - Experimental Performance and Analytical Study of a Retrofitted Structural Model," by J.M. Bracci, A.M. Reinhorn and J.B. Mander, 12/8/92, (PB93-198315, A09, MF-A03).

NCEER-92-0032 "Experimental and Analytical Investigation of Seismic Response of Structures with Supplemental Fluid Viscous Dampers," by M.C. Constantinou and M.D. Symans, 12/21/92, (PB93-191435).

NCEER-92-0033 "Reconnaissance Report on the Cairo, Egypt Earthquake of October 12, 1992," by M. Khater, 12/23/92, (PB93-188621).

NCEER-92-0034 "Low-Level Dynamic Characteristics of Four Tall Flat-Plate Buildings in New York City," by H. Gavin, S. Yuan, J. Grossman, E. Pekelis and K. Jacob, 12/28/92, (PB93-188217).

NCEER-93-0001 "An Experimental Study on the Seismic Performance of Brick-Infilled Steel Frames With and Without Retrofit," by J.B. Mander, B. Nair, K. Wojtkowski and J. Ma, 1/29/93, (PB93-227510, A07, MF-A02).

NCEER-93-0002 "Social Accounting for Disaster Preparedness and Recovery Planning," by S. Cole, E. Pantoja and V. Razak, 2/22/93, (PB94-142114, A12, MF-A03).

NCEER-93-0003 "Assessment of 1991 NEHRP Provisions for Nonstructural Components and Recommended Revisions," by T.T. Soong, G. Chen, Z. Wu, R-H. Zhang and M. Grigoriu, 3/1/93, (PB93-188639).

NCEER-93-0004 "Evaluation of Static and Response Spectrum Analysis Procedures of SEAOC/UBC for Seismic Isolated Structures," by C.W. Winters and M.C. Constantinou, 3/23/93, (PB93-198299).

NCEER-93-0005 "Earthquakes in the Northeast - Are We Ignoring the Hazard? A Workshop on Earthquake Science and Safety for Educators," edited by K.E.K. Ross, 4/2/93, (PB94-103066, A09, MF-A02).

NCEER-93-0006 "Inelastic Response of Reinforced Concrete Structures with Viscoelastic Braces," by R.F. Lobo, J.M. Bracci, K.L. Shen, A.M. Reinhorn and T.T. Soong, 4/5/93, (PB93-227486, A05, MF-A02).

NCEER-93-0007 "Seismic Testing of Installation Methods for Computers and Data Processing Equipment," by K. Kosar, T.T. Soong, K.L. Shen, J.A. HoLung and Y.K. Lin, 4/12/93, (PB93-198299).

NCEER-93-0008 "Retrofit of Reinforced Concrete Frames Using Added Dampers," by A. Reinhorn, M. Constantinou and C. Li, to be published.

NCEER-93-0009 "Seismic Behavior and Design Guidelines for Steel Frame Structures with Added Viscoelastic Dampers," by K.C. Chang, M.L. Lai, T.T. Soong, D.S. Hao and Y.C. Yeh, 5/1/93, (PB94-141959, A07, MF-A02).

NCEER-93-0010 "Seismic Performance of Shear-Critical Reinforced Concrete Bridge Piers," by J.B. Mander, S.M. Waheed, M.T.A. Chaudhary and S.S. Chen, 5/12/93, (PB93-227494, A08, MF-A02).

NCEER-93-0011 "3D-BASIS-TABS: Computer Program for Nonlinear Dynamic Analysis of Three Dimensional Base Isolated Structures," by S. Nagarajaiah, C. Li, A.M. Reinhorn and M.C. Constantinou, 8/2/93, (PB94-141819, A09, MF-A02).

NCEER-93-0012 "Effects of Hydrocarbon Spills from an Oil Pipeline Break on Ground Water," by O.J. Helweg and H.H.M. Hwang, 8/3/93, (PB94-141942, A06, MF-A02).

NCEER-93-0013 "Simplified Procedures for Seismic Design of Nonstructural Components and Assessment of Current Code Provisions," by M.P. Singh, L.E. Suarez, E.E. Matheu and G.O. Maldonado, 8/4/93, (PB94-141827, A09, MF-A02).

NCEER-93-0014 "An Energy Approach to Seismic Analysis and Design of Secondary Systems," by G. Chen and T.T. Soong, 8/6/93, (PB94-142767, A11, MF-A03).

NCEER-93-0015 "Proceedings from School Sites: Becoming Prepared for Earthquakes - Commemorating the Third Anniversary of the Loma Prieta Earthquake," Edited by F.E. Winslow and K.E.K. Ross, 8/16/93.

NCEER-93-0016 "Reconnaissance Report of Damage to Historic Monuments in Cairo, Egypt Following the October 12, 1992 Dahshur Earthquake," by D. Sykora, D. Look, G. Croci, E. Karaesmen and E. Karaesmen, 8/19/93, (PB94-142221, A08, MF-A02).

NCEER-93-0017 "The Island of Guam Earthquake of August 8, 1993," by S.W. Swan and S.K. Harris, 9/30/93, (PB94-141843, A04, MF-A01).

NCEER-93-0018 "Engineering Aspects of the October 12, 1992 Egyptian Earthquake," by A.W. Elgamal, M. Amer, K. Adalier and A. Abul-Fadl, 10/7/93, (PB94-141983, A05, MF-A01).

NCEER-93-0019 "Development of an Earthquake Motion Simulator and its Application in Dynamic Centrifuge Testing," by I. Krstelj, Supervised by J.H. Prevost, 10/23/93, (PB94-181773, A-10, MF-A03).

NCEER-93-0020 "NCEER-Taisei Corporation Research Program on Sliding Seismic Isolation Systems for Bridges: Experimental and Analytical Study of a Friction Pendulum System (FPS)," by M.C. Constantinou, P. Tsopelas, Y-S. Kim and S. Okamoto, 11/1/93, (PB94-142775, A08, MF-A02).

NCEER-93-0021 "Finite Element Modeling of Elastomeric Seismic Isolation Bearings," by L.J. Billings, Supervised by R. Shepherd, 11/8/93, to be published.

NCEER-93-0022 "Seismic Vulnerability of Equipment in Critical Facilities: Life-Safety and Operational Consequences," by K. Porter, G.S. Johnson, M.M. Zadeh, C. Scawthorn and S. Eder, 11/24/93, (PB94-181765, A16, MF-A03).

NCEER-93-0023 "Hokkaido Nansei-oki, Japan Earthquake of July 12, 1993, by P.I. Yanev and C.R. Scawthorn, 12/23/93, (PB94-181500, A07, MF-A01).

NCEER-94-0001 "An Evaluation of Seismic Serviceability of Water Supply Networks with Application to the San Francisco Auxiliary Water Supply System," by I. Markov, Supervised by M. Grigoriu and T. O'Rourke, 1/21/94.

NCEER-94-0002 "NCEER-Taisei Corporation Research Program on Sliding Seismic Isolation Systems for Bridges: Experimental and Analytical Study of Systems Consisting of Sliding Bearings, Rubber Restoring Force Devices and Fluid Dampers," Volumes I and II, by P. Tsopelas, S. Okamoto, M.C. Constantinou, D. Ozaki and S. Fujii, 2/4/94, (PB94-181740, A09, MF-A02 and PB94-181757, A12, MF-A03).

NCEER-94-0003 "A Markov Model for Local and Global Damage Indices in Seismic Analysis," by S. Rahman and M. Grigoriu, 2/18/94.

NCEER-94-0004 "Proceedings from the NCEER Workshop on Seismic Response of Masonry Infills," edited by D.P. Abrams, 3/1/94, (PB94-180783, A07, MF-A02).

NCEER-94-0005 "The Northridge, California Earthquake of January 17, 1994: General Reconnaissance Report," edited by J.D. Goltz, 3/11/94, (PB193943, A10, MF-A03).

NCEER-94-0006 "Seismic Energy Based Fatigue Damage Analysis of Bridge Columns: Part I - Evaluation of Seismic Capacity," by G.A. Chang and J.B. Mander, 3/14/94, (PB94-219185, A11, MF-A03).

NCEER-94-0007 "Seismic Isolation of Multi-Story Frame Structures Using Spherical Sliding Isolation Systems," by T.M. Al-Hussaini, V.A. Zayas and M.C. Constantinou, 3/17/94, (PB193745, A09, MF-A02).

NCEER-94-0008 "The Northridge, California Earthquake of January 17, 1994: Performance of Highway Bridges," edited by I.G. Buckle, 3/24/94, (PB94-193851, A06, MF-A02).

NCEER-94-0009 "Proceedings of the Third U.S.-Japan Workshop on Earthquake Protective Systems for Bridges," edited by I.G. Buckle and I. Friedland, 3/31/94, (PB94-195815, A99, MF-MF).

NCEER-94-0010 "3D-BASIS-ME: Computer Program for Nonlinear Dynamic Analysis of Seismically Isolated Single and Multiple Structures and Liquid Storage Tanks," by P.C. Tsopelas, M.C. Constantinou and A.M. Reinhorn, 4/12/94.

NCEER-94-0011 "The Northridge, California Earthquake of January 17, 1994: Performance of Gas Transmission Pipelines," by T.D. O'Rourke and M.C. Palmer, 5/16/94.

NCEER-94-0012 "Feasibility Study of Replacement Procedures and Earthquake Performance Related to Gas Transmission Pipelines," by T.D. O'Rourke and M.C. Palmer, 5/25/94, (PB94-206638, A09, MF-A02).

NCEER-94-0013 "Seismic Energy Based Fatigue Damage Analysis of Bridge Columns: Part II - Evaluation of Seismic Demand," by G.A. Chang and J.B. Mander, 6/1/94, (PB95-18106, A08, MF-A02).

NCEER-94-0014 "NCEER-Taisei Corporation Research Program on Sliding Seismic Isolation Systems for Bridges: Experimental and Analytical Study of a System Consisting of Sliding Bearings and Fluid Restoring Force/Damping Devices," by P. Tsopelas and M.C. Constantinou, 6/13/94, (PB94-219144, A10, MF-A03).

NCEER-94-0015 "Generation of Hazard-Consistent Fragility Curves for Seismic Loss Estimation Studies," by H. Hwang and J-R. Huo, 6/14/94, (PB95-181996, A09, MF-A02).

NCEER-94-0016 "Seismic Study of Building Frames with Added Energy-Absorbing Devices," by W.S. Pong, C.S. Tsai and G.C. Lee, 6/20/94, (PB94-219136, A10, A03).

NCEER-94-0017 "Sliding Mode Control for Seismic-Excited Linear and Nonlinear Civil Engineering Structures," by J. Yang, J. Wu, A. Agrawal and Z. Li, 6/21/94, (PB95-138483, A06, MF-A02).

NCEER-94-0018 "3D-BASIS-TABS Version 2.0: Computer Program for Nonlinear Dynamic Analysis of Three Dimensional Base Isolated Structures," by A.M. Reinhorn, S. Nagarajaiah, M.C. Constantinou, P. Tsopelas and R. Li, 6/22/94, (PB95-182176, A08, MF-A02).

NCEER-94-0019 "Proceedings of the International Workshop on Civil Infrastructure Systems: Application of Intelligent Systems and Advanced Materials on Bridge Systems," Edited by G.C. Lee and K.C. Chang, 7/18/94, (PB95-252474, A20, MF-A04).

NCEER-94-0020 "Study of Seismic Isolation Systems for Computer Floors," by V. Lambrou and M.C. Constantinou, 7/19/94, (PB95-138533, A10, MF-A03).

NCEER-94-0021 "Proceedings of the U.S.-Italian Workshop on Guidelines for Seismic Evaluation and Rehabilitation of Unreinforced Masonry Buildings," Edited by D.P. Abrams and G.M. Calvi, 7/20/94, (PB95-138749, A13, MF-A03).

NCEER-94-0022 "NCEER-Taisei Corporation Research Program on Sliding Seismic Isolation Systems for Bridges: Experimental and Analytical Study of a System Consisting of Lubricated PTFE Sliding Bearings and Mild Steel Dampers," by P. Tsopelas and M.C. Constantinou, 7/22/94, (PB95-182184, A08, MF-A02).

NCEER-94-0023 "Development of Reliability-Based Design Criteria for Buildings Under Seismic Load," by Y.K. Wen, H. Hwang and M. Shinozuka, 8/1/94, (PB95-211934, A08, MF-A02).

NCEER-94-0024 "Experimental Verification of Acceleration Feedback Control Strategies for an Active Tendon System," by S.J. Dyke, B.F. Spencer, Jr., P. Quast, M.K. Sain, D.C. Kaspari, Jr. and T.T. Soong, 8/29/94, (PB95-212320, A05, MF-A01).

NCEER-94-0025 "Seismic Retrofitting Manual for Highway Bridges," Edited by I.G. Buckle and I.F. Friedland, to be published.

NCEER-94-0026 "Proceedings from the Fifth U.S.-Japan Workshop on Earthquake Resistant Design of Lifeline Facilities and Countermeasures Against Soil Liquefaction," Edited by T.D. O'Rourke and M. Hamada, 11/7/94, (PB95-220802, A99, MF-E08).

NCEER-95-0001 "Experimental and Analytical Investigation of Seismic Retrofit of Structures with Supplemental Damping: Part 1 - Fluid Viscous Damping Devices," by A.M. Reinhorn, C. Li and M.C. Constantinou, 1/3/95.

NCEER-95-0002 "Experimental and Analytical Study of Low-Cycle Fatigue Behavior of Semi-Rigid Top-And-Seat Angle Connections," by G. Pekcan, J.B. Mander and S.S. Chen, 1/5/95.

NCEER-95-0003 "NCEER-ATC Joint Study on Fragility of Buildings," by T. Anagnos, C. Rojahn and A.S. Kiremidjian, 1/20/95, (PB95-220026, A06, MF-A02).

NCEER-95-0004 "Nonlinear Control Algorithms for Peak Response Reduction," by Z. Wu, T.T. Soong, V. Gattulli and R.C. Lin, 2/16/95.

NCEER-95-0005 "Pipeline Replacement Feasibility Study: A Methodology for Minimizing Seismic and Corrosion Risks to Underground Natural Gas Pipelines," by R.T. Eguchi, H.A. Seligson and D.G. Honegger, 3/2/95, (PB95-252326, A06, MF-A02).

NCEER-95-0006 "Evaluation of Seismic Performance of an 11-Story Frame Building During the 1994 Northridge Earthquake," by F. Naeim, R. DiSulio, K. Benuska, A. Reinhorn and C. Li, to be published.

NCEER-95-0007 "Prioritization of Bridges for Seismic Retrofitting," by N. Basöz and A.S. Kiremidjian, 4/24/95, (PB95-252300, A08, MF-A02).

NCEER-95-0008 "Method for Developing Motion Damage Relationships for Reinforced Concrete Frames," by A. Singhal and A.S. Kiremidjian, 5/11/95.

NCEER-95-0009 "Experimental and Analytical Investigation of Seismic Retrofit of Structures with Supplemental Damping: Part II - Friction Devices," by C. Li and A.M. Reinhorn, 7/6/95, to be published.

NCEER-95-0010 "Experimental Performance and Analytical Study of a Non-Ductile Reinforced Concrete Frame Structure Retrofitted with Elastomeric Spring Dampers," by G. Pekcan, J.B. Mander and S.S. Chen, 7/14/95.